

Design of An Innovative, Highly Maneuverable, Stealthy Unmanned Underwater Vehicle with ISR Capabilities

Brian Martin
Ben Saletta
Andrew Blancarte
Ketton James
Abraham Paukar

March 19, 2015

Contents

0.1	Introduction	5
0.1.1	Traditional Issues	5
0.1.2	Competition	5
0.1.3	Our Solution	6
0.1.4	Mission Objectives	6
0.1.5	Operational & Design Objectives	6
0.1.6	Brief Project Overview	7
1	Propulsor Development, SHEILA-D	9
1.1	Overview	9
1.2	Constraints	9
1.3	Design	9
1.3.1	Fluids Calculations	9
1.3.2	Drive Train	10
1.3.3	Power Supply	10
1.4	Construction	10
1.5	Testing	10
2	Summer Research and Testing	12
2.1	Open Mind	12
2.2	Well-Read	12
2.3	Presentation	13
2.4	Summer Research Summaries	13
2.4.1	Shark Skin	13
2.4.2	Vantablack	13
2.4.3	Cephalopod Skin	14
2.4.4	Waterproofing Sensors	14
2.4.5	Arduino	14
2.4.6	CFD and Python	15
2.4.7	Physical Understanding of Fluids Equations and their Application to CFD	15
2.4.8	Optimal Design of an Archimedes screw	15
2.4.9	Tom's Effect	15
2.4.10	WHOI Acoustic Modem	15
2.4.11	CLT Propellers	16
2.4.12	Smart Duct	16
2.4.13	Vortex Generators	17
2.4.14	Wanda II	17
2.4.15	Control Surface Basics	18
2.4.16	Materials and Stealth	18
2.4.17	Funding	19
2.4.18	Testing	19

2.4.19	Thrust Augmentation	20
2.4.20	Owl Stealth	20
2.4.21	Submarine Hydrostatics	21
2.4.22	Submarine Design Process	22
2.4.23	Buoyancy Control	22
2.4.24	Underwater Coatings	22
2.4.25	Currents	23
2.5	TeamUV.org	23
2.6	Summer Testing	23
3	Final Prototype Design and Manufacture, DORY	25
3.1	Lessons Learned	25
3.2	Subsystem Decomposition	26
3.2.1	Propulsor	26
3.2.2	Body	37
3.2.3	Control Surfaces	47
3.2.4	Buoyancy Control	52
3.2.5	Pressure Hull	53
3.2.6	Drive Train	56
3.2.7	Sealing	58
3.2.8	Electronics	58
3.3	Programming	63
3.3.1	Firmware	63
3.3.2	Software, The Graphical User Interface	64
3.4	Fundraising, Pricing, Time Decomposition	66
3.5	Testing	66
3.6	Conferences	66
3.7	Team Bios	66
3.7.1	Ben	66
3.7.2	Brian	67
3.7.3	Andrew	67
3.7.4	Ketton	67
3.7.5	Abraham	67
A	Phase I Report	68
B	Presentation Format	93
C	Electronics Data Sheets	94
D	Senior Project Primer Package	102

List of Figures

1.1	Drive Train Design Section View	10
2.1	Close up of Shark Skin	13
2.2	Vantablack on Aluminum Substrate	13
2.3	Cephalopod Skin	14
2.4	Potting and Conformal Coating	14
2.5	Arduino Uno Microprocessor	15
2.6	Contacted and Loaded Tip Propellers	16
2.7	Thrust Vectoring Smart Duct	16
2.8	Vortex Generators on the Wing of a Fighter Jet	17
2.9	Wrasse-inspired Agile, Near-shore, Deformable-fin Automation	17
2.10	Representation of Euler Angles	18
2.11	Sonar Detection of a Submarine	18
2.12	Underside of a Boat in a Tow Tank	19
2.13	Thrust Augmentation on the Hull of a Ship	20
2.14	Wing Features on an Owl that Provide Stealthy Flight	21
2.15	Center of Buoyancy and Center of Mass of a Submarine	21
2.16	Design Considerations for Underwater Vehicles	22
2.17	Currents and Overall Fluid Transport	23
3.1	Schematic of Control Volume A	27
3.2	Simplified Energy Equation for Control Volume A	27
3.3	Schematic of Control Volume B	28
3.4	Simplified Energy Equation for Control Volume B	29
3.5	K values for Minor Losses due to Diameter Change	29
3.6	Schematic of Control Volume C	30
3.7	Simplified Energy Equation for Control Volume C	30
3.8	Schematic of Control Volume D	31
3.9	Simplified Energy Equation for Control Volume D	31
3.10	CFD Analysis of the Vane Shell	35
3.11	CFD Analysis of the Vane Shell with the Body	35
3.12	CFD Analysis of the Vane Shell and Body with the Nozzle	36
3.13	CFD Analysis of the Entire Propulsor Design	36
3.14	Isometric View of the Von Mises Stresses on the Vane Shell	37
3.15	Conceptual Hand Drawing	38
3.16	A Possible Future Vehicle Design	39
3.17	Possible Body Shapes for Future Design	40
3.18	CFD Analysis of the Body	41
3.19	Creating the Foam Mold for the Body	42
3.20	Final Mold Ready for Body Creation	43
3.21	The Body Manufacturing Process	43

3.22 First Attempt at an ABS Forming Box	44
3.23 Second Attempt at an ABS Forming Box	45
3.24 The Fiberglass Body	45
3.25 Batteries Seated in the Fiberglass Body	46
3.26 The Final Body	47
3.27 (LEFT) Original team designed airfoil, (RIGHT) UIUC airfoil.	47
3.28 EPPLER E838 HYDROFOIL AIRFOIL (e838-il)	48
3.29 Original Control Surfaces Idea with Flaps	48
3.30 Rotary Shaft Driver Idea Design	49
3.31 Torque Transfer for Control Surfaces	49
3.32 3D Printed Pectoral Fin Control Surface	50
3.33 CFD of pectoral fin with surface plot of flow trajectories.	50
3.34 Rudder shape cut out on paper positioned on sheet of ABS	51
3.35 3D printed ABS servo mounts	51
3.36 Control surface assembly: servo, shaft, ball bearing, and shaft seal.	52
3.37 Overview of the Buoyancy Control Device	53
3.38 Details of the Buoyancy Control Device	53
3.39 The Pressure Hull Design	54
3.40 (LEFT) Dome Front Cap fixed to the pressure hull. (RIGHT) Inside Cap Camera Door	54
3.41 Wire standoffs before being trimmed of excess material.	55
3.42 (LEFT) Top view of slider tray. (RIGHT) Logic Command Center on slider tray. Note riveted handle.	55
3.43 Banebots P60 Gearbox. Courtesy of: robotshop.com	56
3.44 Gearbox mounted to pressure hull and shaft seal attached to gearbox shaft.	57
3.45 Gearbox mounted to pressure hull and shaft seal attached to gearbox shaft.	57
3.46 (Left) Loctite Marine Epoxy (Right) Silicone Sealant	58
3.47 Sabertooth 2x60 Motor Driver Courtesy of Dimension Engineering	59
3.48 MicroSD Card Breakout Courtesy of Adafruit.com	60
3.49 HackHD module courtesy of Sparkfun.com	60
3.50 (Left) Waterproofed LiPo Battery. (Right) All five LiPo batteries connected in Parallel	61
3.51 (Top) Turnigy Power Supply. (Bottom) Mega 1000W Charger	62
3.52 The Graphical User Interface	65
3.53 The Orientation Model For Viewing in the GUI	66

0.1 Introduction

Newton's third law of motion states that when two bodies interact, there are equal and opposite reactions that occur. Propulsion works on this principle and it is what allows an object to move forward. In terms of marine vehicles, a propulsion system (typically a propeller) accelerates water (the working fluid) which produces a thrust force on the propeller and body that moves the vehicle forward. In the world of marine propulsion, bladed propellers have dominated since the creation of paddle wheel by the US Navy in the 1840s.

0.1.1 Traditional Issues

Today, bladed propellers are by far the most common means of propelling water crafts, whether above or below the surface. While bladed propellers are effective, relatively inexpensive to manufacture, and available in a wide variety of sizes and geometries, they also exhibit numerous inefficiencies and disadvantages. Among these are that they create flow instabilities (buffeting), cavitate easily (leading to accelerated degradation as a result of surface pitting), produce a significant amount of noise (mainly as a result of cavitation), must be made of heavy, metallic materials (in order to mitigate the effects of cavitation damage), and are exposed to foreign object damage (which can lead to fouling which is detrimental to its primary function). These shortcomings can become greatly exaggerated when bladed propellers are used for fully submerged vehicles; this is especially true for applications in which stealth is key, such as in military submarines, special operator deployment craft, and unmanned undersea drones such as remotely operated vehicles (ROVs), unmanned underwater vehicles (UUVs), and autonomous underwater vehicles (AUVs).

The objectives for this project are to produce the UV to have fluid/smooth maneuvering, be capable of higher speeds (relative to other UVs), require little to no human interaction, and to boast a great deal of stealth (with respect to thermal, magnetic, and flow signatures, noise, cavitation, and ability to be inconspicuous).

The idea of underwater exploration is not new, however, stealthy UVs that can overcome the shortcomings inherent to traditional propellers and designed ISR missions is not a fully developed industry.

0.1.2 Competition

The idea of underwater exploration is not new, however, stealthy UVs that can overcome the shortcomings inherent to traditional propellers and designed ISR missions is not a fully developed industry.

A commercial company called OpenROV sells small tethered, battery powered ROV that is marketed as an underwater exploration vehicle for everyone. It uses three propellers as its propulsion system which achieves a maximum speed of 2 knots, and maximum operational depth of 246 feet. Although its size and price are impressive, it does not improve or acknowledge the aforementioned issues produced by the propellers and therefore does not meet the mission and operational objectives set out.

However, completion exists in the form of a 5 foot, 100 pound, US Navy developed, underwater drone codenamed GhostSwimmer. The US Navy, in collaboration with Boston Engineering, had developed and tested swarms of this new UUV which uses an innovative, biomimetic oscillating tail fin to produce thrust, eliminating the use of a traditional propeller altogether. Visually, GhostSwimmer looks like and replicates the movements of actual tuna and by doing so can achieve an operational maximum speed of 3 knots and operational depth of 300 feet. It is highly maneuverable and versatile, able to operate using battery power and remotely by a 500 foot tether. According to the release from the Navy on December 11, 2014, Ghostswimmer gathered data on tides, currents, wakes and weather conditions – the sort of oceanographic information commonly gathered by meteorologists and submariners for use in finding – or concealing – subs. This UV meets both the mission and operational objectives set out and, in some areas, surpasses them. The fact that GhostSwimmer exists simply means that the work and research Team UV has done is warranted.

0.1.3 Our Solution

As previously demonstrated, the underwater vehicle market has been expanding in recent years to include a number of new vehicles and technologies; however, many of these new solutions fall victim to the same inefficiencies that underwater vehicles have been plagued by for years, especially within the context of stealth. The solution that we put forth in the coming pages aims to revolutionize the way that naval ISR is performed by taking more special operators out of the field to make their jobs easier and less dangerous.

In order to define how our solution will stray from the traditional underwater vehicle, two sets of parameters were defined. The first set is termed the "Mission Objectives" and provides a set of guidelines for the project. The second set is termed the "Operational & Design Objectives" and represents the specific performance goals for the final project; unlike the Mission Objectives, the Operational & Design Objectives are subject to change throughout the evolution of the project.

0.1.4 Mission Objectives

These Mission Objectives are our top priority goals for this project and represent the mandatory deliverables for this project; this is to say that every decision for the project was first evaluated against these Mission Objectives so as to ensure that none of these objectives were violated, as said violation would constitute a breach of mission and thus a failure of objectives. These objectives were developed prior to the start of Phase I in April 2014 and are listed below for reference.

1. Fluid/smooth maneuvering
2. Higher speeds
3. Stealth
 - Thermal Signature
 - Magnetic Signature
 - Noise
 - Flow Signature
 - Cavitation
 - Inconspicuous
4. Little or no human interaction required

*These objectives were set out in the initial concept stage of this project and must be carried through to the final design/testing phases. Violation/endangerment/jeopardizing of these mission objectives is equivalent to a failure of the mission; as such, these mission objectives should be upheld throughout the project period and must be repeatedly referenced for compliance.

0.1.5 Operational & Design Objectives

The Operational & Design Objectives essentially set in place the practical definite parameters of the design (whereas Mission Objectives refer to the more global, superficial characteristics of the vehicle as a whole) and were originally laid out at the beginning of Phase I. These objectives are listed below for reference:

- Depth range of 100-200 ft
- Speed of 5 knots
- Size limited to approximately that of a scuba tank

- Weight which aims to increase thrust-to-weight ratio, but reduce the amount of positive buoyancy that the buoyancy control systems must overcome; the weight might possibly be used to induce neutral buoyancy at a prescribed depth
- Operational times of 1 hour at full power
- Maximization of internal space for stowage of the sensor suite
- Eases of storage and transportation/portability
- Ease of maintenance/reduction in required maintenance

These Operational & Design Objectives were more comprehensively assessed at the end of the Summer 2014 time period as a means of altering the objectives to a refined state consistent with the progress/success of Phase I & II, while keeping in mind the timeline and scope of work for Phase III. The changes to the Operational & Design Objectives that reflect the updated performance goals heading into Phase III are as follows and correspond to the italicized items within the initial Operational & Design Objectives list as noted above:

1. Reduced operational depth range to match the depth capabilities of commercially available buoyancy control solutions as found in preliminary component identification/costing research to a 33 ft (1 atm) test depth capability and 66 ft maximum operational (buoyancy control limiting) depth of 66 ft (2 atm).
2. Reduced speed goals to correspond to the balance between vane shell propulsor optimization, manufacturing challenges (tolerance limitations), and body drag (as effected by the battle between streamlining and manufacturing limitations).

0.1.6 Brief Project Overview

The timeline for this project is split into three phases over a 14 month period; these phases (along with truncated descriptions of the phases) are as follows.

Phase I (ME 325/L_Spring 2014): As the introductory phase of the project, this phase (spanning 36 days from April 2014 to May 2014) focused on the development of the propulsion system demonstrator for the project. Based off of the findings regarding the plausibility and efficiency of Phase I, the developed propulsion system demonstrator would be directly integrated into the full vehicle as the propulsor, adapted towards the vehicle propulsor, or scrapped in favor of a different propulsor for the vehicle.

Phase II (Summer Research/Testing_Summer 2014): This follow-up phase began the same day that Phase I ended (in May 2014) and ran until the day that Phase III began (in September 2014). The focus of this phase consisted of three main goals: future vehicle concept development, literary research, and experimental testing. With regards to future vehicle concept development, the team spent a great deal of time conceiving, visualizing, and documenting ideas for what the final vehicle would look like and what kind of subsystems it would be composed of; this sub-focus of Phase II continued into the early stages of Phase III. The majority sub-focus of Phase II was the literary research, which spanned very many topics in engineering (many of which were extremely advanced, high-level topics), as will be discussed later. The final subset of Phase II, experimental testing, consisted of both propulsion system demonstrator testing and small-scale testing aimed at gaining further insight into the physics associated with the demonstrators flow mechanics and into the requisite considerations that would be associated with future subsystems.

Phase III (Senior Project_Fall 2014, Winter 2015): This phase began the same day as Phase II ended (in September 2014) and will officially end at the end of the Winter 2015 quarter (in March 2015), but will unofficially continue until all aspects of the project are completed (projected June 2015). The official time span of this phase will cover the development of the full vehicle, the building of said vehicle, and the testing of the vehicle. The unofficial appended time span will cover research conferences, presentations, further development, and further testing of the vehicle, with the unofficial end of the phase coming with the

last deliverable for the project (at the time of writing, this would be the senior project symposium/possible show case or the California State University Student Research Conference CSUSRC, both of which will be discussed in the section of conferences/talks). Specific subsystems for further development in this phase consist of:

- Propulsion System
- Maneuverability Systems
 - Control Surfaces
 - Control Electrical Systems
 - Control Programming
- Buoyancy Control Systems
 - Buoyancy Control (Mechanical) Systems
 - Buoyancy Control Electrical Systems
 - Buoyancy Control Programming
- Body
 - Streamlining
 - Subsystem Housing
 - Structural Support System
- Navigation
 - Electrical Systems
 - Programming
- Sensor Suite
 - Navigation Components & Programming
 - ISR Components & Programming
- Graphical User Interface (GUI)

Phase III will require greater incorporation of subjects/theories such as mechanical design, electromechanical systems, materials selection, fluid mechanics, heat transfer, acoustics, computer programming, and many more. More information about the specific phases, Phase III goals/challenges/etc., and scope of work, please see the appended Senior Project Primer Package.

Phase 1

Propulsor Development, SHEILA-D

1.1 Overview

SHEILA-D stands for Subaqueous Hydrodynamically propelled Explorer Implementation Los Angeles - Demonstrator. The driving force behind the development of this unmanned underwater vehicle is the innovative propulsion system. This system was the foundation of the first phase of development, a proof of concept for this screw based propulsion system. As this phase was a deliverable for a Machine Design Class there is a detailed overview of this phase included in appendix A.

1.2 Constraints

As this initial design was part of a class project there were many constraints that came along with it. The primary constraint was time. The project was completed, from design to testing, in 35 days to meet the deadline imposed by the academic calendar. There were also significant cost constraints because this phase was funded completely out of the personal funds of the members involved. The constraints eliminated several custom manufacturing techniques due to extensive lead times and costs. This led to the final construction consisting mainly of parts shaped from hardware store components.

1.3 Design

The initial design phase took the first 5 days in which the foundational fluid mechanics, the drive train and power calculations were completed in these days. Further redesign was included in with the manufacturing process when the aforementioned constraints restricted the construction of the device as designed.

1.3.1 Fluids Calculations

The fluids calculations were an important part of the initial design because of the role they played in moving the device through the water. To complete these calculations the device was broken into two sections. First the cylinder holding the screw and second the cone used to accelerate the fluid. For the cylinder an assumption was made that a constant force would be imparted to the fluid along the surface of the screw blades. This constant force would act on the fluid mass between the vanes therefore, assuming a constant density, the vanes would provide a constant acceleration along this section. With a known length of the cylinder and this calculated acceleration the speed of the fluid exiting the cylinder was calculated. Conservation of momentum was then applied to the fluid as it passed through the final cone and nozzle giving the final thrust force of the propulsion system. These calculations were plugged into an Excel spreadsheet and various geometries

were iterated through to find the optimal configuration. A more detailed walk through of the fluids analysis is included in appendix A.

1.3.2 Drive Train

The fluids calculations provided a value for the required torque and angular velocity. The drive train was designed to meet both of these criterion. The major difficulty with the drive train in this design was transmitting the torque from the motors to the external shell. To solve this problem and provide sufficient torque two motors were fitted with gearboxes then mated to the sun gear in a planetary gear set that transmitted the torque out to the rotating cylinder as seen in Figure 1.1. The planetary gear system was 3D printed to minimize cost and manufacturing time.

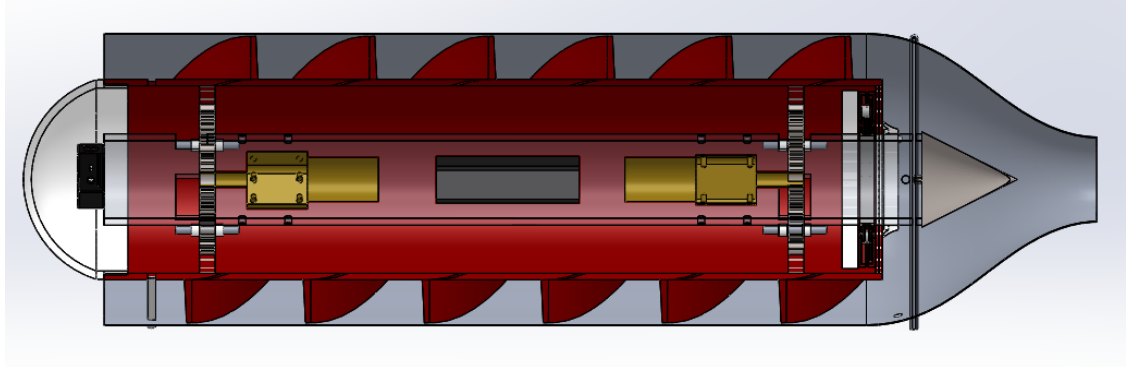


Figure 1.1: Drive Train Design Section View

1.3.3 Power Supply

These motors required a significant amount of current at a constant 12 volts. These requirements went into the power design calculations and searches for sufficient batteries. A single 12 volt lithium battery was selected due to its high current discharge, compact form, and high capacity characteristics. The design of the power supply was integrated into the design of the drive train due to the important relationship between the easily available motors and batteries for a reasonable operational time. The power supply had to fit between the two motors and is shown as a black box in Figure 1.1.

1.4 Construction

The construction of this device was completed in a very short time span using commercial off the shelf components. This involved PVC pipes of various diameters, cutting and thermoforming sheets of acrylic, and fastening components with traditional fasteners as well as epoxy. As the construction proceeded difficulties were discovered and the design was adjusted to compensate for these problems. One of the major difficulties was the manufacture of the helix screw. This was solved by thermoforming cut acrylic then filling gaps created in the vanes with waterproof tape. Other adjustments and quick fixes were applied throughout the process. The construction was a challenge to complete within the time frame at an acceptably low cost.

1.5 Testing

Once construction was completed the device needed to be tested to confirm that the propulsion system did indeed propel the device through the water. To do the testing properly the vehicle was taken to the

Puddingstone reservoir at dawn and ran along the deck of a boat dock. It took a few tests to get the device operational and, while the vehicle could not be set off on its own at this stage, it pumped a significant amount of water though the body and out the cone and nozzle assembly. Many things were learned about the design during the testing session and made note of for future design. The major lessons were that the assumptions that were made in the fluid calculations were wrong and that without control surfaces the vehicle would reach an equilibrium rotation state where the outermost cylinder would rotate and counter the rotation of the center cylinder.

Phase 2

Summer Research and Testing

During the summer of 2014 the group members of Team UV did not entirely part ways for three months. The group decided that it would be in the best interest of the group and design itself to meet twice a month where each member would give presentation on standard material along with research they have found during the two week period between meetings. These meetings started in June of 2014 and ended when the 2014 Fall period started, September 2014. Each of the meetings held were roughly five to seven hours long. The format of the presentations were standardized however each member provided their own research and information. Presentation format can be found in appendix B. In the summer of 2014 Team UV spent roughly 240 hours as a group towards the senior project itself. That number includes research done outside of the meeting along with the meetings themselves. The PowerPoint presentations contained three sections.

2.1 Open Mind

The group was given a situation/problem that has or could happen in the world we live in today and each member had to give insight or propose a solution to the problem/situation. Each member were asked to provide their solution along with reasoning as to why their solution would be efficient. Since Team UV are composed of mechanical engineering undergraduates, the solutions based on the prompts were required to use some aspect of engineering. For example, one open mind prompt addressed the issue that many people in developing countries lack the access to power. The group was asked if they were tasked with developing an inexpensive do it yourself power generation system for use in a 3rd world country, what kind of engineering considerations might you take into account. The idea behind the open mind prompt was to keep the group members mind engaged during the break and keep that engineering mentality sparked. Also, this prompt was to have the members think outside the box and to aid in developing creative/innovative ideas for use in the senior project design.

2.2 Well-Read

Members were asked to look into articles/publications and present something they found to be interesting, innovative, advancements, etc. The articles were not limited to strictly the engineering field however it was recommended. Articles presented from the group ranged from next generation wind turbines to theory behind the process of suction eating of fish. The idea of the well-read was to give insight to the group of remarkable advancements in science and technology throughout the world.

2.3 Presentation

The presentation was an open ended section which allowed for each member to present some research they did during the two week period between meetings. The research was required to aid in the design of the senior project in areas such as theory, analysis, design, controls, manufacturing, and/or testing. Research in CLT propellers, computational fluid dynamics, Arduino coding, wake turbulence, underwater designs and coatings, power management, component selection for marine research, smart ducts, submarine design/research, and many others.

2.4 Summer Research Summaries

2.4.1 Shark Skin

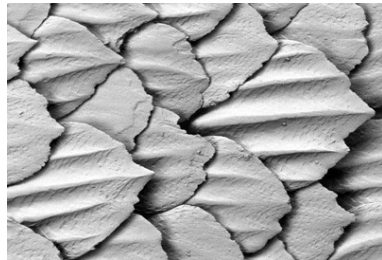


Figure 2.1: Close up of Shark Skin

Sharks move very efficiently thanks to the characteristics of their skin. Anything but smooth, shark skin has individual scales, called dermal denticles, with narrow passages that reduce friction drag and accelerate the flow along its length. These scales also flex and realign to reduce biofouling which can negatively affect flow over the body.

2.4.2 Vantablack



Figure 2.2: Vantablack on Aluminum Substrate

Surrey NanoSystems has engineered a new super-black material called Vantablack. This material composed of Vertically Aligned Carbon Nanotube Arrays absorbs 99.965% of incident light. Photons are allowed into the material and are then blocked and trapped from leaving. This material is already in high demand for space and stealth applications.

2.4.3 Cephalopod Skin



Figure 2.3: Cephalopod Skin

Two teams of researchers from Rice University and MIT were tasked with developing material which could replicate the camouflaging abilities of cephalopods. The class of mollusks which include squid, possess skin that can manipulate its own color and texture. Rice University engineering a rigid aluminum nanorod display panel which displays an intense color spectrum. MIT, on the other hand, created a flexible display that can change color and texture but with limited color spectrum.

2.4.4 Waterproofing Sensors

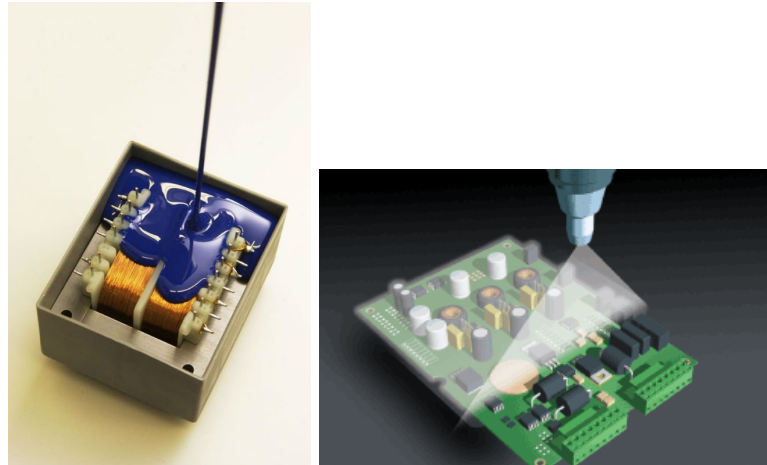


Figure 2.4: Potting and Conformal Coating

Using sensors underwater with a strict budget takes a bit of creativity. Two popular methods used by hobbyists and professionals alike are: Potting and Conformal Coating. Potting is the method of filling an electronic assembly with a solid or gelatinous compound such as a thermosetting plastic or silicone. This blocks water and increases shock resistance. Conformal Coating offers the same benefits of potting but is lighter and non-permanent which allows for reworking.

2.4.5 Arduino

Microprocessing is made accessible to all thanks to companies like Arduino. Boards housing everything from input and output terminals to a microprocessor can link the electrical world to the physical world. Users start out controlling the lighting sequencing of LEDs to eventually controlling more advanced mechanical



Figure 2.5: Arduino Uno Microprocessor

systems. Topics presented to the team include LED control, reading data from sensors, and ways to expand the factory limitations of Arduino boards.

2.4.6 CFD and Python

Computational Fluid Dynamics, CFD, is a powerful tool for the analysis of fluid behavior. The computational techniques used to break down the navier-stokes equations have applications that stretch beyond the realm of fluid dynamics and allow the modeling of many non linear mathematical phenomena within a computational environment. This presentation was an introduction to the ideas behind CFD and the way that an analysis could be written using the Python coding language.

2.4.7 Physical Understanding of Fluids Equations and their Application to CFD

To apply any of the fundamental fluids equations to a device a physical understanding of the meaning behind the mathematics is crucial. This presentation addressed four different ways to address a fluids problem. First analysing a stationary control volume and applying conservation of mass equations to the borders. Secondly selecting a moving control volume of fixed mass and applying conservation of momentum equations to the borders. Thirdly selecting an infinitely small particle and analyzing the fluid that passes through it. Or finally selecting an infinitely small particle and analyzing its path through the fluid. This allows for the analysis of any problem from a variety of different perspectives.

2.4.8 Optimal Design of an Archimedes screw

As the device that we are manufacturing depends upon a screw similar to the original archimedes screw it was important that we analyze the methods used to optimize the design of one of these screws.[1] This introduced the idea of breaking a design down into dimensionless variables that dictated the ratio of the size of components and reduced the amount of unknown variables. These dimensionless numbers were then varied and efficiencies were calculated providing the final, most efficient design ratios.

2.4.9 Tom's Effect

Fish are covered with mucus primarily to cover wounds and promote healing, however this mucus also causes Toms Effect. This is when a high molecular weight polymer is released into a fluid stream it makes the fluid remain laminar for longer because the polymers line up with the streamlines in the fluid. This requires the fluid to use more energy to break the streamlines and become turbulent. With fish this allows them to travel through the water with significantly less drag than they otherwise would have had to overcome. The could be applied to any underwater vessel to provide increased fuel efficiency and stealth.

2.4.10 WHOI Acoustic Modem

Underwater communications have been a long standing challenge because radio waves attenuate rapidly in water. A possible method for communication between several underwater vehicles or even between a vehicle and its home base is an acoustic modem. These work by emitting modulated sound waves that carry data

through the water. Due to the high speed of sound through water these methods of communication become practical.

2.4.11 CLT Propellers



Figure 2.6: Contracted and Loaded Tip Propellers

Fundamentally the goal of the Contracted and Loaded Tip (CLT) propeller is to improve open water efficiency. This means that the tip on the propeller reduces the velocities of water entering the propeller disk which, in turn, reduces the hydrodynamic pitch angle. This reduction of hydrodynamic pitch angle and induced velocities results in many advantages. To list a few, CLT propellers achieve higher top speeds, greater thrust, smaller optimum propeller diameter, better maneuverability, inhibits cavitation and tip vortices (resulting in less noise, less vibrations, lower pressure pulses, and lower area ratio

2.4.12 Smart Duct



Overhead views of the Smart Duct. Neutral (upper) and powered (lower).

Figure 2.7: Thrust Vectoring Smart Duct

A Smart Duct is a deformable shroud that changes the direction of flow of the propeller wash to provide a direct steering force to the vehicle. The duct itself is an electrically actuated structure that is covered by a flexible hydrodynamically smooth sheathing whose primary movers are a set of high strength Nickel-Titanium SMA actuator cables. Shape memory alloys (SMA) make this deformable Smart Duct a reality. Testing has proven flow turning angles of up to 15 degrees at thrust levels of operational submarines is possible with this technology. These results may directly affect the design of future marine vehicles by reducing (and possibly eliminating) the use of control surfaces for maneuvering.

2.4.13 Vortex Generators



Figure 2.8: Vortex Generators on the Wing of a Fighter Jet

For relatively blunt objects like a sphere or wing on a plane the overall drag decreases when the boundary layer becomes turbulent because turbulent flow allows the boundary layer to follow the surface closer which decreases the overall wake region. The larger this wake region is the more you see chaotic flow separation and adverse pressure gradients that can be catastrophic on aircraft because the flow separation can cause them to stall. Vortex generators can be found on the wings of aircraft and even on some high performance cars. With vortex generators there is an exchange between high energy momentum and lower energy momentum by tripping laminar flow into turbulent which allows the boundary layer to remain attached over a greater length of the wing chord or car profile which results in a thinner wake region and smaller adverse pressure gradient on the rear of the object which lowers the pressure drag. This allows for many benefits like lowering the stall speed, improving stability and control during maneuvering, and decreasing the turning radius.

2.4.14 Wanda II



Figure 2.9: Wrasse-inspired Agile, Near-shore, Deformable-fin Automation

Researchers have turned to nature for inspiration trying to model a UUV that uses flapping fins to maneuver through difficult underwater environments. Many fish species use articulation of the pectoral fins to produce appropriate forces and moments propel themselves through the water and to react to dynamic changes in flow, physical obstacles, and wave forces near the shore. A four-fin UUV named WANDA-II (Wrasse-inspired Agile Near-shore Deformable-fin Automaton) is the 2nd generation of this alternative

propulsion UUV. These fins are capable of producing thrust vectors in multiple directions through changes in curvature and stroke angle. All this is in the attempt to replicate the high level of controllability that fish species have near shore and in shallow water environments. A four-fin UUV could be deployed in a variety of missions including harbor monitoring and protection, hull inspection, and covert shallow water operations.

2.4.15 Control Surface Basics

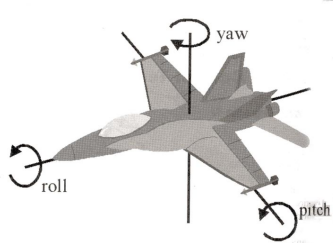


Figure 2.10: Representation of Euler Angles

Control Surfaces are moveable surfaces on wings that allow for maneuverability for both air and marine vehicles. Typically when control surfaces deflect they change the trailing edge of the wing which in turn changes the angle of attack. Angle of attack is the angle of between the wing chord (leading edge to trailing edge) to the Relative Airflow or free air flow (RAF). The amount of lift a wing produces is more a function of the angle of attack rather than the shape of the airfoil (cross section of the wing). The primary control surfaces on an airplane are ailerons (which controls roll/pitch), elevators (which controls pitch), and the rudder (which controls yaw).

2.4.16 Materials and Stealth

five major underwater vehicle requirements. The two key issues are technical feasibility and stealth. The third important issue is survivability. Fourth, and equally important is the need to successfully deliver a payload. And finally, all of these attributes regardless of importance, must be considered within a framework of cost. (Submarine Technology for the 21st Century).

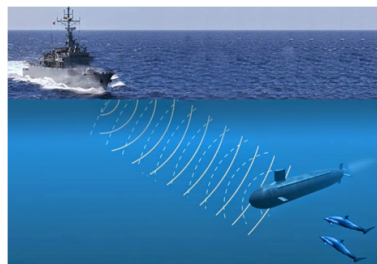


Figure 2.11: Sonar Detection of a Submarine
[3]

Research was done into submarine hull materials and what we could learn from them for our project within the framework of parameters such as weight/speed, strength/depth capability, stiffness, corrosion resistance, magnetic signature, machinability/formability, fatigue resistance, thermal properties, electrical properties, and acoustic properties. Research was conducted into steel, titanium, aluminum, composites (Carbon Fiber-, Titanium-, and Glass Fiber-Reinforced Polymers), and general polymers.

Stealth was investigated with regards to passive control (active control was not looked into owing to the impracticality with regards to the scope/scale of our project). Passive control research centered firstly on the effect of polymeric bodies and polymer secretion on the hydrodynamic boundary layer, skin friction, wake field, general turbulence, vortices, and hydrodynamic noise generation. The next direction for passive control was towards acoustic stealth via the use of anechoic materials (with sublayers for absorbing sonar waves, damping and decoupling of internal signal waves, and transmission layers for areas with intentional signal emission/transmission) and machinery raft beds (for vibration and noise damping), including attenuation ranges, elastomeric viscoelastic mechanical models, porosity effects (on attenuation, damping, and chemical stability), the correlation of relaxation modulus with temperature, signal frequency, and thermal transitions, and chemical stability (hydrolytic stability and water absorption).

2.4.17 Funding

Research was conducting with regards to sources of project financial support. Options looked into included National Science Foundation (NSF) and Department of Defense (DoD) grants, innovation competition awards, (financial, material, product, and service) sponsorships (and the possible development of a sponsorship brochure) and donations, and online crowdsourcing. The final decision was to use crowdsourcing for the majority of the fundraising and to look for sponsors and donors whenever possible. Specific companies further researched for sponsorship, donation, or discount included Proto Labs, Rapid Machining, Quick Parts, Solid Concepts, and the Cal Poly Pomona Southern California Engineering Technologists Association (SCETA).

Websites looked into for hosting the crowdsourcing campaign included KickStarter, Indiegogo, RocketHub, and GoFundMe. Aspects considered included campaign type [Flexible (keep what you raise) vs. Fixed (all or nothing)], timeline, campaign durations, processing/collection timelines and fees, donor rewards, website demographics (aimed at technical or artistic people), website traffic, and connectivity with social media.

At this time, the team also created social media accounts with Facebook, Instagram, and Twitter in order to help spread awareness of both the fundraising campaign and the website (which was created through WordPress.com after consideration and research into the same basic considerations as for the fundraising campaign, with the addition of website cost, domain ownership, and customization considerations).

2.4.18 Testing

Research was also conducted into both industry standard marine vehicle testing (mostly the use of tow tanks and the specific parameters often focused on with industry testing, i.e. the Admiralty Coefficient) and testing that we could perform.

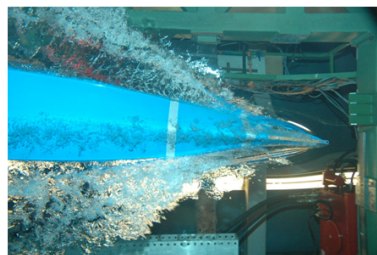


Figure 2.12: Underside of a Boat in a Tow Tank
[4]

The first future test highlighted for our project included powered movement testing with stabilizing surfaces (for cancelling out torque transfer and rotation transmitted to the outer body) and a distributed weight belt (for inducing neutral buoyancy) with the parameters of interest of water speed, thrust, and flow

field visualization. Other test ideas consisted of battery run time tests, sealing tests, and small scale concept tests (i.e. using a cut open 2L bottle, cone to fit into the bottle, and swirling motion to determine the most efficient exit flow type through measuring drain time and waterproofing small DC motors and connecting them to vane shells of various geometries inside submerged tubes).

2.4.19 Thrust Augmentation

Research was conducted into Zone I (hull and pre-shaft inlet sections), Zone 2 (fluid working section), and Zone III (outlet section) thrust augmentation devices, their implementation, and how they influence propulsive efficiency, flow separation, turbulence, propulsor swirl (pre-swirl and post-swirl) (and thus flow equalization), cross flow minimization (and thus bilge vortices), effective thrust, shaft vibrations, wake field magnitude and distribution, open water efficiency, energy recovery, propeller hub vortices, conversion of rotational kinetic energy to directional flow, hydrodynamic lift, and lift-drag ratio. Devices researched include:

- Zone I: Wake equalizing ducts, asymmetric sterns, Grothues spoilers, stern tunnels, semi- or partial ducts, reaction fins, Mitsui Integrated Ducted Propulsion Units, and Hitachi Zosen Nozzles.
- Zone II: Increased diameter-low RPM propulsors, Grim Vane Wheels, propellers with end-plates, CLT propulsors, and propeller cone fins.
- Zone III: Rudder-Bulb fin systems and additional thrusting fins.



Figure 2.13: Thrust Augmentation on the Hull of a Ship
[5]

Research was also conducted into the effect of combination of devices with the conclusion that most combinations were not possible due to one device removing the regime utilized by the other, while a select few combinations led to good benefits.

2.4.20 Owl Stealth

Research was conducted into the mechanisms by which owls derive their acoustic stealth, with the goal of better understanding the turbulent eddies and their amplification/scattering from the trailing edges of wings

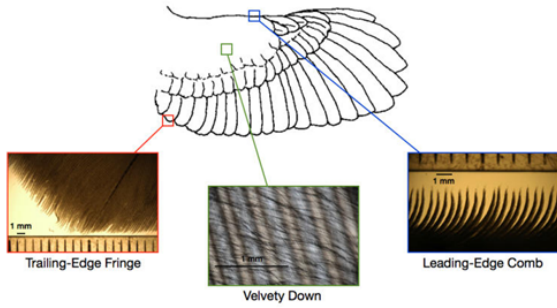


Figure 2.14: Wing Features on an Owl that Provide Stealthy Flight
[6]

(natural or man-made) and how biomimicry might be able to change the way our control surfaces might affect our stealth (acoustic or flow signature). Research centered on the profiles, material properties (most importantly stiffness), geometry, and surface roughness of the leading edge, mid-wing section, and trailing edge.

It was determined that the trailing edge is the dominant noise source on wings and that owl wing stealth was mainly the result of use of leading and trailing edge tubercles and flexible, porous trailing edge material. Tubercles were to be a future feature of our vehicle's control surfaces, time permitting.

2.4.21 Submarine Hydrostatics

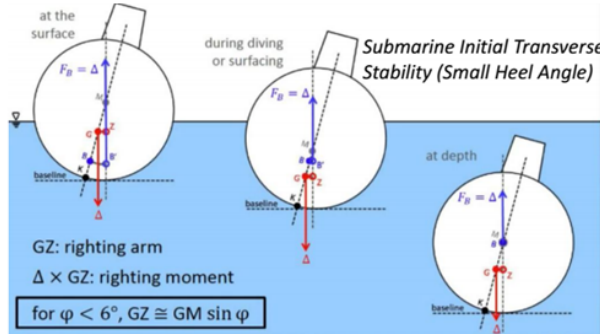


Figure 2.15: Center of Buoyancy and Center of Mass of a Submarine
[7]

Research was conducted into ship and submarine hydrostatics in the surfaced, diving/surfacing, and submerged states. Key factors considered included state of buoyancy, reserve of buoyancy, trim, configuration and use of main ballast tanks (internal and external), free flood spaces, margin ballasts, variable ballasts, superstructures, flexible bag ballasts with flotation collars, freeboard, and a pressure hull.

Methodologies for buoyancy calculation were researched heavily for both intact and damaged vessel states, surface (static), surfacing/diving (transition), and submerged (static) states, conditions of flotation, and disturbance response for small and large values of sway, yaw, surge, heave, and (the most complex case) heel/roll.

Some specific takeaways included the final decision with regards to buoyancy control system and flood/vent hole design (i.e. location and use of a grill if requiring a large hole in order to disrupt noise, vibration, and drag caused by the flood/vent hole(s)).

2.4.22 Submarine Design Process

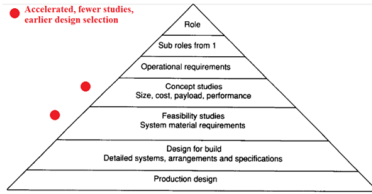


Figure 2.16: Design Considerations for Underwater Vehicles
[8]

Research was conducted into the submarine design process as presented in Concepts in Submarine Design, 2s (Burhcer). This design process is shown below, with the accelerated modifications for our time-sensitive project shown in red.

Note: Bolded text in the following paragraphs highlights the applicability to our project. Specific topics focused on included role designation (**ISR**) [and subsequent subrole (**perform ISR in a covert manner within a variety of environments while retaining high stealth, maneuverability, elevated speeds, and sufficient battery life**)], development of operational requirements (**specifics of speed, maneuverability, battery life, stealth characteristics, etc. requirements**), concept studies (with key parameters of size, cost, payload, performance), feasibility studies (and system material requirements) (**development of weight, space, and power budgets for various sub-systems in design**), *design for build* (detailed systems, subsystems, arrangements, configurations, specifications, etc. (**management of previously developed budgetary allocations with deliverables relating to structures, arrangements, hydrodynamics, subsystems, hydrostatics (both surface and submerged), etc.**), and production design (**final vehicle design**)).

2.4.23 Buoyancy Control

A research article contained information related to buoyancy control of a semiautonomous underwater vehicle and design orientation. The orientation of the design determined what the application of the vehicle. For example, if the design were to be horizontal resembling a manta ray, its use would be for towing and exploration at lower depths. However, due to this orientation it has a higher chance of getting stuck in densely populated sea vegetation or between underwater rocks. If the orientation were to be vertical, resembling a fish, its use would be for a remote controlled mode and towing as well. The vertical orientation makes it easier to maneuver in densely populated sea vegetation. The buoyancy control mechanism contained two compressed air tanks connected to two separate balloons. The air would be released into the balloon when the vehicle needed to raise and the air would be released from the balloon when the vehicle needed to be lowered.

2.4.24 Underwater Coatings

Cathodic protection is used in a variety of underwater applications. Cathodic Protection (CP) is a technique used to control the corrosion of a metal surface by making it the cathode of an electrochemical cell. A simple method of protection connects the metal to be protected to a more easily corroded "sacrificial metal" to act as the anode. The sacrificial metal then corrodes instead of the protected metal. The sacrificial metal that has been corroded provides a protective surface to prevent the base material from being corroded. Alocit by the A&E group is a coating that is used for underwater applications. It is one of three coatings that meet the specs of the US Army Corps of Engineers.

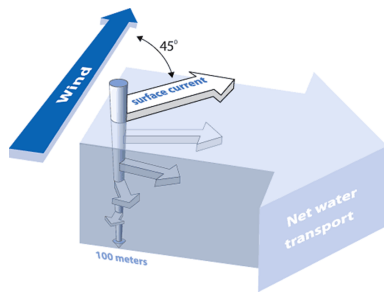


Figure 2.17: Currents and Overall Fluid Transport

2.4.25 Currents

Currents are broken down into two types, surface and deep water. Deep water currents usually occur more than 400 meter (1300 feet) under the surface of the water. The water movements are caused by differences in water density known as Thermohaline circulation. Deep water currents are much slower than surface currents but they move much more water due to water density increase deeper in the sea. Surface currents are due to the Coriolis Effect. The Coriolis Effect occurs due to the rotation of the earth, the circulating air is deflected resulting in curved paths. The winds curved path drags on the waters surface, causing it to move in the direction the wind is blowing. The Ekman Spiral is a consequence of the Coriolis Effect.

2.5 TeamUV.org

Establishing TeamUV.org was the obvious next step after a Summer filled with professional growth and academic exploration. Not only was the website about the current progress of the teams senior project but also about inspiring interest in STEM and facilitating monetary support. Topics covered range from fluid dynamics, robotics, and biomimicry to shining light on what engineering is and how it impacts the world. Inspired by websites often visited by Team UV members, posts were uploaded various times throughout the week to keep followers intrigued without feeling overwhelmed. Well Reads, Presentations, and Open Minds were set to be posted on Tuesdays, Thursdays, and Sundays, respectively. Each post was written by a team member according to a set schedule set for months in advance. A list of website postings can be found in Appendix . Team UV also made sure that the website was linked with companion Facebook, Twitter, Instagram, and GoFundMe accounts.

Team UV.org went live on July 31, 2014 with a welcome post about the site, the project, and ways to help the teams fundraising campaign. The site instantly created buzz pulling in 122 views and 38 visitors the first month. After gaining a steady following from all around the world including 87 countries, TeamUV.org achieved a best month of 670 views and 518 unsubscribed visitors in January 2015. To date, the site has gained a steady, recurring base of 84 subscribed followers that actively visit and participate in leaving comments for the team.

Aside from weekly posts, visitors to the site can also find team member biographies giving background about personal interests, academic experiences, and professional work. Those looking to sponsor the teams efforts with donations or equipment are also able to give directly on the site, follow a link to the Team UV GoFundMe site, or contact the them directly.

2.6 Summer Testing

Along with delving into Summer research pertaining to many aspects of engineering design, Team UV also performed a couple of tests. Another trip to Sailboat Cove was made to test the benefits of attaching control surfaces to Sheila-D. Spring Quarter testing resulted in the formation of a free exit jet but minimal

displacement of the vehicle. Due to stacking inefficiencies with material availability, available manufacturing methods, and unaddressed torque transfer issues, Sheila-D was in need of support. Scrap square pieces of aluminum flashing were roughly attached to the sides of the propulsor which controlled the overturning moments caused by torque transfer in the device. This resulted in linear travel along the dock, verifying the projects potential.

Testing the importance of the exit cone was also performed during the summer session. 2-liter soda bottles were modified to resemble the flow through Sheila-D. Water was passed through the models nozzle, with and without an exit cone, and discharge times were recorded. The use of the exit cone was verified by the faster exit times of the cone-equipped soda bottle. Tests were also performed as to the effects of pre-swirl into the nozzle caused by the vane shell. Tests using modified soda bottles showed promising results as the water look to discharge out the nozzle faster with pre-swirl but were eventually ruled inconclusive. Controlling the swirl of the exiting water was difficult to accomplish giving the tests poor repeatability.

Phase 3

Final Prototype Design and Manufacture, DORY

3.1 Lessons Learned

Even though SHEILA-D was able to provide thrust through the use of the unique propulsion system there were factors that attributed to the inefficiencies of SHEILA-D. For example, SHEILA-D was funded entirely from the group members themselves and was under a deadline of eight weeks to do analysis, design, manufacture, and testing. Contacting vendors to manufacture customized parts where tolerances were very critical was found to be very expensive. Therefore components bought for SHEILA-D were products that could be obtained from readily available sources with little to know lead time from local vendors such as Home Depot or bought online from vendors such as McMaster Carr. SHEILA-D was not designed from components that could be bought locally or online which led to the team adjusting many components ultimately leading to a greater manufacturing timeframe. The main inefficiency during phase I was the high amount of friction that occurred in the system. The main component of the propulsion was experiencing a high amount of friction which caused the first round of testing to fail. The team took these experiences into high consideration when designing the phase III device.

The revised goal resulting from the experiences of phase I was to minimize friction in the system and develop an entire underwater vehicle that overcomes the shortcomings of a traditional propeller system. The new phase III device would have an entirely remote operation which eliminates the need to tether the device. The device would perform its mission in obtaining information, surveillance, and reconnaissance (ISR). In order to achieve this goal several new components were added to the phase III device to ensure enough information is received. To ensure sufficient maneuverability three control surfaces powered by servo motors were added to the design. The phase III device was made to be neutrally buoyant therefore a piston ballast tank was added to control the depth of the vehicle. The vehicles rotational power is going to be provided by only one motor instead of 2 motors to give more room for additional components. The biggest addition to phase III was the use of a graphical user interface (GUI). The GUI is where the user would read all of the information received by the vehicle once it has returned from its mission. The GUI has four separate components that display specific information. One box will display a video of the route the vehicle took. This will be achieved by placing a camera at the face of the vehicle that saves the data onto a SD card. The second box displays information on the vehicles speed, displacement, and orientation. An accelerometer will be placed inside the vehicle in order gain this information. The third box shows the orientation of the vehicle. Orientation data is taken from the accelerometer and the model will update the orientation to show how the vehicle was oriented at a specific time. The fourth box contains a map that plots the route of the vehicle. When the vehicle ends its mission the map will display the route it took. The electronics will be powered by batteries and functionality to be provided by the use of an Arduino. The GUI was to be done using the program, Processing.

3.2 Subsystem Decomposition

3.2.1 Propulsor

Control Volumes

In order to perform our internal fluids analysis on the propulsor with the goal of optimizing the vane shell, we had to treat the problem as a basic fluid mechanics problem and start with the same foundational elements of all fluid mechanics problems; we had to define some control volumes.

Before jumping right into defining our control volumes, we had to identify the parameters of interest to us; of these, we highlighted four main parameters that were to be treated as unknowns:

1. Inlet velocity at the front of the propulsor v_1
2. Pressure at the end of the vane shell and prior to the nozzle P_2
3. Exit velocity at the rear of the nozzle v_3
4. Thrust force produced by the vehicle F_T

Additionally, these values would be evaluated at three main state points:

- The free stream inlet region ahead of the propulsor (1)
- The interface between the back of the vane shell and the start of the nozzle/cone(2)
- The exit region immediately behind the nozzle (3)

To properly solve for these four unknowns, we needed four equations and thus we developed four control volumes (A, B, C, D), each with a distinct equation associated with it as will be shown below. Once we had these four equations developed, the plan was to use an iterative programming technique to solve the four equations for the four unknowns, thus yielding the parameters necessary for finding the basic performance characteristics associated with the propulsor. This will be discussed in greater detail in the programming section of the report that follows.

As will be seen below, the basic types of equations utilized in the analysis consisted of the conservation of energy and the conservation momentum; conservation of mass was not utilized as it did not yield any helpful information with regards to the problem solving process.

$$\frac{P_i}{\gamma} + \frac{v_i^2}{2g} + h_{L_{i-f}} = \frac{P_f}{\gamma} + \frac{v_f^2}{2g} + h_{s_{i-f}} \quad (3.1)$$

$$\Sigma F = P_i A_i + \dot{m} v_i + P_f A_f - \dot{m} v_f - F_T + F_D = ma \quad (3.2)$$

Control Volume A For control volume A , the energy equation was adopted, with the unknowns of v_1 and P_2 .

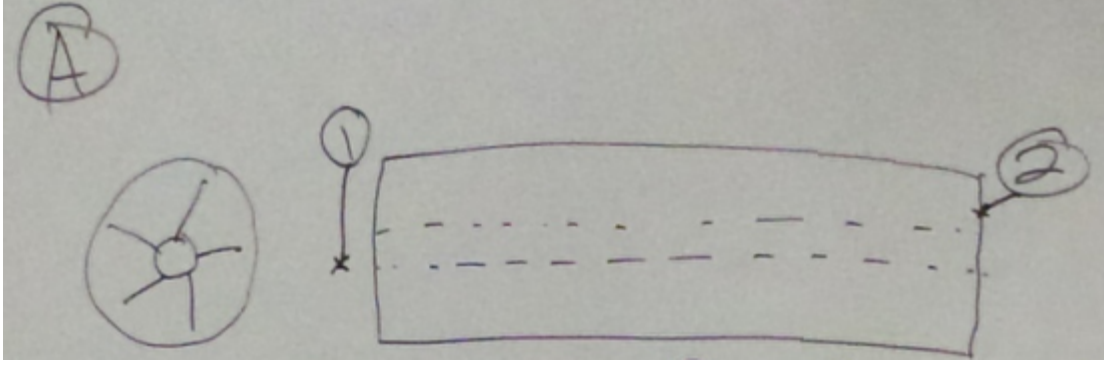


Figure 3.1: Schematic of Control Volume A

$$\cancel{\frac{P_1}{\gamma} + \frac{v_1^2}{2g} + z_1} + h_{L_{1-2}} = \cancel{\frac{P_2}{\gamma} + \frac{v_2^2}{2g} + z_2} + h_{s_{1-2}}$$

0 (gage)

Figure 3.2: Simplified Energy Equation for Control Volume A

As can be seen, the inlet pressure term was set equal to zero, as this was taken to be gage pressure since it is simply the free-stream hydrostatic field pressure. The two elevation terms also cancel, because even if the propulsor was stood up vertically, the change in elevation would only be one to three feet (this length had yet to be determined), which would be negligible; additionally, the vast majority of the time, the vehicle would be travelling at roughly zero angle of attack (and therefore would not have a change in elevation from front to back of the propulsor).

This leaves a few terms remaining; g is simply the gravitational acceleration ($32.2 \frac{ft}{s^2}$), γ is simply the specific weight of the fluid (water; $62.4 \frac{lb}{ft^3}$), v_1 is the inlet velocity (an unknown, as defined earlier), P_2 is the pressure at the end of the vane shell (another unknown, as defined earlier), v_2 is the velocity at the end of the vane shell, $h_{L_{1-2}}$ is the energy loss term from front to back of the vane shell, and $h_{s_{1-2}}$ is the shaft input energy term from front to back of the vane shell.

In order to reduce this equation further to the original two unknown values we wished to solve for, we had to come up with equations for the v_2 , $h_{L_{1-2}}$, and $h_{s_{1-2}}$ terms.

Using the fact that v_2 represents the maximum speed our vane shell could get the fluid moving without slip, we defined the maximum vane shell axial fluid speed to be equal to the angular velocity times the effective screw pitch associated with the vane shell, which is a function of the average radius (average between the base radius, or outside radius of the cylinder onto which the vanes attach and the maximum radius, or the radius to the tips of the vanes) and the angle of twist of the vanes:

$$v_2 = \omega P; p = \frac{2\pi r_{avg}}{\tan(\theta)} \quad (3.3)$$

The next term is the head loss term along the length of the vane shell ($h_{L_{1-2}}$); this term would normally include both major (due to friction) and minor losses (due to components), but since there is not any major bends/corners/etc., the minor losses were neglecting, reducing the head loss term to that of purely major loss.

$$h_{L_{1-2}} = f \frac{L}{D_h} \frac{v^2}{2g} \quad (3.4)$$

The velocity (v) used above would be taken as the average between the free stream velocity (v_1 , an unknown) and the maximum/end of vane shell velocity (v_2) and thus would require iteration in the program. The length of the vane shell (L) would be assumed in the iteration at different values in order to determine the desired unknown values over a range of lengths. The hydraulic diameter (D_h) would be determined for each set of iterations on the basis of assumed vane shell geometry (just like the length), through the formula:

$$D_h = \frac{4A}{P} \quad (3.5)$$

where A is the area of the flow (determined by finding the sum of all inter-vane flow areas, as restrained by vanes on either side of the flow, the rotating cylinder on the bottom of the flow, and the stationary body cylinder on the top of the flow). Lastly, the friction factor (f) was determined as the Darcy-Weisbach friction factor through the use of the Swamee-Jain approximation of the Colebrook-White equation:

$$f = \begin{cases} \frac{64}{Re} & : Re \leq 2000 \text{ Laminar} \\ .25[\log(\frac{\epsilon}{3.7D_h} + \frac{5.74}{Re^{.9}})]^{-2} & : Re > 2000 \text{ Turbulent} \end{cases} \quad (3.6)$$

$$Re = \frac{v_{avg}D_h}{\nu} \quad (3.7)$$

where η is the material roughness, Re is the Reynolds number as defined in equation 3.7, and ν is the kinematic viscosity of the fluid. Lastly, the shaft head ($h_{s_{1-2}}$) was taken as:

$$h_{s_{1-2}} = \frac{T\omega}{\gamma Q} \quad (3.8)$$

where ω is the rotational speed (as defined earlier), γ is the specific weight (as defined earlier), Q is the volumetric flow rate (the product of the average velocity and the flow area, as both defined earlier), and T is the torque. Torque was defined as a fluid torque through its relation to the rotational speed of the screw-like vane shell and the twist of the path of water (more details about this may be found in the appended original Phase I report calculations, appendix A):

$$T = \frac{(r_a v g \omega)^2}{2g} \gamma A \cos(\Phi) (r_a v g) \quad (3.9)$$

With all of these equations developed, it becomes apparent that the original energy equation (after substitution of assumed geometry and iterated angular velocities) has been reduced to two unknowns (v_1 and P_2), albeit in a highly intertwined fashion.

Control Volume B For control volume B , the energy equation was again adopted, this time with the unknowns of P_2 and v_3 .

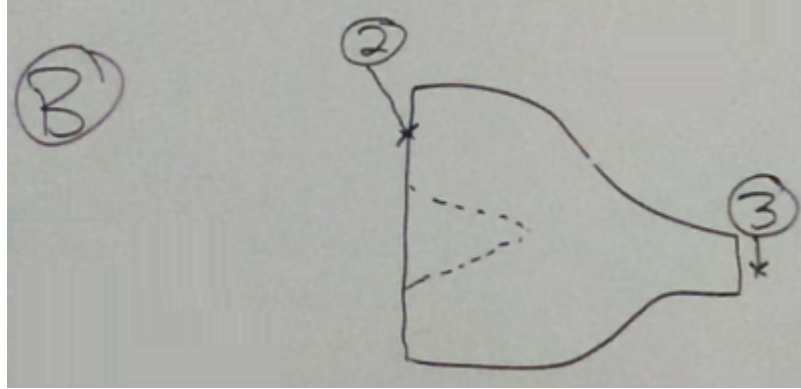


Figure 3.3: Schematic of Control Volume B

$$\frac{P_2}{\gamma} + \frac{v_2^2}{2g} + z_2 + h_{L_{2-3}} = \cancel{\frac{P_3}{\gamma}} + \frac{v_3^2}{2g} + z_3 + h_{s_{2-3}}$$

0 (gage) **0 (no energy input)**

Figure 3.4: Simplified Energy Equation for Control Volume B

Once again, elevations cancel, one pressure (this time the exit pressure) interfaces with the hydrostatic pressure field and is thus set to zero gage pressure, and this time the shaft input energy term is set to zero because we are now beyond the vane shell and only have stationary components. P_2 (an unknown) is defined the same as before, v_2 is the maximum/end of vane shell velocity (as defined earlier), and v_3 (also an unknown) is the free jet exit velocity, as defined earlier. This just leaves the head loss term, which unlike before now contains both major (due to friction and calculated the exact same way as before, except between points 2 & 3, rather than 1 & 2) and minor losses (due to components). The minor losses were modeled through use of the following general minor loss equation:

$$h_{L_{2-3}(\text{minor})} = K \frac{v_{avg}^2}{2g} \quad (3.10)$$

where K is the component loss coefficient, which in this case was taken conservatively as the worst case non-reentrant scenario entrance loss coefficient ($K = 0.5$), although our situation would never come near this scenario.

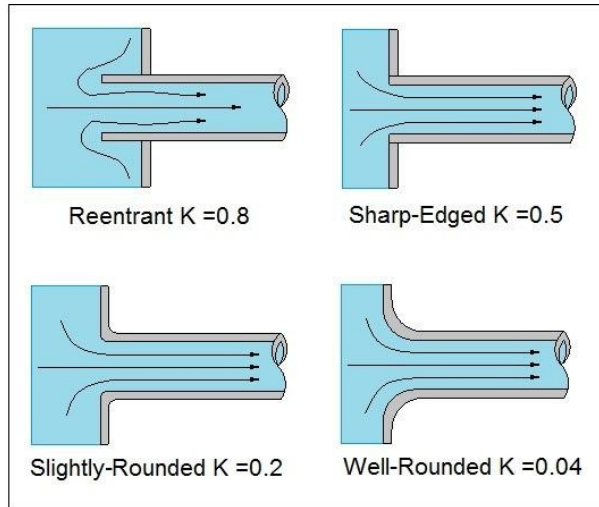


Figure 3.5: K values for Minor Losses due to Diameter Change

With all of these equations developed, it becomes apparent that the original energy equation (after substitution of assumed geometry and iterated angular velocities) has been reduced to two unknowns (v_3 and P_2), albeit in a highly intertwined fashion.

Control Volume C For control volume C , the momentum equation was adopted, with the unknowns of P_2 , v_3 , and the thrust force F_T .

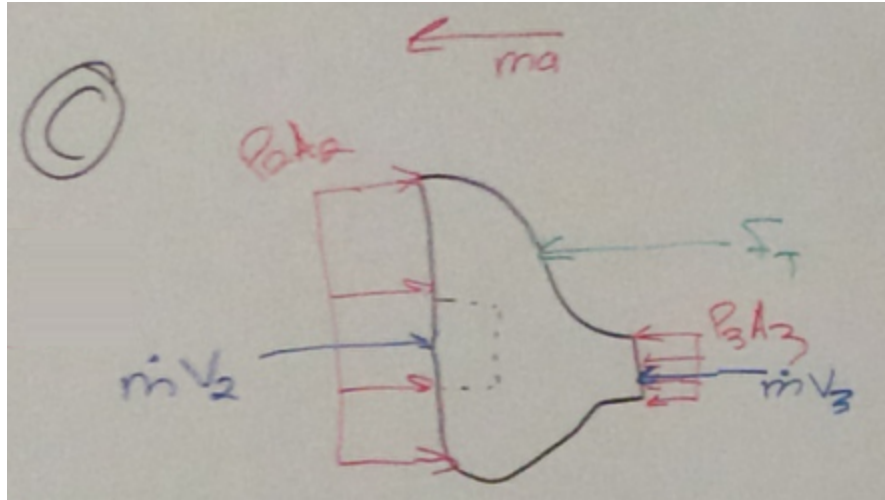


Figure 3.6: Schematic of Control Volume C

$$\Sigma F = P_2 A_2 + \dot{m} v_2 - \cancel{P_2 A_3} - \dot{m} v_3 - F_T + \cancel{F_D} = \cancel{m a}$$

$\cancel{P_2 A_3}$ 0 (gage)
 $\cancel{F_D}$ Assumed 0 (negligible/small section)
 $\cancel{m a}$ 0 (Steady State)

Figure 3.7: Simplified Energy Equation for Control Volume C

P_3 is once again set to zero gage as it is the hydrostatic field pressure, drag force (F_D) is assumed zero for the small nozzle section, and acceleration (a) is taken to be zero due to the assumption that steady state velocity (no acceleration) has been reached. P_2 , v_2 , and v_3 are defined as before and the thrust force (F_T) is one of the desired unknowns. A_2 is the area of the annular flow region between the circular nozzle and the circular pressure hull/start of cone (not pictured). This just leaves the mass flow rate (\dot{m}), which is the product of the average velocity from point 2 to 3, the density of the fluid (water), and the effective flow area as previously discussed.

Once again, with all of these equations developed, it becomes apparent that the original momentum equation (after substitution of assumed geometry and iterated angular velocities) has been reduced to three unknowns (v_3 , P_2 , and F_T).

Control Volume D For control volume D, the momentum equation was adopted, with the unknowns of v_1 , v_3 , and the thrust force F_T .

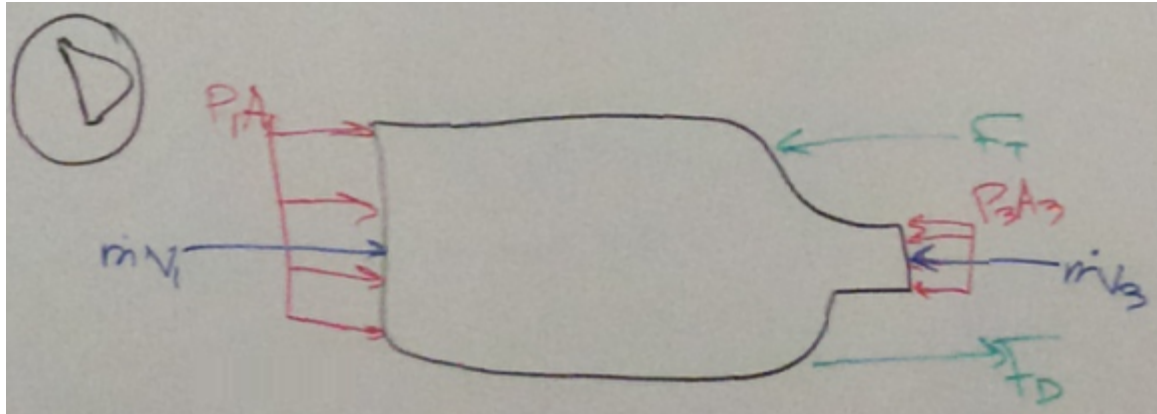


Figure 3.8: Schematic of Control Volume D

$$\sum F = P_1 A_1 + \dot{m} v_1 - P_3 A_3 - \dot{m} v_3 - F_T + F_D = \cancel{\dot{m} a}$$

0 (gage) **0 (gage)** **0 (Steady State)**

Figure 3.9: Simplified Energy Equation for Control Volume D

Just as before, P_1 and P_3 are both taken to be zero gage due to their interfacing with the hydrostatic field pressure and the acceleration is set to zero due to assumed steady state operation; also as seen previously, v_1 , v_3 , and F_T are all desired unknowns and mass flow rate is calculated the same as before, with the average velocity being taken between points 1 and 3. The only new term being introduced here is the drag force (F_D).

The drag force is calculated with the classic algebraic form of the drag force equation:

$$F_D = 0.5 \rho C_D v^2 A \quad (3.11)$$

where ρ is the fluid (water) density, v is the average velocity between points 1 and 3, A is the reference area (in this case taken as the outermost circular cross-sectional area of the body cylinder), and C_D is the drag coefficient, which has been taken conservatively to be 1.2.

One last time, with all of these equations developed, it becomes apparent that the original momentum equation (after substitution of assumed geometry) has been reduced to three unknowns (v_1 , v_3 , and F_T).

Integration of Control Volumes With all of these control volumes and the associated equations, it can be seen that we have developed four equations (the ones boxed in red in the previous sections) as a function of four desired unknowns (v_1 , P_2 , v_3 , F_T). As can be seen the system of four equations is statically determinant with the right assumptions made, but is nonlinear in nature and highly inter-dependent, requiring a very complex computer program to be written in order to integrate the four equations together to solve for the desired unknowns, as will be discussed in the next section. A summary of the desired unknowns for each control volume is provided below.

1. Control Volume A (Energy Equation from 1 to 2): v_1 and P_2
2. Control Volume B (Energy Equation from 2 to 3): P_2 and V_3

3. Control Volume C (Momentum Equation from 2 to 3): P_2, v_3 , and F_T
4. Control Volume D (Momentum Equation from 1 to 3): v_1, v_3 and F_T

MatLab Code

The mathematical model rendered through the above control volume analysis still contained many unknowns. With the above equations the relationship between these unknowns could be determined, however finding the optimal value of each of the 5 geometrical dimensions and the one dynamic variable would have required exhaustive iterations and guess work. To facilitate the design process and ensure optimal design a program was written in the MatLab coding environment that would cycle through ranges of each of these variables, creating every possible combination of designs and rank them on an efficiency. This would allow for the most efficient design to be selected.

The majority of the variables in question described the geometry of the propulsor. To reduce the complexity of the design some variable were designated before the program began. The length of the nozzle was fixed to 5 inches, providing a reference size so that the most efficient design would still have a reasonable package size. The number of vanes was set to 5, in previous iterations of the program a value of 5 vanes commonly populated the highest efficiency and therefore it was set, freeing up processing time for more volatile variables. The outer radius, inner radius, length, angle of the vane helix, and nozzle radius were allowed to vary. Each variable had to have a range to vary within because without a finite range the program would loop infinitely. The maximum outer radius was set to 5 inches, the minimum inner radius was set to 2 inch, length ranged between 18 and 26 inches, the vane angle varied between 42 and 48 degrees, the minimum nozzle radius was .75 inches.

Variable	Minimum Value	Maximum Value
Outer Radius, r_o		5 in
Inner Radius, r_i	2 in	
Length, L	18 in	26 in
Vane Angle, θ	42°	48°
Nozzle Radius r_n	.75 in	
Rotational Velocity ω	220 RPM	320 RPM

Table 3.1: Iteration Ranges for Design Variables

The dynamics of the system also had to be coded into the program. The angular velocity was the only parameter allowed to vary from a low speed of 50 rad/sec to 200 rad/sec. A pump efficiency of .75 was used to account for losses in energy transfer from the vanes to the fluid itself, the surface roughness of PVC was used because it most accurately modeled the material we anticipated the vane shell to be made of. A drag coefficient of 1.2 was used as a conservative estimate, the real drag will be much less because the outer surface will be streamlined.

Variable	Value	Source
Acceleration due to Gravity, g	$32.2 \frac{ft}{s^2}$	[9]
Specific Weight, γ	$62.4 \frac{lb}{ft^3}$	[9]
Kinematic Viscosity, ν	$12.1 \times 10^{-6} \frac{ft^2}{s}$	[9]
Surface Roughness, ϵ	0.0015mm	[9]

Table 3.2: Material Constants for Design

Not every variable needed a range to vary within because certain relationships were established. This allowed for more accurate results while still minimizing the amount of processing time. The minimum

outer radius was limited to be at least .25in greater than the inner radius to allow for a practical vane height. The nozzle maximum value was limited so that the exit area would never exceed the area of the annular region between the inner cylinder and the outer cylinder. This was done to ensure that the the nozzle would be converging and provide increased thrust rather than the diverging nozzle that would slow the fluid and reduce the overall thrust.

With these relationships and ranges established the order of the nested loops needed to be established. The loops were ordered so that the more depended on the variable being changed the farther out of the nest it was placed. This led to the following order: angular velocity, inner radius, outer radius, nozzle radius, length, then vane angle. By nesting the loops in this order all of the relationships between the different range limits could be satisfied and once in the center of the loops one complete set of design variables was established.

In the center of the nested loops two finite difference loops were used to assist in the solving of the mathematical models derived from the control volume analysis. The first finite difference loop calculated the friction factor used to find the losses along the length of the vane shell. The second finite difference loop was used to find the friction factor for the losses through the nozzle. These losses were used with the established design variables to find the overall thrust, the pressure at the end of the vane shell, the speed of the device at steady state, and the speed of the free jet leaving the end of the nozzle.

These results from the fluid analysis were used to determine the efficiency of the device. The energy added to the fluid increased the velocity up to the end of the vane cylinder. A 100% efficient device would move at the speed of the fluid at this point. Essentially a fully efficient device would accelerate until it could no longer add energy to the fluid. This means that the efficiency of the device could be calculated by taking the steady state speed of the device and dividing it by the steady state speed of the fluid after the vane shell. $\eta = \frac{V_1}{V_2}$. These calculations were done for all the possible combinations of design parameters within the given ranges resulting in thousands of possible designs each with their own efficiency.

Excel Narrowing of Results

All of the designs were exported in a comma separated value format to be manipulated in Excel. First all efficiency values less than or equal to zero were removed as poor designs, then each variable was graphed with respect to efficiency. Due to the cyclic nature of the analysis data was plotted as clusters around certain values. Using these plots the clusters of data with low efficiency could be eliminated. Certain geometrical values were limited by realistic manufacturing constraints. This means that very small clearances between the inner radius and outer radius were removed along with excessively small nozzle radii. By narrowing these results in this fashion final design values were arrived upon with a resulting efficiency of between 77.8% and 80.7% for a range of angular velocities. The final geometry was.

Variable	Value
Outer Radius, r_o	4.45in
Inner Radius, r_i	3.2in
Length, L	19.6in
Vane Angle, θ	48°
Nozzle Radius r_n	1.218 in

Table 3.3: Final Geometry for the Propulsor Design

CFD

Computational Fluid Dynamics, or CFD, is a numerical technique for solving the Navier-Stokes equations and mathematical modeling a fluids behavior under specific circumstances. The Navier-Stokes equations do not have an explicit analytical solution but they are commonly used to model ideal cases where certain

simplifying assumptions can be made, such as neglecting viscosity or compressibility. Before these computational techniques complicated fluid analysis was performed using experimentation with models. As designs involved more complicated geometries and fluid reactions such as with a super sonic jet iterative modeling experiments became excessively expensive in both time and money. This, along with the evolution of computers, led to the development of these computational techniques. To understand further look at the Navier-Stokes Equaton:

$$\frac{\partial \vec{V}}{\partial t} + (\vec{V} \cdot \nabla) \vec{V} = \frac{-\nabla P}{\rho} + \nu \nabla^2 \vec{V} \quad (3.12)$$

The $(\vec{V} \cdot \nabla) \vec{V}$ adds non-linearity to the equation while $\nu \nabla^2 \vec{V}$ makes the system second order. These added complexities make the analytical solution of the equations practically impossible. For a numerical solution to be achieved first a numerical grid must be set up. Each node in the grid represents a position in space with an added dimension of time. This is because the dynamics of the fluid depend on the surrounding fluids as well as its position at the previous time. To understand the full dynamics of the fluid in question the whole grid must be solved for every point in time. Computational techniques can only handle addition, subtraction, multiplication, and division, no calculus. This means the equation needs to be transformed into a numerically solvable form. For this the Taylor Series expansion can be used.

The generic Taylor Series is as follows:

$$u(x) = \sum_{n=0}^{\infty} \frac{f^{(n)}(x_i)}{n!} (x - x_i)^n \quad (3.13)$$

Solving the Taylor series for the $f^{(n)}$ term allows for the numerical solving of the differentials in the Navier Stokes equations. If the Taylor Series is solved on the previously discussed numerical grid for a one dimensional flow the following relationship is achieved:

$$\left. \frac{\partial u}{\partial x} \right|_i = \frac{u_{i+1} - u_i}{x_{i+1} - x_i} - \frac{x_{i+1} - x_i}{2!} \left. \frac{\partial^2 u}{\partial x^2} \right|_i - \dots \quad (3.14)$$

If the grid spacing, $(x_{i+1} - x_i)$, is close enough the equation can be truncated with an error of $\frac{x_{i+1} - x_i}{2!} \left. \frac{\partial^2 u}{\partial x^2} \right|_i$. This allows for a simply algebraic solution to a partial derivative and is the function that gives CFD its power.

These solutions still need set boundary conditions, such as velocity or pressure, the properties of the fluid, such as density and viscosity, as well as the properties of the design being tested, most significantly the geometry. Once these characteristics are imputed the program iterates through each point in space, solving the Navier-Stokes equations with the appropriate Taylor substitutions, then it moves to the next point in time and solves again until the designated amount of time has passed. The inputed conditions give the program a place to begin and therefor are an important consideration in the overall solution.

With a good understanding of the basics of CFD the student version of AutoCAD CFD was used along with SolidWorks FlowAnalysis to find the solutions for our specific geometry. To prove our concept with CFD the design was steped through and analysis was done with each added flow component.

Analysis of the Vane Shell Traditional propellors have no ducting around them and this is one of the major things this design improves. As a starting point CFD analysis was done on just the vane shell.

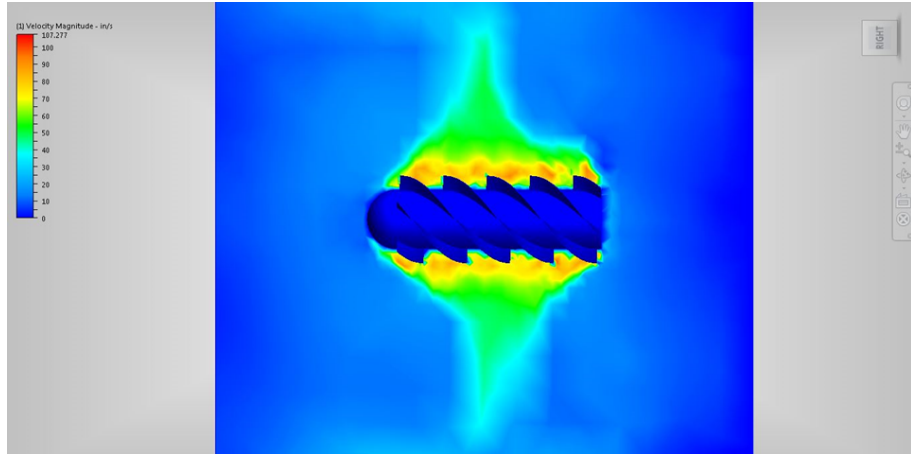


Figure 3.10: CFD Analysis of the Vane Shell

This image shows that much of the energy added to the fluid by the propulsion system is lost by accelerating the fluid radially.

Analysis of the Vane Shell and Body Analysis was run again with the addition of a bounding duct around the vane shell to constrain the fluid so that all acceleration of the fluid will be along the length of the propulsor.

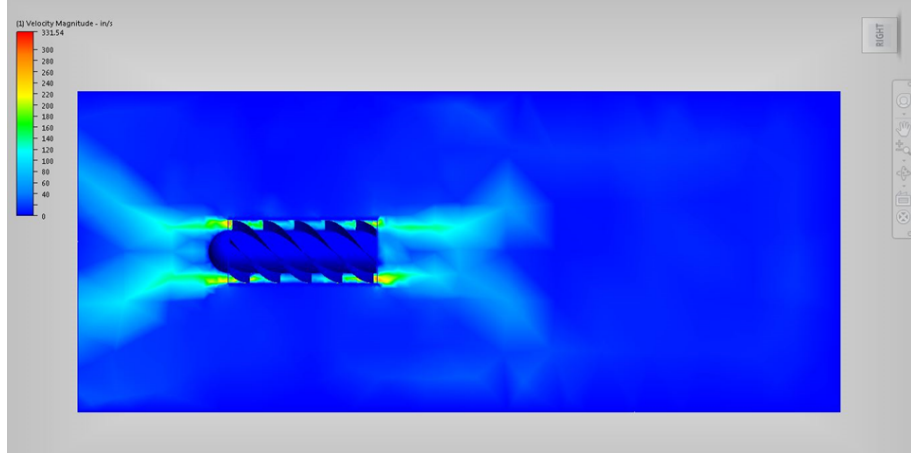


Figure 3.11: CFD Analysis of the Vane Shell with the Body

As this figure shows the fluid is now directed along the length of the device, however at the tail end there is a triangular section of flow recirculation and the flow is not fully constrained and deviates at the rear. This reduces the amount of thrust produced as well as increasing amount of drag acting on the device.

Analysis of the Vane Shell, Body and Nozzle The addition of a nozzle at the end of the device constrains the flow and increases the velocity of the fluid leaving the device increasing the amount of thrust produced due to the conservation of momentum.

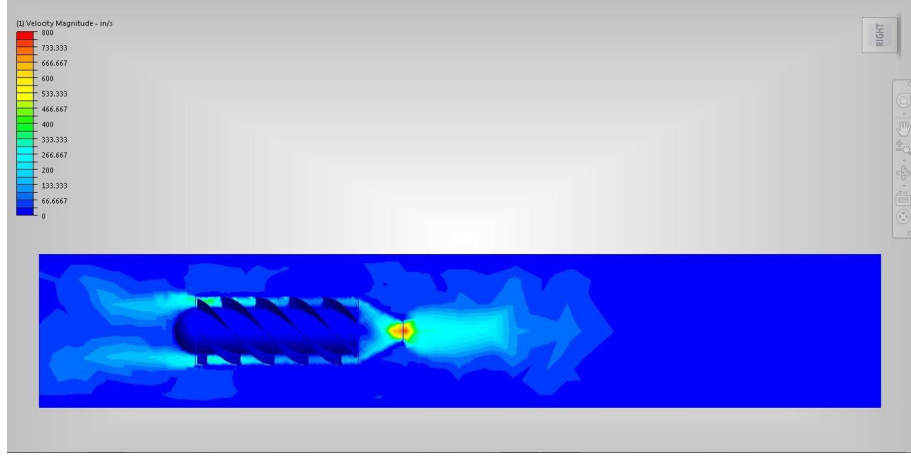


Figure 3.12: CFD Analysis of the Vane Shell and Body with the Nozzle

The CFD analysis shows a maximum velocity right at the nozzle where it would be expected, however there is still a large area of recirculation and low velocity at the end of the vane shell. This reduces the total fluid velocity.

CFD Analysis of the Whole Propulsor Design The addition of the cone completes the propulsor design and removes the area of recirculation behind the vane shell. By removing this section the nozzle steadily converges the flow and increases its speed, sending a jet of high speed fluid out the back of the device.

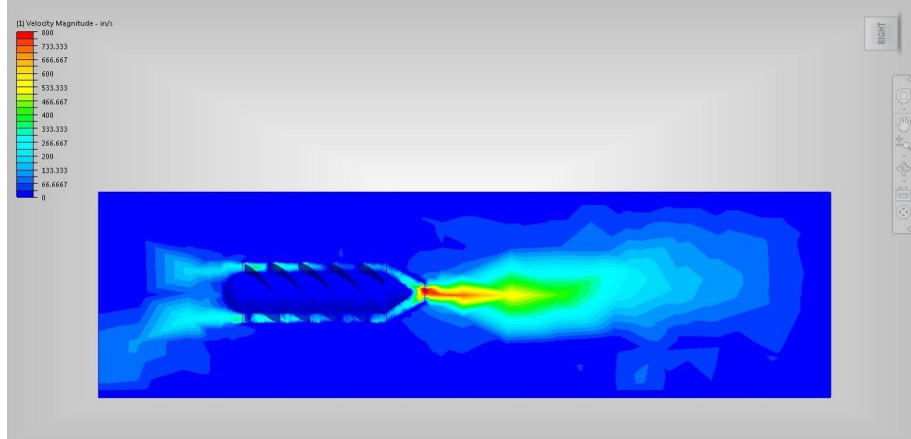


Figure 3.13: CFD Analysis of the Entire Propulsor Design

As seen in the figure the high speed jet of fluid generates the thrust that propels the vehicle through the water.

Manufacturing

The complicated geometry of the vane shell presented a challenge for manufacturing due to our limited resources. Any form of traditional manufacturing via removal of material, such as CNC milling or lathing, presented to high of a cost. Aluminum would be used for these methods due to the development of a protective Aluminum Oxide coat in a corrosive environment as well as the materials ease of manufacturing.

Selective Laser Sintering, SLS, was also considered due to the ease of production for complicated geometries. This method would be expensive, but has a shorter lead time than traditional manufacturing. This process would also produce a metal part. Metal parts would be significantly heavy, which would remove some of the need for permanent balast, however it would add a significant inertial load to the drive train.

Using an ABS 3D printer was also considered. This process had the lowest cost and lead time. There were some concerns about the strength of the part and the fact that it was quite large. Some further analysis was done on the part and was found that the loads would be low enough to be handled by the ABS. The vane shell was broken into six identical pieces so that it would fit within the print volume.

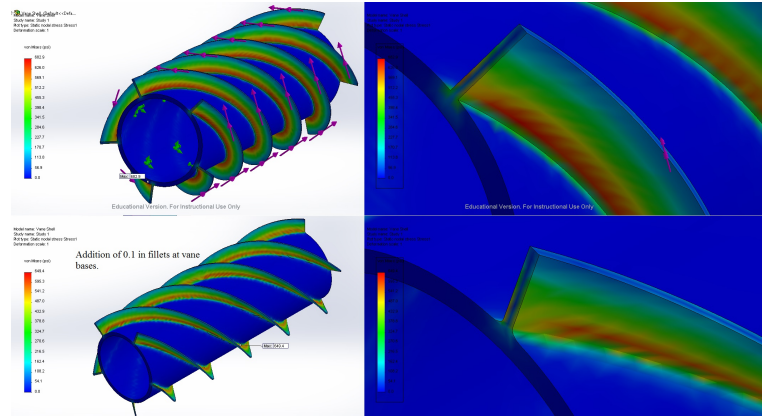


Figure 3.14: Isometric View of the Von Mises Stresses on the Vane Shell

The Cal Poly Chapter of the Southern California Engineering Technologists Association, SCETA, was chosen to manufacture these six sections that comprised the vane shell. Once these parts were received they were linked together using aluminum rods along the length and marine epoxy on the surfaces. This provided a strong bond between each of the six pieces. Once the epoxy had hardened the surfaces were sanded to remove epoxy overspill and printing errors. Then the entire surface was coated with ABS cement to smooth the surface, ensure bonding, and fortify strength.

3.2.2 Body

Initial Considerations

One of the major subsystems highlighted for improvement in Phase III of the project was the body. In Phase I the body was really not a subsystem at all, but rather a section of 8 HVAC ducting that only serves to position the vane shell and constrain the flow through it. For a vehicle that was to be stealthy, maneuverable, and capable of higher speeds, this clearly would not suffice and so a new streamlined body was to be a major focus of Phase III.

From the beginning of the project (even in the ideation and concept development that took place about four years prior to the start of Phase I), the vehicle was always a major focus and was meant to be advanced both scientifically and aesthetically; however, simple streamlining was far from the only goal for the body. In fact, the body really has a whole list of vital parameters pertaining to its design, a short sampling of which is included below:

- Streamlining for better performance
 - Ease of manufacture
 - Choice of materials
- Ease of manufacture (repeated)

Cost of manufacture

Effect on the flow

Structural support (supports all other subsystems of the vehicle)

Weight (ease of transportation as well as buoyancy considerations)

- Incorporation of flow control measures
- Incorporation of stability measures
- Stowage area/volume constraints
- Permanent ballast (for decreasing buoyancy)
- Free flood space (for decreasing buoyancy)
- Thermal/magnetic/acoustic shielding

and the list goes on. With regards to the actual shape of the vehicle as it related to streamlining, the original shape was purely influenced by a sense of biomimicry in that it was always meant to look like some sort of fish; this was for two main reasons:

1. Fish have been already optimized through natural selection and so rather than starting from nothing, it would cut down on work and improve the caliber of the final design significantly if the vehicle were to be designed within the framework of a biomimetic solution.
2. As has been documented previously in this report, one of the mission objectives is to produce a design that exudes stealth, at least in part with regards to inconspicuousness. This design intent can be seen below both in the conceptual hand drawing that was produced near the end of Phase I and in the SolidWorks Future Vehicle Concept model below that was developed at the same time.

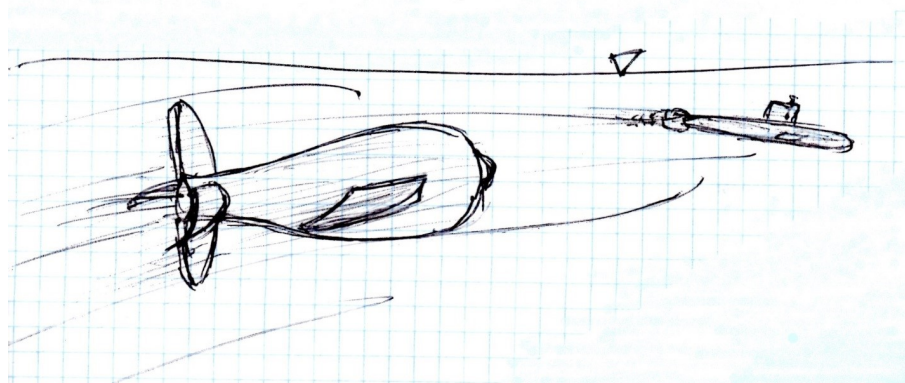


Figure 3.15: Conceptual Hand Drawing

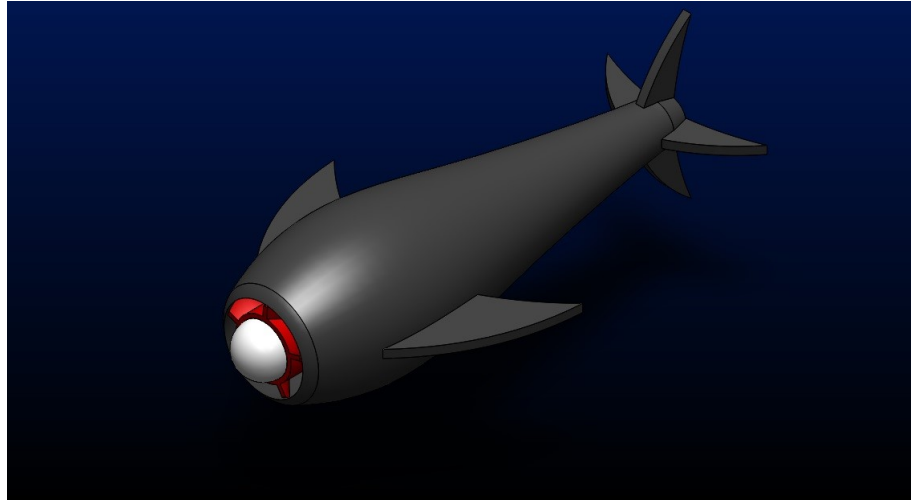


Figure 3.16: A Possible Future Vehicle Design

The next step that followed in the design process after this ideation phase was the general practicality parameters. This essentially began with an overall estimated desired size for the vehicle, which was set to be roughly the size of a scuba tank as this was seen as a size that would allow for all of the components to be fit into the body while still keeping the vehicle relatively portable.

Following this the next step was to start nailing down the manufacturing process, as the part would obviously need to be custom made and this introduced a large deal of complexity to the project, while also augmenting projected costs and imposing more stringent cost constraints. As a first approximation to the build solution, additive manufacturing and CNC quotes were sought purely to get an idea of what it would cost to have it made professionally (rather than by the team), as having it made professionally would significantly decrease manufacturing time and help to produce a much more polished solution; additionally, this would serve as a jumping off point with regards to both developing an idea of how much it would take for the team to make it ourselves and to how high we should set our fundraising goal, as will be discussed later. After receiving quotes for everything from aluminum CNC to injection molding to polyurethane casting, it was found that a professional build would cost anywhere from \$4k to \$10k; obviously this was completely unrealistic, but it served to shine some light on what kind of manufacturing processes the team should look at as well as the materials associated with the processes.

General Body Shape

Following this, a few different body styles were created in SolidWorks as conceptual studies to inter-relate location and size of propulsor, control surfaces, pressure hull, sensor suite, and buoyancy control. A few sample designs can be seen below.

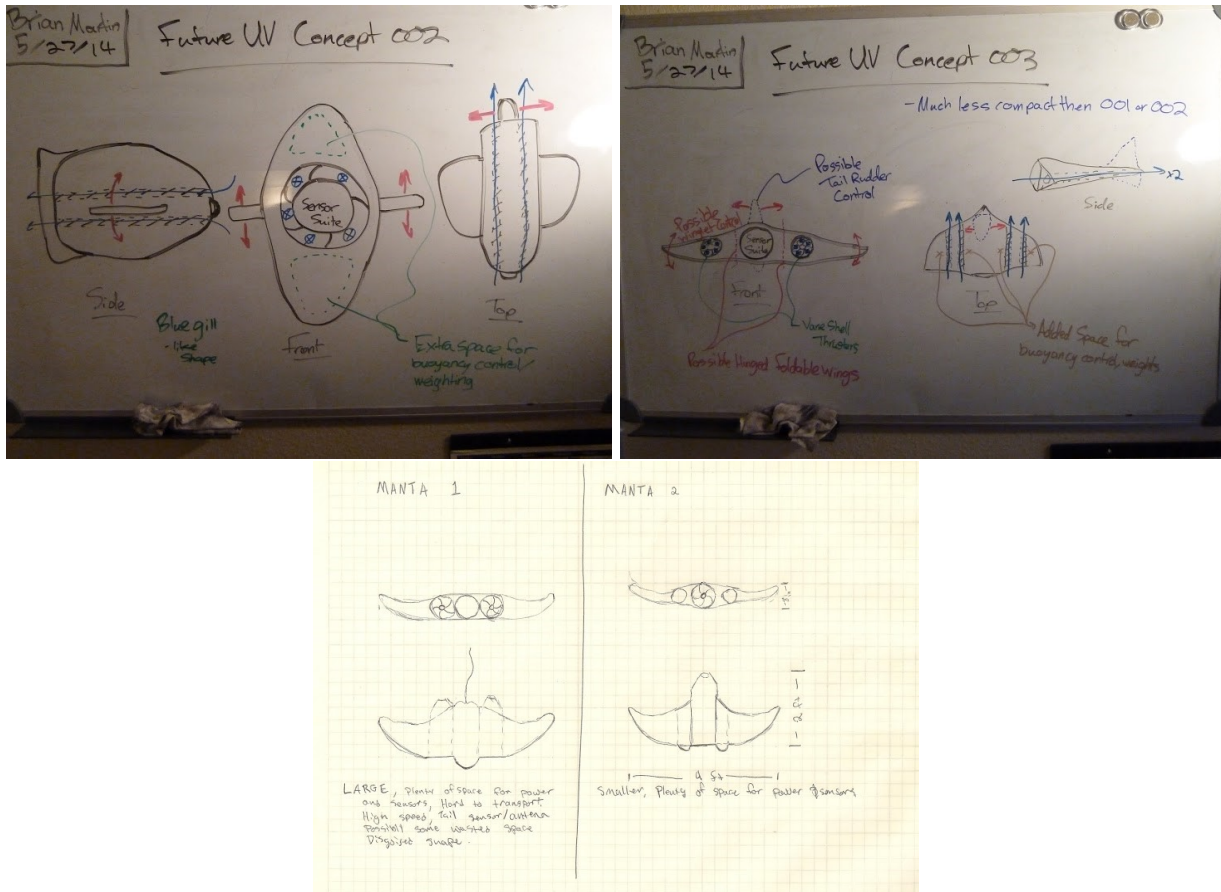


Figure 3.17: Possible Body Shapes for Future Design

Eventually it was decided that it was best to stick to the original design due to the stability, associated external hydrodynamics, internal stowage capabilities, and overall maneuverability (rising and falling movement is strongly influenced by the buoyancy control and thus is less of a concern, but movement in the horizontal plane is dependent more on the control surfaces, therefore if the vehicle is excessively tall, wide, or has a less than optimal slenderness ratio, rolling and yawing can become inhibited).

Solid Modeling and Computational Fluid Dynamics (CFD)

At this point the SolidWorks model of the entire assembly was coming together and so as the assembly became more complete, the body had to be adjusted repeatedly in order to get all of internal components to fit within the body while also keeping the vehicle relatively slender and tight against the internal components as excess volume would mean more positive buoyancy that would need to be combated using more permanent ballast and/or free flood space as well as a negative influence on vehicle maneuverability. This process of sizing was repeated multiple times over the months leading up to (and into) the start of manufacture.

With the body shape and size essentially set, CFD studies were performed to validate the hydrodynamic integrity of the design. Initially this led to more redesign due to issues such as recirculation regions, possible flow separation/reattachment, and other turbulent phenomenon. Eventually the body got to the point of showing promising streamlining as shown in the below CFD image.

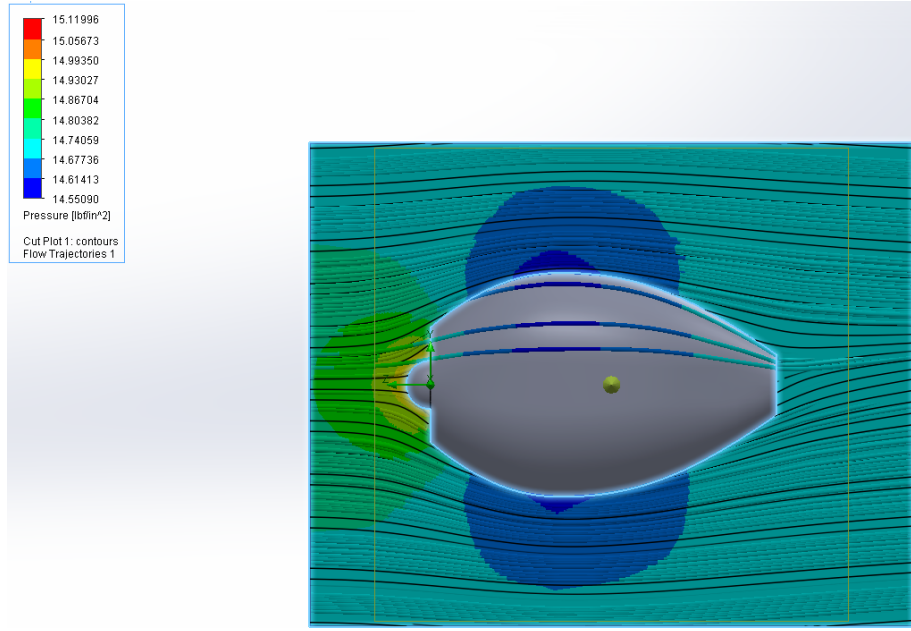


Figure 3.18: CFD Analysis of the Body

An interesting note to make is that the position of the dome forward from the body actually has a significant effect on the flow in that a stagnation point exists at the tip of the dome providing higher pressure for enhanced fluid acceleration into the inlet, helping to overcome initial chop created by the vane leading edges.

Materials & Manufacturing

With the final design completed and the manufacturing period fast approaching, a body mold had to be created and materials had to be selected.

For the body mold, the body solid model had to be re-created in SolidWorks using a multi-level loft. Next the actual cross sections of the loft were printed out to full scale and then used to make cardboard cross section cutouts which were then inserted into a large foam block at regular precisely sized intervals corresponding to the lofting in the solid model. Next a maximum height profile was also printed out and used to cut a cardboard piece that was mounted to the side of the foam. Next this max height profile was used to remove large chunks of material from the foam block, yielding the proper axial curvature.



Figure 3.19: Creating the Foam Mold for the Body

Now the max heights profile cardboard was removed and the cross sectional rounds were used to further whittle down the body foam using a combination of a hot wire cutter, bone saw, and bread knife. This process was extremely time consuming and consisted of one member slowly shaping the body and checking streamlining by eye for about six hours straight until the original visualization of the body was recreated.



Figure 3.20: Final Mold Ready for Body Creation

At this point the body mold was wrapped in wax paper pieced together with duct tape in order to keep any molding material from sticking to the foam. Now that the body mold was built, it was time to move on to the material for the body itself.

Originally carbon fiber had been looked at due to structural, moisture, and aesthetic properties, but due to price point, the team moved on to considering other materials. Eventually the team looked into casting materials and found a Smooth-On Smooth Cast 385 mineral filled polyurethane casting material. This specific casting material was selected based on its strength, moisture properties, curing time, impact resistance, ability to be colored, and viscosity (if it was not viscous enough, it could drip during the casting process). In order to deal further with possible viscosity complications, it was decided that the body mold would be made out of cardboard and Styrofoam and that we might design in ridge-like bulkheads to confine dripping material to quadrants.

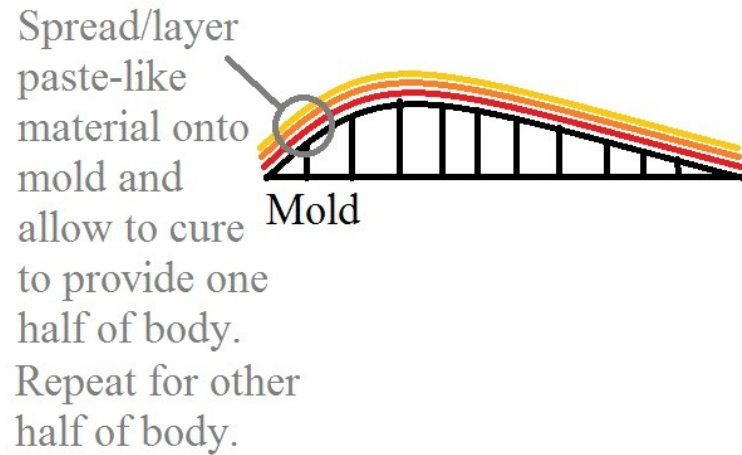


Figure 3.21: The Body Manufacturing Process

Upon receiving and testing the material, it became clear that the material was much more brittle than we thought and that it would require at least 0.5 in wall thickness to toughen up the material, but even then there was major concern for when we drilled into the body (poor machinability due to the brittleness)

to mount servos for the control surfaces as well as for how we would fix the two halves together (original idea was to drill in some sort of hinge).

To remedy this we tried to reinforce the material with cut up strips of old t-shirts, which actually worked pretty well; however, there was still concern about maintaining even thickness and because it took a long time for it to cure, there was a chance we could invest a lot of time and still end up with something that didn't work. So we decided to move on to using heat moldable ABS sheets.

First off, we ran to the local hardware store and bought pipe end caps made out of ABS both 1/8 in and 1/4 in thick and conducted informal impact testing with a sledge hammer to see the difference between the ABS and the casting material; the casting material shattered with hardly any impact, but the ABS took whatever impact was thrown at it even literally when we conducted throw-against-the-wall-really-hard impact testing of both materials. Additionally, we tried to heat form them using 1500W heat guns and quenching them in place with water. This system worked relatively well and so we went ahead and bought 2 large panels of ABS that could be used from each side of the body; unfortunately, when the material showed up it was actually $\frac{1}{4}$ in thick, but we did not have time to re-order the material and thus went ahead trying to form it to our mold. First we tried with two handheld 1500W heat guns but found that we were losing heat to the environment at too rapid of a rate, so we built a tin-foil lined cardboard and plywood enclosure with two holes for the heat guns at the top.



Figure 3.22: First Attempt at an ABS Forming Box

This worked well for about 10 minutes and was partially deforming the ABS, but the heat gun nozzles began to melt (they were poor quality bought from Harbor Freight for about \$15). The ABS had already partially formed though, so we removed the heat guns and ducted the heating element of a propane patio heater into the makeshift oven.



Figure 3.23: Second Attempt at an ABS Forming Box

This only worked for about 5 minutes as the heat was greater and the duct tape all melted; as a last ditch effort we tried using butane blow torch for localized deforming, but due to the thickness and large size as compared to the small flame, the ABS began to vaporize and the ABS sheet could not deform on a large scale.

At this point, a family member of the team informed us that he could get fiberglass for relatively cheap and so we decided to go back to the original idea of using composites. Prior to using the fiberglass, the body mold was wrapped in a few layers of duct tape since the fiberglass resin reaction is exothermic and we did not want to risk the body mold melting. Over the next few weeks we worked on building up the fiberglass and adding resin then sanding back in order to get the body nice and smooth with plenty of structural integrity at about a 0.5 in sidewall.



Figure 3.24: The Fiberglass Body

The next step was to integrate the propulsor subassembly into the body at which point we first cut a lid out of the top of the body and took a long time to center the drawn holes and then drilled the 8 entrance hole and 2.25 exit hole and seated the body cylinder into the front hole and the axial gap between the nozzle and the aft body hole was bridged with a straight aft extension coupler. Before everything was

locked into place, the body mold was reused by cutting it down significantly and using it to support the weight of the body cylinder/propulsor subassembly. This worked perfect for this purpose since it already conformed to the shape of the body. Once the foam was cut to the right height, a cavity was cut out of the foam to house the batteries and a cardboard door was added to protect the waterproofing of the batteries from getting snagged on metal. Lastly all of the foam and cardboard was wrapped with duct tape to keep it from getting damaged in the case of a leak.



Figure 3.25: Batteries Seated in the Fiberglass Body

This foam support was then locked into place with silicone form-a-gasket and then used fiberglass, marine epoxy, and silicone caulking to seal the body cylinder, nozzle, and straight aft extension coupler into place on the body.

The next step was then to carefully over a long period of time align all of the servo mounts, servos, and control surface hardware into their appropriate places of the body and then drill tight fitting holes in the body to mount up the control surfaces using fasteners and marine epoxy. Lastly, a hole was drilled at the base of the body to route the buoyancy control to a lower section of the body using polyurethane hosing since while surfaced, the body would not be able to pull in water from above the waterline; this hole was also epoxied around.



Figure 3.26: The Final Body

Once ready for testing, the permanent ballast will be configured by setting the vehicle in the water and continually adding weight until neutral buoyancy is reached and the buoyancy control system is capable of bringing the vehicle up and down in the water column.

The last step was to spray paint the body black to lower its observable visual signature and then, after some testing, to apply the superhydrophobic coating to observe its effect on drag reduction.

3.2.3 Control Surfaces

Hydrofoil/Airfoil Design

The purpose of including control surfaces into the vehicle design was to add maneuverability. They would ultimately control roll, pitch, and yaw for the vehicle by a combination of biomimetic pectoral fins and tail fin. Initially, the team designed an original foil shape, as seen in Figure 1. This design was arbitrary as it only served as an example to run CFD analysis, however, the pressure distribution at the leading edge would cause excessive drag as it was too bulbous. It was decided to use a hydrofoil/airfoil found in a UIUC Airfoil Coordinate Database as CFD results for lift force and torque the vehicle would experience were more reliable also seen in the figure.

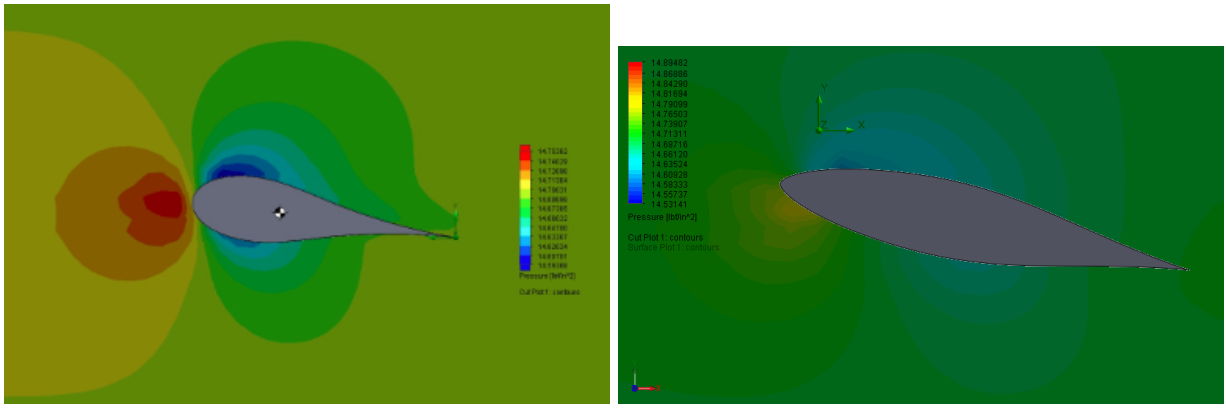


Figure 3.27: (LEFT) Original team designed airfoil, (RIGHT) UIUC airfoil.

The control surfaces were designed using a symmetric foil as opposed to a cambered geometry that most airplanes use. The reason for this was to not create lift fluid forces when the angle of attack is at 0°

relative to the axis of propulsion of the UV. Also, the control surfaces would be operating at lower angles of attack (up to about $\pm 12^\circ$) both symmetric and cambered airfoils would produce near identical amounts of lift. With this design criteria in mind the vehicle would be able cruise at a certain plane of depth without moving vertically. The EPPLER E838 HYDROFOIL AIRFOIL (e838-il), seen in the below Figure, was chosen for the design of the two pectoral fins and the tail fin and their angle of attack would be controlled by revolute servos. Servos were chosen over stepper motors because of the accurate feedback on position that servos provide.

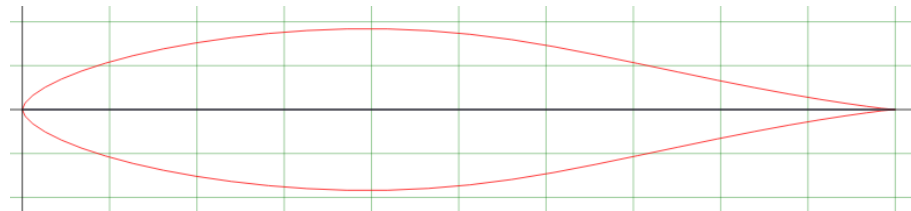


Figure 3.28: EPPLER E838 HYDROFOIL AIRFOIL (e838-il)
Courtesy of: <http://airfoiltools.com>

Design of Control Surfaces

Originally, the control surfaces were designed to have moveable flaps via a rotary shaft driver assembly, as seen in the following two figures, which would only control the trailing edge much like the design of ailerons on airplanes.

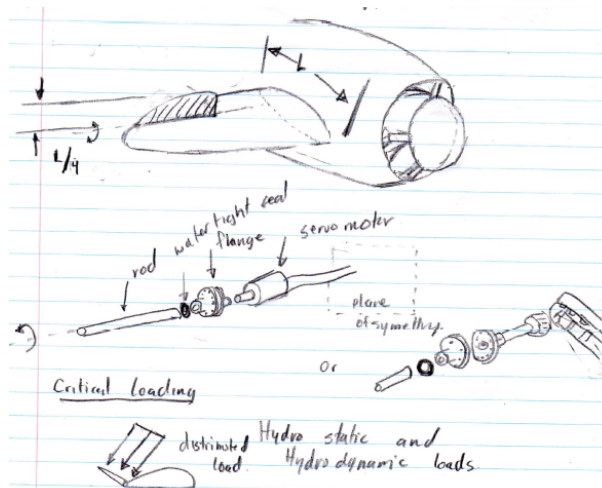


Figure 3.29: Original Control Surfaces Idea with Flaps

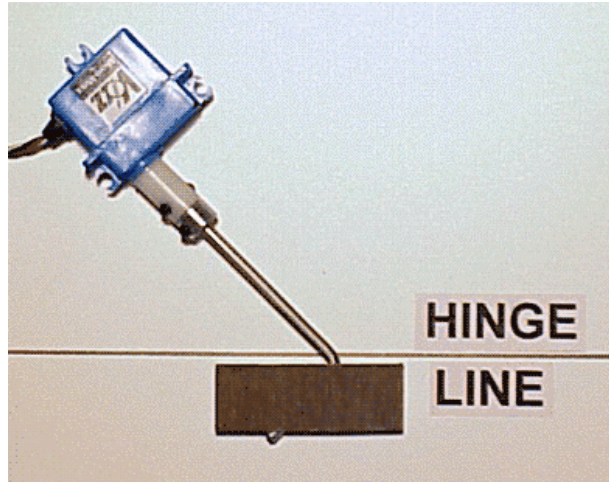


Figure 3.30: Rotary Shaft Driver Idea Design
courtesy of: <http://www.irfmachineworks.com>

However this design was abandoned as it would put high torque loads on the flaps themselves which would increase the cost of the servos as they would have been larger and rated for a much higher holding torque. It was later decided that the entire control surface would revolve around the axis of rotation of the servo and through the, as seen in the following figure, center of mass of the control surface and an angled driver shaft would transfer torque.

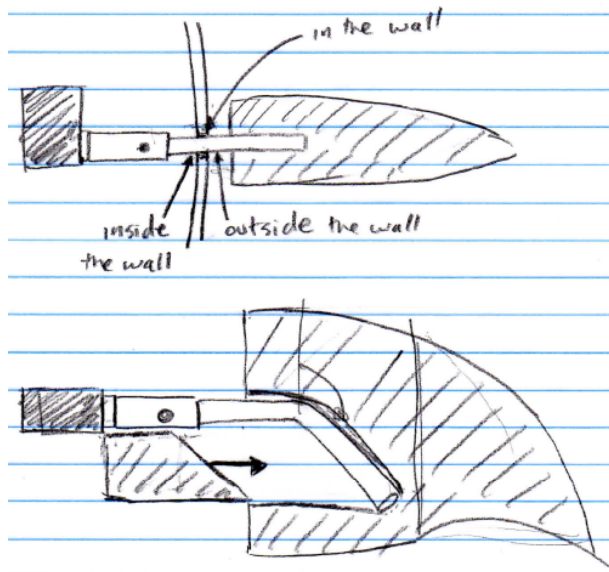


Figure 3.31: Torque Transfer for Control Surfaces

This would theoretically cancel out most reactant torque couples that the control surface would experience from incoming flow of water, making the design holding torque for the servos much lower than originally planned. Generic High Torque Servos (rated at about 5.2 lb-in of maximum deliverable torque) were chosen to control the surfaces. The shape of the control surfaces was biomimetic in terms of geometry as it tapered away from the body, was curved at both the leading and trailing edge, and ended at point almost

resembling a sharks pectoral fin as seen in the following figure. They would be 3D printed in ABS, for its corrosion resistance and high fracture toughness, in two parts and marine epoxied together and coated with ABS cement to strengthen and fill in voids and discontinuities that may have occurred in manufacturing.



Figure 3.32: 3D Printed Pectoral Fin Control Surface

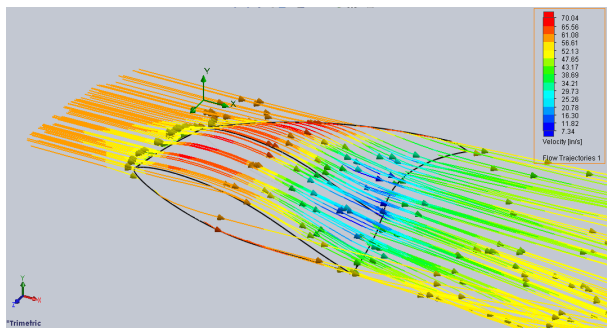


Figure 3.33: CFD of pectoral fin with surface plot of flow trajectories.

The tail fin (rudder) was designed using the same foil as mentioned above but larger and angled near the base to avoid seizing with the body of the vehicle upon changing angles of attack. Unfortunately due time and size constraints in 3D printing, the design could not be manufactured the same way as the pectoral fins. Instead, the geometry was cut out from three sheets of $\frac{1}{4}$ ABS and fastened together using threaded screws as seen in the following figure. Then it was coated with ABS Cement to increase smoothness and fill voids and discontinuities.



Figure 3.34: Rudder shape cut out on paper positioned on sheet of ABS

Control Surface Assembly

For the pectoral control surfaces, servos were fastened onto 3D printed ABS mounts, as seen in Figure 9, which would mate with to the outer surface of the body cylinder. Marine epoxy would be used to fix the mounts at the theoretical center of mass of the vehicle, perpendicular to the vertical line of symmetry, on both sides of the vehicle.



Figure 3.35: 3D printed ABS servo mounts

The rudder however would have the servo epoxied directly to the straight aft extension coupler as time constraints did not allow for a 3D printed mount like the pectoral fins. The angled shaft was made of precision ground 0.25 inch 6061 aluminum rod mainly due to the oxide layer that would form when the rod was submerged, allowing it to passivate and not corrode any further. The shafts would mate to the servos spline via a shaft coupler made of 316 stainless steel. A 0.25 inch steel ball bearing was added to the assembly to react to any misalignment or deflections that shaft might experience in positioning and/or operation to avoid applying that load to the body entirely. A graphite-reinforced, spring loaded, corrosion resistant PTFE shaft seal was used to seal out water due to its high corrosion resistance and high maximum pressure

resistance (250 psi) for slow rotary motion of the control surfaces. The maximum amount of operational hydrostatic pressure the seal would experience would roughly be around 30 psi but the dynamic load was still unknown during the design phase so a 250 psi rated shaft seal was the best choice for the price allowing for a high factor of safety to account for the unknown maximum pressure. The shaft seal and ball bearing were set into a 3D printed cylindrical mount that would be epoxied to a bore in the wall of the body of the vehicle.

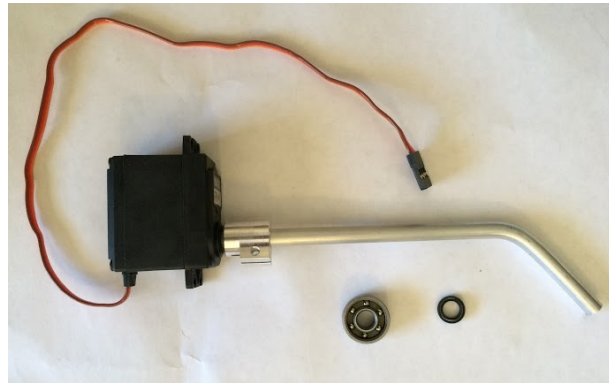


Figure 3.36: Control surface assembly: servo, shaft, ball bearing, and shaft seal.

Further Development of the Control Surfaces

The final size of the control surfaces were about 30% smaller than originally desired. This was due the size of the control surface being incorrectly dimensioned for the size of the propulsor, not the overall length of the vehicle which includes the straight aft extension coupler and nozzle.

3.2.4 Buoyancy Control

The underwater vehicle was designed to be neutrally buoyant. Therefore the need of a device to control the device to dive deeper into the water or rise to the surface was important. Buoyancy force is determined by the following equation $F_b = \rho g V$. Since the density of the water does not change significantly with respect to depth the team decided to change the density of the device itself by changing its mass by using a piston ballast tank. The piston ballast tank is made by the company Alexander Kengel KD located in Germany. Components of the ballast assembly are the following: 12V motor, threaded rod with piston, gear reduction system of 15:1, hollow metal cylinder, and limit switches. The main function of the ballast tank is to intake and expel water to control the buoyancy of the underwater vehicle. Voltage is run through the motor that is connected to the gear reduction system. The gear reduction system is attached to the threaded rod and with rotational power given from the motor displacement of the threaded rod occurs to expel or intake water. A figure of the device is seen below. The ballast tank itself can intake up to 30.5 cubic inches with an overall length of thirteen inches. When the correct voltage is applied the tank can go from full stroke to no stroke in eleven seconds. Limit switches (white components seen in the figure above) are used to determine the position of the threaded rod and piston assembly. One limit switch will indicate that the piston is located at the halfway point. The other limit switch is to indicate the piston has been fully retracted and shuts off power to the motor to ensure no damage to the ballast tank occurs. The piston ballast tank is suitable up to a depth of 34 feet. This piston ballast tank assembly is connected to the brains of the device to submerge the underwater vehicle where depth can be measured by the accelerometer. Once depth is achieved the vehicle will be able to run its mission. The dimensions of the ballast tank can be seen in the figure below. Dimensions noted in figure are in millimeters.



Figure 3.37: Overview of the Buoyancy Control Device

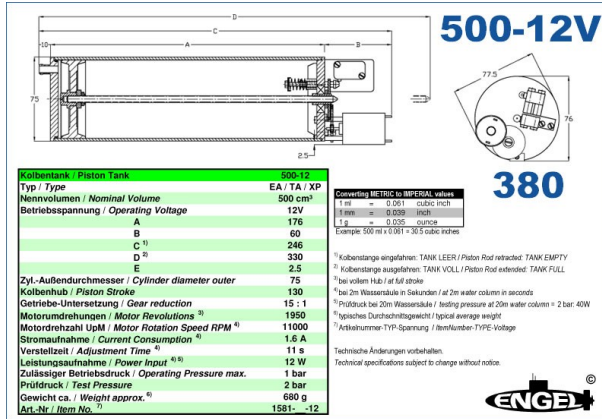


Figure 3.38: Details of the Buoyancy Control Device

3.2.5 Pressure Hull

Drawing from the concept found in SHEILA-D, the pressure hull is used to house vital components that power the project. Located at the center of the vehicle, within the vane shell, the pressure hull was designed to satisfy numerous challenges associated with underwater operation. After seeing how vulnerable SHEILA-D was to flooding, we knew that limiting entry points and creating obstacles for any water that may leak in was of top priority. Our new design of powering the vane shell through a shaft located at the rear of the pressure hull eliminated the need to cut holes into the PVC pipe to transmit power. This left the two pipe openings at either end and any holes needed to pass communication and power wires to external actuators.

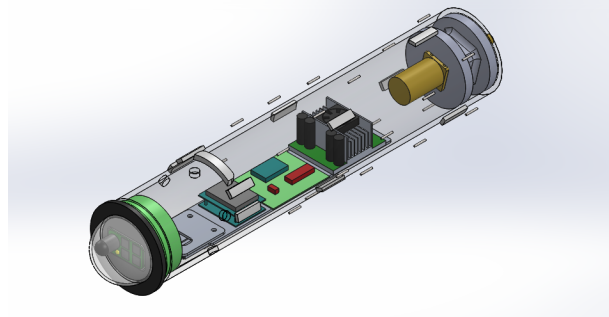


Figure 3.39: The Pressure Hull Design

The front of the pressure hull was slightly redesigned to allow for better sealing and the integration of a smaller, micro-controlled camera. A dome was ordered off the shell and mated to a PVC end cap using marine epoxy and then covered in ABS cement for good sealing measure. To allow for easy access to the camera, a custom hinged door was then fabricated onto the back of the domed front cap. Upon ending a session and removing the cap, the SD card containing video footage could be easily ejected without hassle. The front cap can then be slipped on and sealed with silicone for non-permanent but water proof sealing.



Figure 3.40: (LEFT) Dome Front Cap fixed to the pressure hull. (RIGHT) Inside Cap Camera Door

Five holes were cut at the front of the pressure hull, along the circumference, to do two things: run wire to external electronics found within the body and rigidly connect the body to the pressure hull. The holes were mated to a matching set found on the body cylinder and the two sets were then connected by aluminum standoffs. Wires from the logic command center could then be routed to the control surface servos, buoyancy control subsystem, and battery bank safely avoiding contact with water and the rotating vane shell. The main purpose for the standoffs was to address the torque transfer issues from Phase 1. We noticed that when rotating the vane shell in SHEILA-D, the torque transmitted to the vane shell would also cause the pressure hull to rotate relative to the body cylinder. Rigidly connecting the body and pressure hull cylinders would keep them oriented properly and allow for full energy transfer to the vane shell. Locking the body and pressure cylinders relative motion also keeps our wiring safe from being pulled in any one direction which could disconnect important navigational actuators or tear the wires completely.



Figure 3.41: Wire standoffs before being trimmed of excess material.

The middle of the pressure hull is the home of Dorys logic command center which includes an Arduino Uno, IMU, SD card breakout board, and Sabertooth motor controller. The electronics sit atop a hand-fabricated, aluminum slider tray aimed at high accessibility. The tray is a two-piece assembly made out of C channels and flat plate aluminum stock with the track permanently fixed to the bottom of the pressure hull with marine epoxy. Aluminum was chosen here to wick heat away from the electronics under heavy usage. The tray is easily slid on and off the track to gain access to the logic command center between running sessions and when data is to be collected. The tray is able to be removed 2 feet from the body fully wired and can be completely removed in a few steps. The detachable tray is locked in place by rubber stoppers in the back and pressed in from the front by the front dome cap. A fixed position was crucial in ensuring that the logic command center doesn't slide around freely during underwater sessions as any unwanted movement in the tray can lead to disturbances in the IMU readings or even damage to electronics themselves. The slider tray was then completed by the addition of a rubberized, aluminum handle which was fixed rivets. The handle was incorporated to easily pull the tray out for data collection and protect the users in the case of electrical shock.



Figure 3.42: (LEFT) Top view of slider tray. (RIGHT) Logic Command Center on slider tray. Note riveted handle.

The rear of the pressure hull houses the driving motor for the vane shell and the motor mounts. The motor mounts were designed to completely fill the inner circular area of the pipe. Two mounts were 3D printed to support the motor and gearbox at two points with an annular open region between the two. The motor mounts also would act as bulkhead as seen in many water or air based vehicles. Bulkheads are walls that separate regions of a hull to minimize overall damage in the event of an accident. In our application the bulkheads are used to block water from reaching the electronics package from the rear of the vehicle. Water will have to reach the rear of the pressure hull by first going through the vane shell, vane shell coupler, and motor shaft seal, before reaching the bulkheads. In the event that water gets through the first bulkhead, the

second bulkhead will help contain the water. The motor mounts are fixed to the vane shell by marine epoxy and sealed with silicone.

To complete the package, the outer surface of the pressure hull is lined with three sets of plastic strips epoxied in place. These strips are used to both space out the vane shell and provide a low friction surface for the vane shell to ride on. Another strip of plastic is placed on the pressure hull which mates to the front of the vane shell to act as a thrust bearing, relieving some of the thrust load on the motor.

3.2.6 Drive Train

The drive train in the assembly converts the electrical supply from the batteries into rotation motion for the vane shell. The Banebots RS-550 Motor provides 70.55oz-in (4.41 lbf-in) of torque and when coupled with the Banebots P60 Gearbox gearbox provides 4515.2oz-in (282.2 lbf-in) of torque to be transferred to the vane shell. The reason for designing the vehicle with such high torque was to ensure that any resistance to rotation, whether due to traction or due to inefficiencies from manufacturing, would be overcome.



Figure 3.43: Banebots P60 Gearbox. Courtesy of: robotshop.com

3D printed ABS mounts were used to concentrically fix the motor and gearbox to the pressure hull. The mounts served as bulk heads to seal water out of the pressure hull section that contained vital electronics. A Stretch-Fit Rotary-Shaft Seal was also used in conjunction with marine grease to seal water from getting into the gearbox as seen in the following figure. A 3D printed ABS flange coupler was mated and epoxied to the gearbox shaft and to the vane shells inner diameter to transfer torque to the vane shell. The design of the torque transfer assembly used epoxy intentionally to create a semi-rigid connection rather than a rigid connection. If the vane shell were to seize during operation, the epoxy bond would be the first to fail rather than the motor or vane shell which are both costly to repair and replace.



Figure 3.44: Gearbox mounted to pressure hull and shaft seal attached to gearbox shaft.

The end of the shaft would rest and freely rotate inside the cone which would be rigidly fixed to the body cylinder. This would allow for support of the aft side of the pressure hull and to prevent erosion of the cone with a Lubrication-free Acetal Ball Bearing as seen in the following figure.

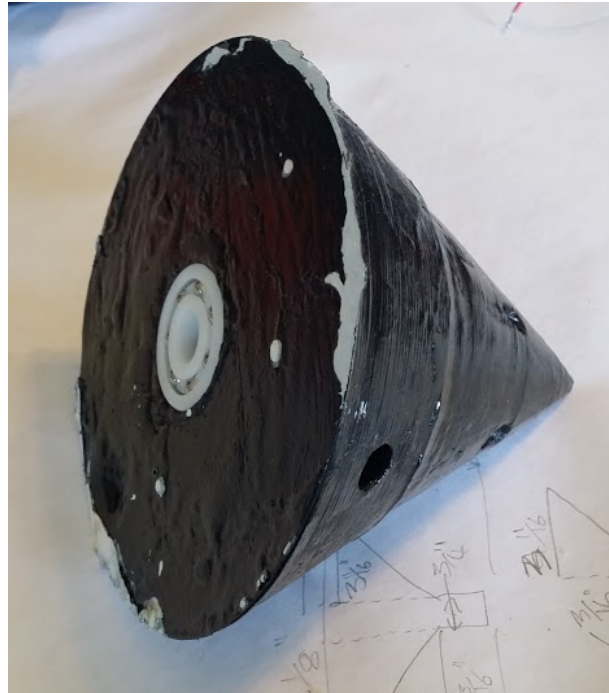


Figure 3.45: Gearbox mounted to pressure hull and shaft seal attached to gearbox shaft.

Future Drive Train Development

A lower torque motor and gearbox are desired pending on testing and performance data of operational conditions of the vehicle. The future design of the vehicle will move towards higher operational speeds to become more competitive with other UVs currently being developed. Also, possible replacement of the

Acetal Ball Bearing with a steel ball bearing would be wanted in future designs as the acetal would eventually erode and no longer be useful to support pressure hull.

3.2.7 Sealing



Figure 3.46: (Left) Loctite Marine Epoxy (Right) Silicone Sealant

One of the most challenging aspects in designing a UV is sealing against the environment for prolonged periods of time. For our design we opted to use Loctite Marine Epoxy at all mating surfaces and potential water pathways. Marine epoxy is formulated to bond wet surfaces and can be handled underwater in two hours. After curing for 24 hours, marine epoxy dries to a final strength of about 3000psi[LOCTITE] with no shrinkage or expansion. Epoxy was applied throughout the entire vehicle but most heavily around the pressure hull to prevent water leaking into the sensitive electronics tray. At mating locations where a permanent bond is not desired but water proofing is, silicone was the caulking of choice. Supreme Silicone is water ready in 30 minutes and dries to a flexible, waterproof seal. This was applied to the dome front cap before mating to the front of the pressure hull and around the body lid. Lastly, ABS cement was used to fill in any gaps present on 3D printed parts. Abs cement dries in 15 minutes and can be sanded to obtain any desired surface finish.

3.2.8 Electronics

A major leap forward from SHEILA-D is the integration of controls and electronics in Dory. Our Phase I attempt was merely a 12V 2A LiPo battery undersupplying two powerful 12V DC motors with a switch to turn the motors on at full speed. Not only was this not adequately safe for the user but it wasn't safe for the vehicle. During Phase II, our team set out to learn as much about electronics and controls of machinery as possible. Our goal was to deliver a well-controlled vehicle with data collection capability that was much more sophisticated than SHEILA-D. After becoming familiar with the world of Arduino and robotics, we applied our new found and self-taught knowledge to develop Dory's Logic Command Center. With a few choice parts, we were able to piece together an electronics package that can generate position and orientation data, save it to an SD card, record synced video, and control various actuators found throughout the vehicle.

Motor Controller

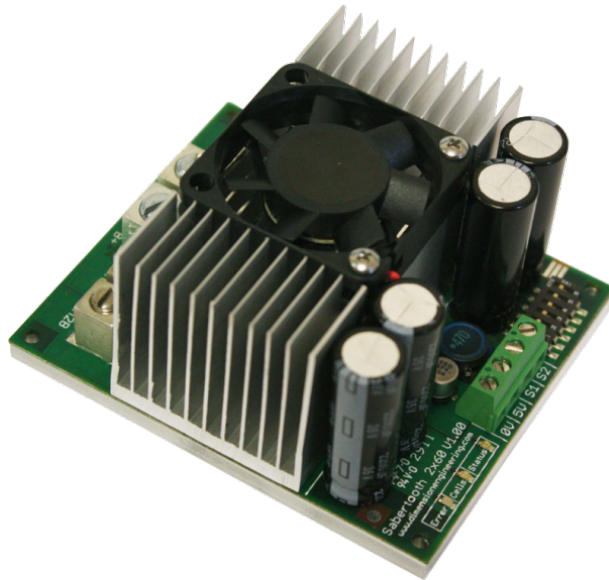


Figure 3.47: Sabertooth 2x60 Motor Driver Courtesy of Dimension Engineering

Obtaining full control of the powerful vane shell motor is made difficult by the needs of the motor at stall. The specific motor we chose consumes upwards of 80A at stall torque which is higher than any readily available motor controller on the market except for one. The Sabertooth 2x60 Dual Motor Driver is the most powerful and user-friendly controller on the market today. Each channel is capable of providing a burst current of 120A with normal operation around 60A; making it a perfect fit for our application since we will also be driving a DC motor to actuate the buoyancy controller. Using the onboard DIP switches we used the driver in Simplified Serial mode to make coding as simple as telling the driver which motor channel to engage and at what speed to run the motor. The Sabertooth also contains a 5V 1A Battery Eliminator Circuit (BEC) which drops the supply voltage low enough to drive the control surface servos. Since servos have higher current draw than the logic board (Arduino) can provide, the Sabertooth fulfills two power needs in one package.

Micro SD Card Breakout Board

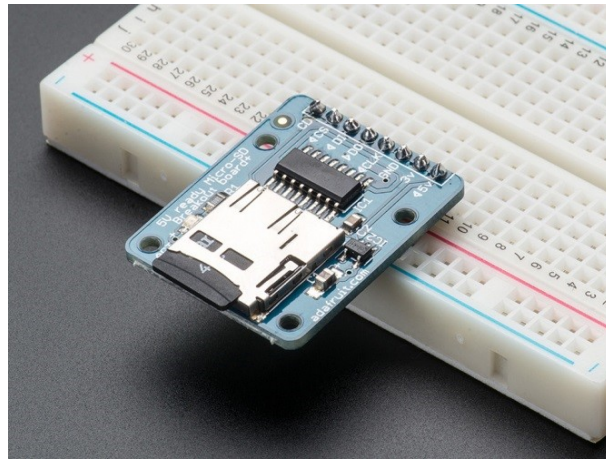


Figure 3.48: MicroSD Card Breakout Courtesy of Adafruit.com

Adafruit supplied the Micro SD breakout board which worked perfectly for saving the data generated by the inertial measurement unit(IMU). The board is driven directly by the Arduinos 5V power supply and only uses four digital pins. Once data is made ready by the IMU, a file is opened and saved to in a commonly found, class four Micro SD card formatted to FAT32.

Camera



Figure 3.49: HackHD module courtesy of Sparkfun.com

Finding a high quality camera to fit within the 4in dome of the front cap boiled down to one choice, the HackHD 1080P camera. The camera is a completely standalone PCB with a 9MP sensor that is simply

grounded by the Arduino for switching between on and off states. The PCB saves videos in up to one hour files on an on board Micro SD card. It is powered by its own 3.7V battery pack offering hours of run time.

Inertial Measurement Unit

An inertial measurement unit, or IMU, is a micro-electromechanical system, MEMS, that consists of a combination of some of the following: accelerometers, gyroscopes, and manometers. The one selected for our project is a LSM9DS0 9 degree of freedom IMU from STmicroelectronics. Selected pages from the device's datasheet are posted in Appendix C. The 9 degrees of freedom represented are acceleration in the x,y, and z direction measured in gs, the change in angle in the x,y, and z direction measured in degrees per second, and the strength of the magnetic field in the x,y, and z direction measured in gauss'. These 9 degrees of freedom allow for the on board processor to locate the device in three dimensional space given an initial location. The IMU was selected over GPS because the signals required to get a GPS fix attenuate rapidly through water making it impossible to make a submersible device that relied on these signals. The use of and IMU and dead reckoning techniques is the most practical way to get a position for a device of this size.

Batteries, Charging, and Power Budgeting

One of the key goals of our vehicle was to provide at least one hour of run time. With a design torque of at least 100 lbf-in and a rotational speed between 250-300 rpm, the vane shell motor is consuming about 40A. The consumption was rounded up to account for servos and the buoyancy control which will not be running very long compared to the vane shell motor. Taking the current and researching available batteries on the market, we chose Lithium Polymer (LiPo) batteries to power our complete system. LiPo batteries are known for their light weight, small size, large capacity, and high discharge rates. In short, LiPos provide high energy storage to weight ratios in any physical size needed. Since we didnt have enough room in the pressure hull for the batteries, they were placed in the underside of the vehicle to act as permanent ballast. This allowed us to go the route of fewer batteries with larger capacities.

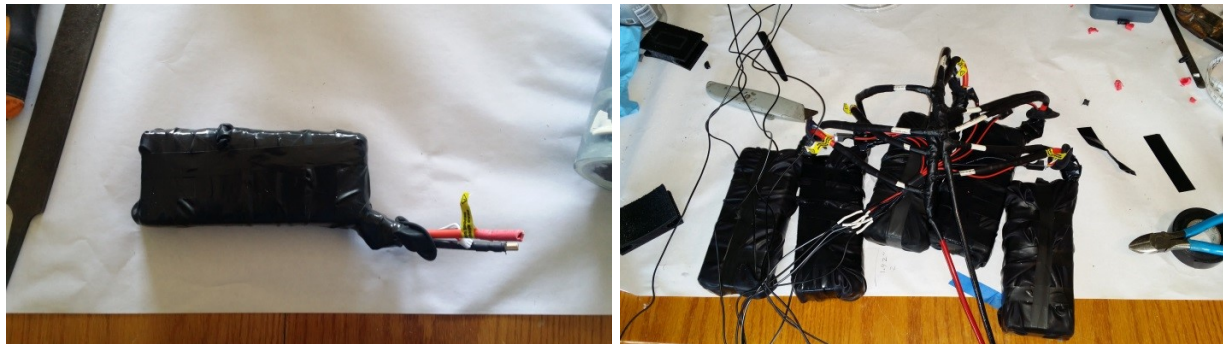


Figure 3.50: (Left) Waterproofed LiPo Battery. (Right) All five LiPo batteries connected in Parallel

The largest available batteries for the least amount of cost while also being from a trusted company where the Zippy Flightmax 8Ah. Each battery pack is configured as four cells in series boasting a total of 14.4V and 8Ah at a discharge rate of 30C. By using the discharge rate and multiplying it by the capacity, each battery provides 240A of discharge which is more than enough to meet our stall current of 80A. To achieve our one hour of run time, more than one battery was needed to meet the requirement. By wiring five 8Ah batteries in parallel, we were able to achieve 40Ah of capacity while maintaining a total nominal potential of 14.4V which grants our targeted run time of an hour. Hand-made parallel cables for both the positive and negative leads were made to link the batteries in parallel and heat-shrunk at all junctions for protection against any water that may leak into the body. Although LiPo batteries are already air proof thus water proof, we took preventative measures by slipping them into latex balloons and zipped tying the openings.

After waterproofing the batteries, they were placed in a foam battery bank under the body cylinder. The foam battery bank serves dual purposes of protecting the batteries from contact with the body cylinder and vertically locating the body cylinder.



Figure 3.51: (Top) Turnigy Power Supply. (Bottom) Mega 1000W Charger

Charging the batteries easily and quickly between sessions was another challenge to overcome. Once the batteries were in place under the body cylinder, accessing them would be nearly impossible unless the body cylinder was removed. Charging the LiPos in parallel would reduce the amount of cables coming out of the pressure hull and reduce charging time. The idea of charging LiPo batteries is fairly new because LiPos have a tendency to explode when mishandled. By parallel wiring the balancers already included in each battery pack and using the same parallel cables used for powering the motors the charger would recognize all five batteries as one large battery with four cells. What the charger doesn't know is that each cell is composed of a cell from each battery. The charger then fills each cell completely and moves to the next cell until they are all full. To find the right charger, the appropriate output to the batteries needs to be calculated. Too little output to the batteries will prolong the required charging time. According to the calculations below, fully charging the batteries would take about one hour if the charger outputs at least 40 Amps, 672 Watts, and is set a charging rate of 1C.

$$\begin{aligned}
 \text{Total Capacity} &= \text{Capacity per battery} * \text{Number of batteries} \\
 &= 8Ah * 5 \text{ Batteries} \\
 &= 40Ah
 \end{aligned} \tag{3.15}$$

$$\text{Total Required Amperage from Charger at 1C Charge Rate} = 40A$$

$$\begin{aligned}
 \text{Total Required Wattage} &= \text{Total Capacity} * \text{Voltage per cell} * \text{Number of cells} \\
 &= 40Ah * 4.2V/\text{cell} * 4 \text{ cells} \\
 &= 672W
 \end{aligned} \tag{3.16}$$

To fulfill this requirement a Turnigy MEGA 1000W charger was purchased for its ability to output up to 40 Amps and 1000 Watts. Like many LiPo chargers on the market, this model doesn't come with a built in power supply so a Turnigy 1080W Power Supply was purchased to provide enough power to support the charger at its highest potential.

Future Logic Command Center Development

In the near future, other electronics will be implemented to the Logic Command Center to further expand the functionality of the vehicle. A conductivity sensor can be added to the outside of the device to act as a start trigger upon contact with water. Another conductivity sensor can be added to the inside of the pressure hull to trigger an emergency shutdown of all systems and blowing of the ballast tank. This will result in an emergency surfacing of the vehicle. Adding audio recording capabilities will also expand on

the UVs abilities while 3D mapping will help with underwater navigation and exploration. Finally, better lighting of underwater environments would be achieved by incorporating LEDs to the front of the vehicle. This would lead to better photo and video quality in dark environments.

Wire Routing and Layout

As stated in the Pressure Hull assembly section, half- inch outer diameter aluminum standoffs were used to connect the body cylinder to the pressure hull. In order to power and communicate with the external actuators found in the body, wires were passed through the standoffs with each external component receiving one dedicated standoff. Also, the positive and negative power leads from the parallel batteries each received their own pass through. Once fed into the pressure hull, the wires were sent back to their final location on the tray. Five feet of cable was reserved for each component to ensure that they could reach their final connection and be pulled out without snagging when the tray is removed.

3.3 Programming

3.3.1 Firmware

For the device to operate independent from a human pilot it needed to have an on board processing system that could navigate, log data, and control the motors for the control surfaces, buoyancy control and the main propulsor. The physical components that are used are described in the electronics section of the report. In this section the software techniques used to handle the data produced by each component will be discussed.

Inertial Measurement Unit

The inertial measurement unit, IMU, outputs data for the acceleration, change in angle, and magnetic field strength. This can be used to find position, however this particular IMU picks up normal forces caused by resisting gravity which need to be canceled out to find the forces that are causing the overall vehicle to move. These forces can then be integrated over time to find the velocity and then the position of the vehicle. The position given will be an offset from an initial position because there is no way for the device to relate its position to absolute coordinates using only the degrees of freedom provided. This must be done in several steps.

Initial Filtering The raw data received from the IMU must be filtered to remove noise due to a non-ideal sensor. Each part of the IMU has a different kind of error that must be filtered in a different way. The accelerometer has noise that can be modeled a zero mean gaussian noise. This means that a low-pass filter can remove most of this noise and return a clean acceleration for later use. This was achieved by taking 10 readings from the accelerometer and averaging them thus creating a simple low-pass filter. The gyroscope tends to drift over time but is accurate in the short term. This means that a high-pass filter will attenuate the long term drift while allowing quick changes to be picked up.

Orientation After the initial filtering cleaned up some of the noise from the sensors the orientation of the device had to be determined. This is where the normal forces measured by the accelerometer become useful. They provide an absolute reference for down. Which can be calculated as follows:

$$\begin{bmatrix} \theta_{x_a} \\ \theta_{y_a} \end{bmatrix} = \begin{bmatrix} \arctan\left(\frac{Y}{\sqrt{X^2+Z^2}}\right) \\ \arctan\left(\frac{X}{\sqrt{Y^2+Z^2}}\right) \end{bmatrix} \quad (3.17)$$

These, along with the change in angle due read from the gyroscope integrated over time, provide means for finding the Euler angles with respect to the normal gravitational inertial reference frame. The are combined

using a complementary filter as follows:

$$\begin{bmatrix} \theta_x \\ \theta_y \end{bmatrix} = \begin{bmatrix} K_g(\theta_{x_{t-1}} + \theta_{g_x} \Delta t) + K_a \theta_{x_a} \\ K_g(\theta_{y_{t-1}} + \theta_{g_y} \Delta t) + K_a \theta_{y_a} \end{bmatrix} \quad (3.18)$$

In this equation K_g and K_a are the gains for the two sensors that can contribute to the orientation. They must add up to 1. A small value for K has a large impact in the short term orientation but is over powered in the long term, while a large value of K has the opposite effect, it is over powered in the short term but in the long term has a large impact on the long term value of the orientation.

With these techniques the pitch and roll Euler angles can be found. For yaw the magnetometer can be used, the noise from the magnetometer has more to do with the environment it is in, what magnetic sources are around it and what kind of metals will redirect the field. These are hard to account for so a low-pass filter like the one created for the accelerometer was created to filter out environmental noise and pick up the natural magnetic field that surrounds the earth thus giving the final Euler angle, the yaw.

Acceleration of the Vehicle With all three Euler angles calculated the acceleration needed to be transformed from the local inertial frame to the normal gravitational inertial frame. This was done with the following Euler transform:

$$\begin{bmatrix} A_x \\ A_y \\ A_z \end{bmatrix} = \begin{bmatrix} 1 & 0 & 0 \\ 0 & \cos \theta_x & -\sin \theta_x \\ 0 & \sin \theta_x & \cos \theta_x \end{bmatrix} \begin{bmatrix} \cos \theta_y & 0 & \sin \theta_y \\ 0 & 1 & 0 \\ -\sin \theta_y & 0 & \cos \theta_y \end{bmatrix} \begin{bmatrix} \cos \theta_z & -\sin \theta_z & 0 \\ \sin \theta_z & \cos \theta_z & 0 \\ 0 & 0 & 1 \end{bmatrix} \begin{bmatrix} a_x \\ a_y \\ a_z \end{bmatrix} \quad (3.19)$$

Once the transformation is complete normal forces due to gravity can simply be removed by subtracting 1g from the acceleration in the Z direction.

Velocity and Position Calculating the velocity and position of the device was a simple matter once the acceleration had been transformed. This acceleration needed to be integrated with respect to time to get a dead reckoning position and acceleration. Simply,

$$\begin{aligned} \vec{V} &= \vec{V}_{t-1} + \vec{A} \Delta t \\ \vec{P} &= \vec{P}_{t-1} + \vec{V} \Delta t \end{aligned} \quad (3.20)$$

Through this method the displacement from initial position and the velocity of the device can be found. This can be used later in the analysis of data collected by the vehicle and is a major part of the mission objectives previously stated.

Error Analysis This method of position estimation is full of error and cannot be fully trusted with the current sensors. This is because if the angle calculated is off, even slightly this will calculate an acceleration due to the normal force that wasn't fully canceled out. And through this acceleration an exponentially increasing error will occur in position. It is exceedingly difficult in these circumstances to filter out the real acceleration from the false acceleration without rendering the sensor useless. Due to this a large error must be considered in the final data analysis. A higher quality sensor, well above the price range for this project, would provide much more accurate data. This improved sensor will make the device much more accurate and yield a more capable ISR vehicle.

3.3.2 Software, The Graphical User Interface

While the vehicle was designed to collect and log data while maneuvering through a marine environment there still needed to be a way to visualize the collected data in a manner that facilitated understanding. Most of the data for this design comes from the 1080p camera positioned to film through the front dome while the rest of the data serves to provide the context for the footage, specifically orientation and position.

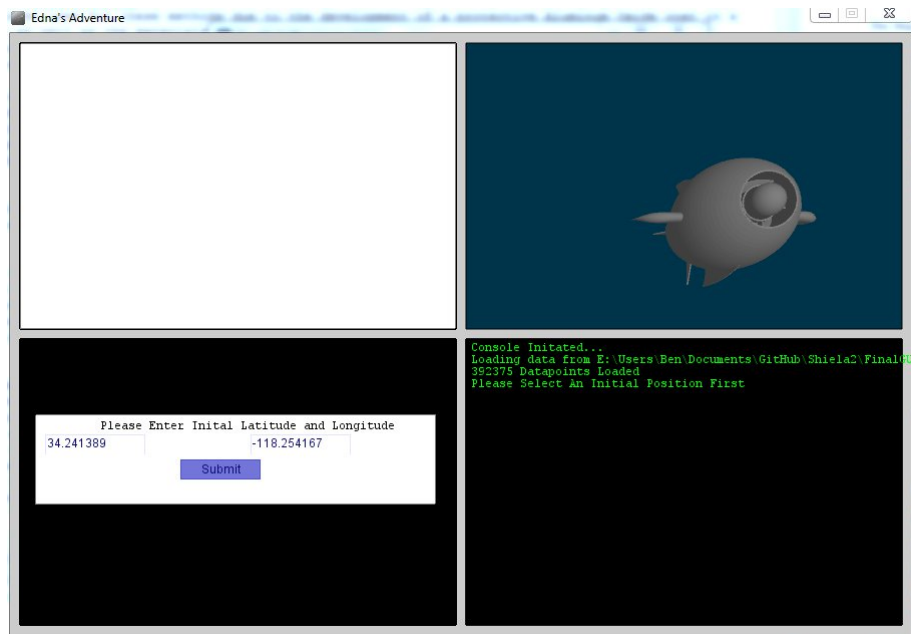


Figure 3.52: The Graphical User Interface

With this the analyst needed a way to easily watch the footage and know where it was taken and where the camera was pointed. This led to the creation of a graphical user interface. The GUI was broken down into 4 parts: the video, the orientation model, the map, and a control screen thus fulfilling the needs of the analyst.

Video Box

The video from the camera is saved onto an SD card while the device is in the water. This SD card can be retrieved from the device once it returns and the video can be analyzed to further understand the underwater environment in question. The coding for the video box is used to synchronize the updating of data in all of the other boxes because a factor of time is inherent in the video. The video is shot at 30 frames per second, and position and orientation data is logged every half a second. This means that for every 15 frames all the other boxes need to be updated. This relationship is easily used to maintain synchronization across the entire interface.

The Orientation Model

While the vehicle is on its mission and looking at the video it is hard to determine where it is facing. The accelerometer is able to read data regarding the orientation of the vehicle. This information is stored into an array to be used to display the orientation of the vehicle when the user runs the GUI once the vehicle's mission is complete. The accelerometer stores three separate values regarding orientation; rotation about the x-axis, rotation about the y-axis, and rotation about the z-axis. These three values are used to rotate the vehicle model on the GUI to show the orientation of the vehicle with respect to the video.

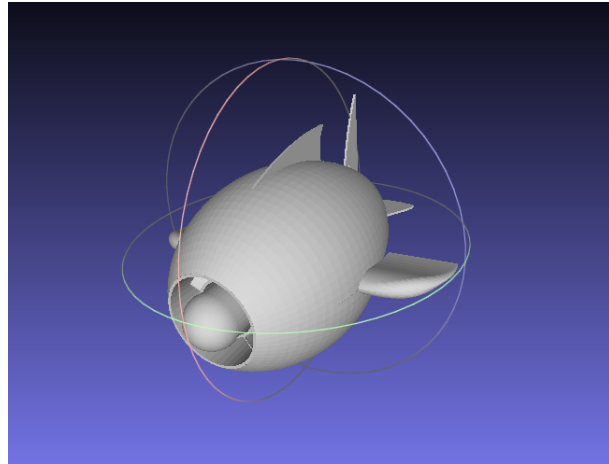


Figure 3.53: The Orientation Model For Viewing in the GUI

The Map

The location of the device at the time of the recording is another very important aspect required to satisfy the ISR capabilities. If some anomaly is seen in the footage it is imperative that the analyst can retrieve the location of the device at the time of the siting for further inspection. The map on the GUI requires the user to input a starting position and then displays the vehicles offset from the designated location thus plotting the path of the vehicle over the length of the mission. The map will further develop to allow the user to input waypoints relative to a selected starting position and therefore plot the path of the device for a future run.

The Control Screen

The control screen is located in the bottom left of the interface and reports important text to the user. The information about loaded files and the raw position data is shown here so that numerical values can easily be retrieved for a specific orientation and map position. In future development this is where the user would input the waypoints in a raw displacement form.

3.4 Fundraising, Pricing, Time Decomposition

3.5 Testing

3.6 Conferences

3.7 Team Bios

3.7.1 Ben

Ben Saletta a Mechanical Engineering student at California State Polytechnic University, Pomona joined Team UV during the Spring of 2014 for the initial phase of the design, the production of SHIELA-D. An idea man, Ben is always coming up with new and creative approaches to traditional problems. In his final year at Cal Poly he has found himself the leader of various campus organizations ranging from organizing fraternity meetings for Pi Kappa Phi to supervising teams of Resident Advisors (RAs). All of these jobs have honed his rapid creative problem solving skills and prepared him to be a unique design engineer. His curiosity and

drive have lead him to do several independent projects, from a low cost olive oil production method to small scale aquaponics systems. When he can grab a bit of free time he likes to rock climb, SCUBA dive and generally adventure.

3.7.2 Brian

Graduating from Cal Poly Pomona in March 2015 with a BS in Mechanical Engineering and a minor in Materials Engineering, Brian is a member of the American Society of Mechanical Engineers (ASME), has made the Deans List 9 times, the Presidents honor list, and passed the NCEES Fundamentals of Engineering (FE/EIT) Mechanical Engineering-specific exam. Brian has interned at the C. Erwin Piper Technical Center where he did machining, 3D CAD modeling, and prepared patent drawings, Hyperion Treatment Plant where he did hydraulic design, structural design, and air flow analysis, produced technical proposals for Department of Defense (DoD) contract solicitations through the SBIR and STTR programs (subject: materials science), and has been interning at the Naval Surface Warfare Center since June 2014. Brian's future interests include attending graduate school to earn multiple degrees in fields such as materials science, fluid mechanics, mechanical, automotive, naval, and/or aerospace engineering, obtaining his Professional Engineer (PE) license, working as a design engineer within the defense industry on vehicles of all kinds (sea, air, land, manned, unmanned, etc.), and eventually starting his own small engineering design firm that works on special projects such as this project.

3.7.3 Andrew

From muscle cars to next gen cell phones, Andrew is interested in all things related to technology. He is currently in the final year of mechanical engineering curriculum at Cal Poly Pomona where he has established strong leadership roots. Aside from working on many design projects and participating in engineering clubs, Andrew has worked for University Advancement where he has led a team of students, alongside other departments, to raise about \$500,000 yearly for various campus needs. He can see a future in engineering as well as in advancement, making possible career paths very exciting. With his free time, you can find Andrew barbecuing with his family and working on his 1970 Camaro.

3.7.4 Ketton

One of the 5 (probably the coolest of them all) members of Team UV. Grown up helping his Father work on cars and doing construction around the house. You can say hes a jack of all trades. Currently in his final year at Cal Poly Pomona as a mechanical engineering student and during his time has gotten valuable experience from classes as well as Internships. Ketton worked three summers as a mechanical engineering intern for Hamilton Sundstrand (who created the first spacesuit) doing analysis of all sorts and even designed a part for the Orion space capsule. Ketton is now working as a project associate for Otis Elevator overlooking the construction and installation of elevators. Ones that you may be riding on in the near future. Ketton is located in Riverside, CA and spends his free time playing recreation softball and playing league of legends.

3.7.5 Abraham

Part-time bassist. Part-time photographer. Full-time student. Known to the team as the lube man, Abraham is a 6th year student at Cal Poly Pomona graduating in the Spring of 2015. Adopting the scientific principle of Occams Razor, he finds that in both engineering and life often the best solution is the simpler one. Currently open-minded in professional goals, he aspires to be masterful in many fields of engineering as well as in playing the blues. Apart from school and work, Abraham spends his free time listening to various indie rock groups, wandering the trails in the wilderness, and actively traveling outside of Downey, California where he currently resides.

Appendix A

Phase I Report

SHEILA-D

(Submerged Hydro-dynamically propelled Explorer
Implementation: Los Angeles - Demonstrator)

5/20/2014

ME325-02 Machine Design

Dr. Todd Coburn

California State Polytechnic University, Pomona

100%
100%
Excellent!!

Team UV
Brian Martin
Ben Saletta
Andrew Blancarte
Ketton James
Abraham Paucar

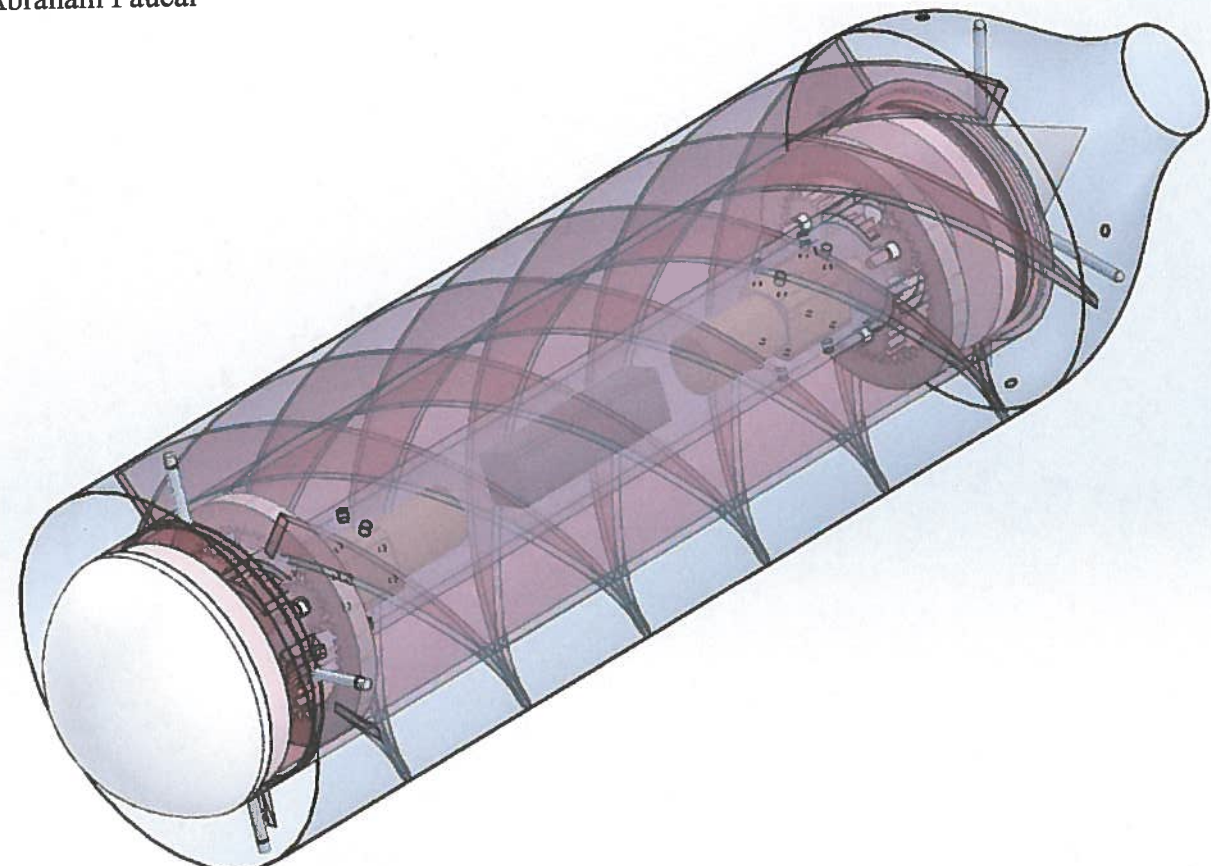


Table of Contents

TABLE OF CONTENTS.....	1
INTRODUCTION	2
BACKGROUND.....	3
COMPETITION.....	5
DESIGN PROCESS.....	7
1. DESIGN CRITERIA	7
2. INITIAL DESIGN/SETUP	7
3. APPLICABLE FLUIDS THEORY.....	7
4. DESIGN REFINEMENT.....	8
5. FLUIDS CALCS.....	8
6. DYNAMICS CALCS	9
7. MOTOR/GEARBOX RESEARCH AND SELECTION	10
8. MACHINE DESIGN CALCS	10
9. BATTERY SELECTION.....	11
10. ITERATIONS (OPTIMAL SETUP)	11
11. PURCHASING/ACQUISITION/SUBASSEMBLY REFINEMENT	11
12. MANUFACTURING/TROUBLESHOOTING/FURTHER SUBASSEMBLY REFINEMENT	12
13. TEST DESIGN/LOCATION SCOUTING	13
14. TESTING	14
RESULTS.....	16
ROLES AND RESPONSIBILITIES.....	18
SCHEDULE	19
MARKETABILITY.....	20
CONCLUSION	21
APPENDIX A: DRAWINGS.....	22
APPENDIX B: CALCULATIONS	38
APPENDIX C: PHOTOGRAPHS	54

Introduction

The objective of this project was to make a demonstrator for a new, powerful, and innovative propulsion system for an underwater vehicle. As it stands currently, there are numerous different types of underwater research and transportation vehicles all using the same propeller propulsion system. Propeller propulsion, although proven effective, has the risk of blades breaking off, cavitation issues, choppy unreliable thrust, and many other problems. This newly designed system corrects these issues and improves in many other areas. The design exchanges propeller blades for a set of winding extruded vanes pushing fluid through a nozzle-end producing a reliable, steady stream of flow that can be controlled and directed. Inside the propulsion system, SHEILA-D, are a pair of motors each connected to high ratio gear boxes; both of which are powered by a user controlled, rechargeable power source. From the gearboxes a pinion rotates 3 idling planetary gears connected to an internal gear which turns the outside cylinder that has the vanes attached. A majority of materials chosen for the design are corrosion proof polymers to reduce the weight but future designs will be of higher quality to ensure better strength and final finish. Having stated this, it should also be noted that for this demonstration phase of the design, in order to cut down production costs, many less than optimal materials were used (e.g. the sheet steel outer cylinder, and a few areas in which different metallic materials are in contact producing galvanic cells). SHEILA-D is a new, compact, safer propulsion system that provides reliable thrust to an underwater vehicle which vastly improves on what propellers and similar systems are currently capable of.

Background

The world of marine propulsion has been ruled by the use of bladed propellers for hundreds of years ever since the first deviation from paddle wheel propulsion by the US Navy in the 1840s. Today, bladed propellers are by far the most commonplace means of propelling water craft, whether above or below the surface.

While bladed propellers have the advantages of being tried and true, relatively inexpensive to manufacture, and available in a wide variety of sizes and geometries, they also exhibit numerous inefficiencies and disadvantages. Among these are the facts that they create uneven, buffeting flow, cavitate easily (leading to accelerated degradation as a result of surface pitting), produce a significant amount of noise (mainly as a result of cavitation), must be made of heavy, metallic materials (in order to mitigate the effects of cavitation damage) and are frequently exposed to foreign object damage. These shortcomings can become greatly exaggerated when bladed propellers are used for the propulsion of fully submerged vehicles; this is especially true for applications in which stealth is key, such as in military submarines, special operator deployment craft, and unmanned undersea drones such as remotely operated vehicles (ROVs), unmanned underwater vehicles (UUVs), and autonomous underwater vehicles (AUVs). For these reasons and more, an innovative approach to the development of a submersible propulsion system based on unconventional mechanics may be warranted. Enter SHEILA-D.

 Submerged Hydro-dynamically propelled Explorer, Implementation: Los Angeles-Demonstrator (SHEILA-D, or SHEILA for short), is a proof of concept demonstrator that has been developed in order to explore the capabilities associated with using a ducted vane screw for submersive propulsion. SHEILA is based off of a concept that is in its fifth year of maturation; however, prior to April this concept was nothing more than an abstract dream. Currently, this concept is being brought to fruition by a highly capable, highly motivated five person team. Upon completion of this project, based off of the results realized and the performance data collected during testing, the propulsion system will be either directly utilized as a subsystem in a planned underwater vehicle senior project starting in the Fall 2014 quarter, partially adapted for the senior project, or (if unsuccessful or determined to be unfeasible) used as a jumping off point for research into other new propulsion systems.

By moving away from the traditional bladed propeller and towards the propulsion system detailed in the following pages, a wealth of advantages may be realized, including:

- Even, steady flow as produced by the entrainment of the working fluid, followed by merging of the annular water entrainment tracks prior in a convergent acceleration nozzle.
- Increased maneuverability as afforded by the newfound steady flow.
- Reduced threat of cavitation as a result of the lower rotational speeds required to produce the same amount of thrust.
- Reduced noise as a result of prevention of cavitation [STEALTH].
- Reduced fouling susceptibility due to the protective concentric vane enclosure

- Reduced weight due to the enabling of the use of non-metallic materials as a result of lower fouling exposure
- Reduced magnetic signature due to the enabling of the use of non-metallic materials as a result of lower fouling exposure [STEALTH]
- Reduced thermal signature due to the enabling of the use of non-metallic materials (and therefore insulating materials) as a result of lower fouling exposure [STEALTH]
- Reduced materials costs due to the enabling of the use of non-metallic materials as a result of lower fouling exposure
- Increased safety due to enclosure of the prime movers (motor/gear/vane assembly)
- Provision of increased speed capabilities without cavitation (also as a result of lower mass)

These benefits are but a small sampling of the plethora of advantages that can be attributed with the propulsion system demonstrated here.

While there are many areas in which a water propulsion system based off of this annular screw vane geometry can prove revolutionary, it should be noted that as with any good research and development, there are many obstacles that need to be overcome. Among the most prohibitive of these barriers are the facts that this type of system is not currently used to this effect for the propulsion of undersea vehicles and as a direct consequence of this fact, the research required for the development of this system has been, is, and will continue to be very challenging and the initial development costs have been, are, and will continue to be (at least for a while longer) quite high. As a result of these high costs, less than optimal materials have been used as most of the design has had to be based off of commercially available off the shelf components (COTS) and items which could be bought for low financial costs that, while are not at all meant for these purposes, could be adapted to serve the required/desired purposes.

Shouldnt change font size

As mentioned before, the research required for the development of this propulsion system demonstrator is quite challenging by nature of the scope of this project. There exists virtually no literature concerning the use of screw-like mechanisms (other than bladed propellers, which are also adaptations of the mechanics set forth by the pioneering work laid down by Archimedes' screw) for the purpose of vehicle propulsion. As a result of this fact, the design work performed here has been largely based off of the extrapolation of known principles to the parameters of this design, as so much is unknown with respect to the specific principles used by this system. In order to define the equations necessary for the optimization of this system, an interdisciplinary approach has been adapted in which principles from fluid mechanics, classical mechanics, and machine design have been used in concert to develop approximating equations of motion which enable simplified determination of some of the performance characteristics/output variables of interest, including: the nozzle exit jet velocity, nozzle exit thrust, stall torque requirements, running torque, running time (based on suitable battery packs that meet the current/voltage and power density requirements), gearing parameters, and numerous other variables. For more on the actual design process, see the section titled "Design Process".

Great Lecture!

Competition

Commercially available, under water vehicles (UV's) don't come in all shapes and sizes. The idea of underwater exploration is not new and most UV's for public consumption follow the same basic principles: pvc tubing frame, modified water pumps with propeller attachments, and a large price tag. SHEILA-D is designed to take the idea of underwater exploration and point it towards the future. Gone are the high drag inducing shapes and propellers, and in their place, well thought out design and propulsion systems. There are a few companies out there that are direct competition but with a slightly different goal in mind.

OpenROV is a company which makes remotely operated vehicle (ROV) kits with an emphasis on open source development. They want to build a community of explorers of all backgrounds, from engineers to children, interested in UV's. A kit of off the shelf components is sold by OpenROV and assembled by the customer. The finished product, called OpenROV v2.6, captures video and transmits the feed to a computer. The customer is able to control the ROV from a remote control and has the option of adding functionality to the ROV at any time. The customer can freely share any findings or product enhancements to the OpenROV community. The strongest features of this design are the use of LED's to flood areas of exploration with light and the ability to control direction. Since SHEILA-D is purely a proof of concept in the area of propulsion, lighting and control features to rival OpenROV will be incorporated at a later time. The idea behind this company is unique but falls short to the same problems associated with UV's of the past. Their design, although easy to assemble, is boxy and prone to getting stuck in kelp beds. SHEILA-D is designed to be hydrodynamic and to be able to navigate through various underwater environments with ease. Since the vanes are enclosed in an exterior shell and direct driven, SHEILA-D is more able to overcome troubling environments.

Other UV's available for purchase such as the Apogee Kits Mini ROV have far less features than SHEILA-D. Most of these smaller and more affordable vehicles are prone to buoyancy issues and high drag. They are designed to be low speed explorers with most of the focus being on image capturing. The modified pumps used for creating thrust for these smaller UV's are underpowered and easily stalled when tangled in kelp beds. Other issues with common UV's are leakage and noise. These issues will have to be addressed by Team UV as well. Epoxy, waterproof duct tape, and silicone sealer will be used to protect electronics and prevent water from reaching critical areas. For a phase 1 project, this approach is adequate and common practice when building any underwater project. For later phases a more sophisticated approach can be designed. As mentioned before, noise is a common issue for underwater vehicles. Most UV designs have high operating noise from the motors and propellers. SHEILA has deleted propellers which make the vehicle run more quietly and can be a future candidate for military applications and stealth operations.

Finally, SHEILA is designed to be more affordable with more features than other underwater vehicles. The proposed total cost of this project is to be \$800 for the propulsion system with later phases integrating controls and better manufacturing. So far, the project is coming in under budget with all parts adding to \$700. Our direct rival, OpenROV, is retailing an unassembled kit

for \$850 designed for the hobby market. SHEILA is offering a better propulsion system with high speed capabilities and potential for more functionality in later phases.

Excellent.

Design Process

The design process contains a lot of detail which is broken into small sub-topics to better follow the production of SHEILA-D from the drawing board to the final water testing.

1. Design Criteria

The objective for this project was to provide a compact and innovative underwater propulsion system that differs from the traditional propeller in today's water vehicles. The underwater propulsion system, SHIELA-D, needed to be compact, about the size of an average scuba tank, yet still be able to produce enough thrust to travel at a rate of 1 knot. SHIELA-D would use a steady, constant laminar flow to produce thrust thus causing less wake when running. SHEILA-D will be a fully submersible system that will need to be able to withstand any drag and hydrostatic pressures underwater and still provide a satisfactory seal to run efficiently.

2. Initial Design/Setup

The aforementioned criteria dictated a compact design with minimal flow interferences and the capability to be autonomous. By removing the life sustaining space and power requirements, the initial design was reduced to a simple screw extending the length of the vehicle and driven by an external power source. To remain portable and easy to use, the design was restricted to approximately the size of a compressed air scuba tank. Many boats already have fittings for this shape of a package, especially in the market that this design is directed towards. With this size requirement in mind, the design was adapted to appear more cylindrical. Instead of driving the screw from externally mounted motors, a design involving three concentric cylinders was adopted. The innermost cylinder houses the motors, their power supply, and provides a space and support system for a future research or observation cell. This design focused mainly on the propulsion systems while providing space for future advancements. The middle cylinder, the vane shell, would serve as a mounting point for the threads of the screw, the vanes. Initially these vanes would only travel about 1/6th of the way around the cylinder over the entire length. The idea behind this was that the water would move faster along the length of the cylinder and therefore produce more thrust. The outermost cylinder contains the flow between itself and the vane shell. This was done to have more control over the flow and ensure that the energy produced by the rotating of the vanes went towards the propulsion of the device and not wasted as turbulence to the external body of water. The external shell also provides a mounting point for future control surfaces to stabilize and steer the device. The external shell terminates in a cone to increase the final speed of the flow accelerated by the vane shell. The increased speed of the exiting flow provides the thrust that propels the device through the water.

3. Applicable Fluids Theory

The design considered very much resembled a turbine which has a constant flow of fluid coming into the system and becoming energized by the work put in by the motors and gears. One of the main loadings that needed to be overcome was the hydrostatic forces associated with starting the propulsion system underwater. Through the two motors and gears, the initial torque that was needed to overcome these initial static loads was applied and transmitted to the vanes which then

input the energy into the working fluid. Considering SHEILA-D would be moving water through its length, there were many dynamic fluid considerations to implement into the design. The choice of the extruded vanes meant that there was drag components to the fluid moving along the length as well as along the walls of the external cylinder and surface of the rotating cylinder. To avoid mixing and unwanted turbulence and drag forces the design must control the flow in such a way where it stays laminar. Once the number of vanes and angle at which the vanes are attached are chosen, the friction factor can be determined to calculate all the associated drag forces. To avoid stagnation and to control the flow at entrance, a hemisphere is placed at the front for a more streamlined input of fluid into the device and a cone at the end for a more controlled output. This dome also acted to help accelerate the flow in that it creates a high (stagnation) pressure at the tip of the dome, forcing the moving fluid to accelerate around the dome into the lower pressure flow field within the vanes. Considering the choice of materials was going to be less than optimal, the drag forces on the outside of the external shell need to be overcome in addition to the weight of the device.

4. Design Refinement

As highlighted above, a large portion of the initial planning/conceptual development stage was spent in an attempt to think through the specific design challenges to be faced in the coming weeks. This was accomplished by thinking through such things as the shortcomings of the initial concept, some of the more remarkable/noteworthy features of the initial concept, how the theories as born from fluid mechanics could be adapted and further developed for the purposes of optimizing the design of SHEILA-D, and of course the many design criteria as laid out by the team, the problem statement, and the environment to which this demonstrator would be forced to immerse itself (both figuratively and literally). Thus, after having spent many hours discussing and analyzing some of the issues, some key alterations and upgrades were made to the additional design, a small sampling of which included the radial and axial location of the components (along with the required constraints) as well as the means by which the vane shell would be allowed to rotate (and thus produce thrust) without transmitting that rotary motion to the exterior shell and motor housing. Some of the actual physical innovative solutions that arose in this stage of the design process included the use of front support rods riding in a running track and through-rods (which also resist rotation of the motor housing and exterior shell) in the rear section to keep the components located radially (which the planetary gear sets also helped with) and the use of a thrust bearing (actually a rotary ring/"Lazy Susan" style bearing) for axial location. These are solely a small sample of the design decisions made at this stage; however, these are also some of the more lasting solutions from this stage, as the design of this demonstrator has been ever evolving and as will be seen in the following pages, was constantly updated as a result of iterations pertaining to the theory, calculations, component purchasing/availability, manufacturing difficulties, and testing parameters/constraints.

5. Fluids Calculations

In order to relate the torque from the motor to the final thrust of the device, the dynamics of the fluids between the vanes and through the final nozzle needed to be considered. The torque required to rotate the vanes through the fluid was calculated through the following procedures mathematically described in Appendix B. The first step was converting the angular velocity to an

instantaneous tangential velocity at the average radius of the vane. Then Bernoulli's equation was used to find the pressure on the vanes due to their rotation. This pressure was converted to a force by multiplying it by the area of the vane multiplied by the cosine of the angle that the vane made with a line along the length of the cylinder. This force was then multiplied by the average radius to provide the relationship between the angular speed and the required torque. This relation went directly into the design of the gear train and the motor selection. Once the torque required by the motor was found the thrust provided by the motor needed to be calculated. This ended up being a simple conservation of linear momentum equation. The rotation of the screw through the water applies a force both along the length of the cylinder and along the circumference of the cylinder. The circumferential component is equal to the drag previously calculated and the lengthwise component is equal to the tangent of the angle that the vane makes with a line along the length of the cylinder multiplied by the circumferential component. The lengthwise component of the force was then divided by the mass of the water between the vanes to provide acceleration. The force on the water is assumed to be constant over the length of the cylinder and the velocity of the fluid is assumed to vary linearly meaning that drag is neglected for this calculation; it will be applied later. These assumptions allow the use of the equation $V^2 = a * x$ where V is the velocity, a is the previously calculated acceleration and x is the length of the vane. This provides an exit velocity, however head loss needed to be accounted for. This was done by taking the average velocity, fluid constants and the hydraulic diameter of a vane to find the Reynolds number for the flow. The Reynolds number was then used to find the pipe friction factor and finally the head loss. The head loss was converted into a velocity loss using Bernoulli's equation and then subtracted from the previously calculated exit velocity. This corrected exit velocity, along with the basic geometry of the device allowed for the completion of linear momentum calculations which resulted in the final thrust provided by the flow.

6. Dynamics Calculations

As stated previously, the calculations performed here within consisted of an interdisciplinary approach which focused on fluid mechanics (to figure out how to produce the desired flow), classical mechanics (to figure out what kind of machine kinetic requirements needed to be imposed to create the flow), and machine design (in order to figure out how to provide the necessary machine kinetics to transfer torque from our power source into torque at the vane shell, which would then be transmitted to the working fluid in the form of kinetic shat input energy). Thus, the dynamics calculations bridge the gap between the fluid mechanics requirements and the machine design requirements.

As the inputs for the dynamics calcs, the vane geometry, geometry of the annular flow region, the vane shell length, the vane shell material properties, and the desired flow acceleration were implemented, with a desired output of the maximum (stall/starting) torque that the demonstrator would need to provide in order to provide movement of the fluid. This was accomplished by assuming that the demonstrator would be starting from stall, and therefore each vane would have to provide enough force (torque over the centroidal moment arm) at the vane-fluid interface in order to accelerate the mass of water in the annular regions between vanes at various accelerations while combating the maximum pressure exerted on the vanes by the fluid (hydrostatic, or stagnation pressure, which is the maximum pressure in the flow field for this incompressible working fluid). This was done by developing a dynamic free body diagram and

deriving the equations of motion as presented in the sample calculations. A factor of safety of 1.5 was tacked onto the output total stall torque requirement to account for the rotational inertia of the vane shell cylinder itself. Once these mathematical relations had been derived, they were programmed into an excel spreadsheet just as the other calculations were, in order to facilitate more efficient design iterations down the road.

7. Motor/Gearbox Research and Selection

The previously discussed fluids calculations dictated the amount of torque per RPM required from the drive train. The challenge was to find a motor with minimal power consumption and a small package that fit these requirements. Stepper motors were initially considered because of their high torque and great control. These motors were eliminated from the selection process because they required complex control circuitry, take up a lot of power and space, and are not practical to rotate at high speeds. Off the shelf gear motors were also looked at but the majority of these motors have shafts that are off center thus making it difficult to mount them to the planetary gear set that is required to transmit the torque radially. The final option was to purchase a gear box and find a motor that mated to it. This provided more flexibility in gear ratios and package size. The planetary gear set that was designed spanned too great of a radial distance with too unusual of a diameter. This made it impossible to find off the shelf gears that would serve the purpose. The decision was made to 3D print the gears out of ABS plastic for custom sizing and less expense. To increase the strength of these gears they were designed to have large teeth and a large face width. These two decisions made it necessary for the majority of the speed reduction to be done by the gearbox attached to the motor while the plastic planetary gear set would mostly serve to transmit the load radially. The fluids calculations provided a relationship between the angular velocity of the vane shell and the torque required. The characteristics of the hobby motors that would mate to gearboxes were listed along with the gear ratios of the possible gear boxes and compared to the fluid requirements. An RS-555 motor was selected along with a mating 1:16 gearbox to satisfy the fluids requirements while remaining near the maximum efficiency of the motor.

8. Machine Design Calculations

A lot of assumptions had to be made for the machine design gear calculations. Using the overall gear ratio of 1:36 and using very basic design equations, the following parameters were calculated: number of teeth (N), pitch diameters (d), and diametral pitch (P) for the pinions, idler planetary gears, and internal gears. A lot of assumptions had to be made for the design calculation because the gears had to be designed and 3D printed from Acrylonitrile Butadiene Styrene (ABS) (imposing some serious stress concerns). It was assumed that an overload factor of 1 should be used, due to a power source and driven machine, the pinion, were both assumed uniform. Looking at the Shigley's text, it was also assumed that the gears were of the lowest quality of commercial gears, 3, to keep the design conservative. The teeth were also uncrowned making the C_{mc} factor 1 and the C_{pm} factor to also be 1 because of the lack of data for non-straddle mounted gears. In addition to this, it was decided to make the assumption of open gearing condition for the entire gear system. Since the design incorporates 2 sets of gears with

two separate motors, the transmitted load was found to be divided by 2 making it only 36lb that runs through the gears. The Shigley's text only gives S_c and S_f factors for steels and other alloys and no other data to calculate the allowable stresses. Therefore, the S_c and S_f factors were assumed as our flexural yield that was taken from the ABS material data sheet.

9. Battery Selection

The power source came into careful consideration after the motor and gearbox selection was completed. Initially it was decided to use an external power source for the motors but this was dangerous as the system would be submerged underwater and thus it was decided to look for a rechargeable power source connected to a switch and potentiometer to control SHEILA-D from the surface and not worry about it running out into the water until the battery died. The battery needed to be able to power the motors for long enough to be able to collect accurate data when testing underwater. It was assumed that an hour of testing would also be unreasonable for run time (due to scarcity of high enough capacity batteries) and that 15 minutes of testing would be too short a run time before the battery packs would have to be recharged, due to the inconvenience posed by recharging. A number above 30 minutes was selected as a run time goal and the battery that was selected was the Lynxmotion 11.1V 28000mAh 3S 30C LiPo Battery which met all of the requirements. Once such met requirement was that the current draw it could handle (seeing as it is a 30C rated battery which means it can handle to release 30 times its rated 2.8A continuously for one hour). This also yielded about 50 minutes of testing time to collect data from SHEILA-D which met the imposed test run time requirement.

10. Iterations (Optimal Setup)

Once the important electrical and mechanical items were decided (gearbox, motor, and battery) the first stage of calculations needed to be reiterated to reflect our updated design. The gear box provided a 16:1 ratio which provided great support in designing the planetary gearset which was designed to be a 2:1 ratio thus giving the gear system as a whole a 32:1 ratio. Calculations such as drag, speed, stresses, and overall thrust of the system needed to be reevaluated due to this change. A battery was chosen that would be powerful enough to power two motors in the core of SHEILA-D. This battery was sufficient to produce 30A in order to start both motors so 12 AWG wire was chosen since the nature of it's size would be able to withstand the current produced from the battery. However, since the battery would produce such high power at startup the system needed a slow starting mechanism so the gears would not undergo great initial force therefore a potentiometer was included in the wiring setup. There would be two switches wired in parallel, one that included a potentiometer that would be used for startup purposes only and the other just with a switch alone that would be activated once SHEILA-D was at full speed. Switches that were rated anywhere close to 30A were chosen as to make sure nothing would burn leaving the system stranded in the water.

11. Purchasing/Acquisition/Subassembly Refinement

In trying to hit the early presentation date, purchases were made at brick and mortar locations whenever possible. This allowed for in person inspection of quality and to ensure timely acquisition. In-person purchases were made at Home Depot and Orchard Supply Hardware for PVC components, exterior shell ducting, small hardware, and sealants. Specialty items such as

electrical wire and small connectors were purchased at Pegasus Hobbies and Fry's Home electronics for their more refined selections. These locations were relatively near or along the way, to SHEILA's manufacturing site. As with any unique project, not all components can be purchased off the shelf or in person. More critical components such as the LiPO battery and electrical components had to be ordered online. Specialty online shops such as RobotShop.com and McMaster-Carr allowed access to parts that best fit the project requirements. These components needed to be ordered quickly to ensure timely delivery. Most deliveries were expedited by upgrading to priority or next day shipping. During manufacturing, quick runs had to be made to local hardware stores to pick up small parts. These small parts such as clamps and washers were not part of the initial design but essentially made SHEILA-D a possibility.

This phase of the project is heavily limited by the availability and cost of possible materials. Purchasing more effective and premium materials would have cost the team a tremendous amount of capital. Decisions to use less optimal components warranted timely construction and a reasonable budget. A spreadsheet of purchases and purchasers has been compiled to make sure that a detailed budget can be made. This is also a great way to make sure correct distribution of cost among all members.

12. Manufacturing/Troubleshooting/Further Subassembly Refinement

The first stage of manufacturing was to construct the vanes. The vanes needed to form along the rotating cylinder at a 45 degree angle leading to about a one and a half cycle per vein from top to bottom. The material for the vanes was acrylic and the rotating cylinder would have 5 vanes total. Each vane started from a rectangular shape that was 2 inches in width and roughly two feet in length. Several slits were cut about one and three-quarters of an inch in the acrylic so it could be formed around the rotating cylinder without breaking the material. A heat gun was used to soften the material at each slit so it could be formed around the cylinder then cooled with ice or water to quickly form the angle desired, this process was repeated for each of the vanes. Once the final shape was obtained for each of the vanes they were epoxied to the rotating cylinder and waterproof tape was applied to both sides of the vanes to cover the spaces produced by the slits after forming the material around the cylinder. The tape was also to provide a solid constant surface area to move the fluid through the system.

The planetary gearset was made of ABS plastic and 3D printed. They were printed as one long extrusion and cut to length. It was found that the printed gears were not solid as expected, but consisted of a honeycomb shape throughout the internals of the gear. Since these gears are undergoing a considerable amount of torque along with them being plastic they were then filled with epoxy in order to provide a more rigid gear that could take the sufficient load. The pinion gears were press fit onto the gearbox and sealed with epoxy in order to ensure the gear would not strip from the gearbox shaft. Quarter-inch diameter rods were cut in lengths of roughly 3 inches that would hold the planetary gears connecting the pinion to the internal gear; these shafts sat inside nylon bushings that are mounted to the motor housing to provide stability during motion.

The motor housing (innermost cylinder) contained the power source, motor, gearbox, pinion gear, partial of the planetary gears, support rods and wiring. The motor housing was made of PVC and cut to a length of two feet. Several cuts were made to this such as holes for mounting

the gearbox, slits to provide room for the planetary gears that connects the pinion to the internal gear, and holes for the support rods in the rear of the system. The rotating cylinder (2nd innermost cylinder) has a separate clear plastic hemisphere on the front of it where a camera would sit as well as provide a seal to protect the battery and the motors from any water. The inner diameter of the rotating cylinder was bored out so the globe to fit inside along with a gasket to provide sufficient sealing when underwater. A track was cut on the outside of the cylinder, roughly an inch from the font. This track would sit on nylon tubes to provide support for the front of the system from any flow induced vibrations and keep the rotating of the cylinder as concentric as possible.

The length of the motor housing is longer than the rotating cylinder so in order to provide a seal in the rear a three in diameter hole was cut in an acrylic plate that would sit on the back of the rotating cylinder and the motor housing would stick out of the plate. A rubber shaft seal was placed on the motor housing that extended past the acrylic plate to create a seal as well as allowing the shaft to rotate. On the inside part of the rotating cylinder a plastic turntable, aka "Lazy Susan", was used to act as a thrust bearing. It was placed inside toward the rear end of the rotating cylinder that mounted on the motor housing and would provide support for any axial loads as well as keep a low friction force if it may come in contact with the plate that provided the seal in the rear. A cone made of thin aluminum was placed on the back of the motor housing to provide a smoother flow of the fluid and reduce any losses in the system before the water reaches the nozzle.

The external shell (outermost cylinder) consisted of thin sheet metal, like those used in air conditioner ducting, and a separate cone attached to the back to act as a nozzle. The cone was also material used in HVAC application and was modified to have a small exit area in order to provide a higher exiting velocity therefore increasing thrust. Holes for the support rods were drilled in the back to provide support between the two non-rotating cylinders (innermost and outermost). Nylon tubes were mounted inside on the front of the external shell that would sit on the track cut out on the rotating cylinder.

SHEILA-D consisted of two motors powered by one battery that lead to two switches connected in parallel. On one side of the parallel wiring was a switch along with a potentiometer and the other side of the parallel was a switch alone. In startup the side that contained the potentiometer and switch was used first in order to provide a slow startup then at full speed the other switch would be activated and thus be the official "on/off" switch.

13. Test Design/Location Scouting

In order to successfully complete this project, a few tests were developed to ensure functionality of the design. SHEILA-D would undergo go testing to determine: Run capability, air speed, water exit jet speed, water thrust, submerged top speed, stall acceleration and time, flow field, and battery discharge time. Four tests would ensure capturing of this data with the first one being an Air Test. This test would offer run capability and air speed out the back. To run this test an anemometer is needed to read air speed and testing supports would have to be constructed to constrain SHEILA-D.

The second planned test is an Open Water Test. This test will also determine run capability but provide submerged top speed, stall acceleration and time. In order to run this test, an apparatus called Rectilinear Motion Constraints (RMC) and a tow line will be deployed to control SHEILA-D. A testing location for test two was found at Frank G. Bonelli Park. Puddingstone Lake, found within Bonelli Park, is often used for recreation and project testing. After talking to another project team performing tests at Sail Boat Cove, a decision to test at the same location was finalized to meet all test requirements. Sail Boat Cove has a depth of 10ft and a length of 50ft in which to test SHEILA-D. Although the water clarity is poor and there can be some foot traffic, this location is perfect for easy and quick setup.

Test three is the Bath Tub Test which will be used to obtain water exit jet speed, water thrust, and flow field. This test will need a spring scale, dye, a waterproof anemometer, and use of the RMC. An inspection of SHEILA-D will have to be made prior to this test to ensure no damage was done during test two. The last test will be the Full Battery Discharge test. This will be performed right after test three as the same setup can be used. This test will provide battery run time and fade out.

14. Testing

Testing was first scheduled to begin on Monday, May 12th 2014 but a potentiometer failure delayed the testing schedule by a few days. Testing was conducted a few days later on Friday, May 16th 2014 at Puddingstone Lake. Team UV arrived at the test location at 0600 and promptly performed final sealing of the motor housing and camera location.

The RMC was positioned and after placing SHEILA-D in the water, the motors were powered on. The demonstrator began to move but power was quickly shut off after water was noticed to leak into the critical motor housing. Opening the motor housing through the observation dome allowed for draining of the water and quick drying. A second test was performed swiftly to obtain video footage for the presentation and to save the motors from frying. This test also failed as the vane shell stopped rotating due to high friction in the system.

An assessment day was scheduled for the following Saturday (5/17/2014) to improve the meshing of the gearset and to improve motor housing sealing. Filing of the gear faces to remove excess material and applying more epoxy to failed sealing areas provided an adequate solution to problems faced during the first test. Team UV also noticed that the vane shell was under a lot of friction. This was fixed by adjusting the location of the rear seal and thrust bearing. After air testing the improvements made to SHEILA-D, a planned water test was made for Monday, May 19th 2014.

On May 19th, 2014 SHEILA-D successfully completed an underwater test. Not only did the demonstrator move linearly in the water, it showed a striking free jet out the rear nozzle. Multiple runs were made to show the free jet and each run was video documented.

Additionally, testing of sub-assemblies was performed at various stages of the manufacturing timeline. Waterproof duct tape, which will be used to seal various components, underwent a submersed test to ensure sealing abilities. The conclusion was no decline in adhesion but water

did penetrate the dry interior of the tube. Another critical test was the confirmation of motor power and rotation. The final electrical circuit to power the motors was wired and allowed to run for a few minutes to confirm desired operation. Meshing of the gears once located on the motor housing was also video documented.

Future plans to test SHEILA-D have been made to collect performance data.

Need more testing

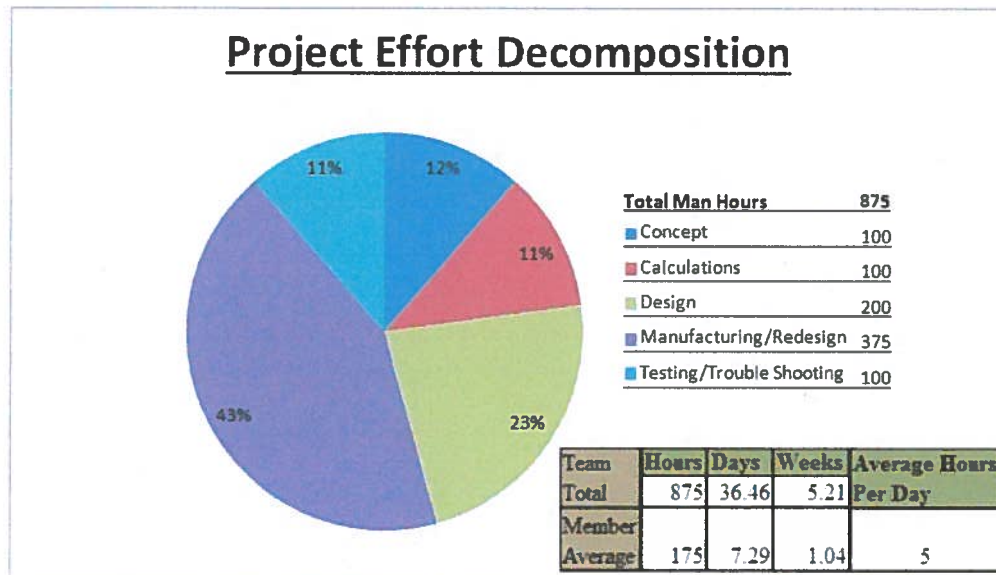
Great Section!

Results

Successful testing solidified the vision of SHEILA-D as an adaptable propulsion system demonstrator. Some very noteworthy results were realized through the second round of testing, including: successful production of a *initially laminar* freejet (and the thrust that is associated with this jet), minimal wake regions stemming off the front edges of the demonstrator, and steady flow out the rear of the convergent nozzle; the first two of these effects may be spotted by the trained eye in the flow field displayed in Figure 10. These positive results verify this type of propulsion as a viable option for the future, thus validating the intent of this project.

Having noted some of the good results associated with the successful testing, it is also necessary to note some of the pitfalls of the current design that were made more than apparent in testing: the current design is *not* hermetically sealed, in order to make efficient use of this type of propulsion (including reducing noise and thrust), much higher tolerances must be used in the manufacturing (and thus financial support must be obtained for the next phase of the project), and the buoyancy must be controlled (as is the demonstrator has a very high degree of positive buoyancy, thus causing SHEILA to float during testing). The upside to these negative results is that any bad things encountered in this phase will directly influence what will be learned from this phase (and thus what can be done in the next phase), none of these results were unforeseen (this is after all simply a propulsion *demonstrator*), and all of these results are things which can be fixed in the future; as a matter of fact, these are all things that currently have conceptual solutions in the planning stage for the next phase.

Lastly, it is important to comment on the time/effort required in this phase; this commenting will be done in reference to the figure below:



Moving down the list of subsections, the following may be noted:

- The concept phase was quite short in duration; this is in no way indicative of the level of thought that has gone into this project, this underwater vehicle (UV) concept is actually nearly five years old in planning (the initial concept was dreamt up in late 2009/early 2010).
- The calculations phase was lengthy, but not as long as it could have been; there does not exist a magical set of calculations that corresponds perfectly to this means of propulsion. This is to say that this concept is highly unconventional and many theories had to be applied, mixed, and adapted in order to do any calculations at all (and the ones done thus far in this phase have been simplified since there is much unknown about this type of flow or how to apply it).
- The design process was highly iterative and thus actually existed in some form or another throughout every stage of the project; the listed 200 hours is only considering meetings that were *purely* called with design-intent in mind.
- The manufacturing process was extremely difficult and time consuming as this really has not been done before, and thus even with having gone to great lengths to think the manufacturing through as much as possible prior to starting, it was simply impossible to foresee all the issues that the team came across. In addition to this, the design and manufacturing stages were highly intertwined as redesigns were constantly necessary to solve issues come across in manufacturing.
- Testing went off for the most part without a hitch in the end; initially there was a great deal of trouble with testing, and the demonstrator had to be torn down, modified, and built back up quite a few times, but eventually very highly promising results were obtained through testing.
- Lastly, it should be noted that the total man hours listed above is *highly* conservative; to give some sort of idea of the time involved in this project, it will be noted that the weekend of Friday May 9th to Sunday May 11th contained three back-to-back 15 hour days (that's 15 hours per member present per day). Weeks like this were quite typical and over the 35 day project period (April 15th-May 19th) many meetings ran to about 0400 the following day.

Roles and Responsibilities

	Role	Responsibilities
Brian Martin	Leader	Team leader for project. Designate tasks to group members, supervise design process, and assist in all aspects of the project. Create concept/preliminary drawings of system to build off and improve throughout the project. Report Roles: Background and Design Process
Ben Saletta	Member	Lead in design meeting. Coordinator for manufacturing methodology and material purchasing. Assist in drawing package, manufacturing, and design. Report Roles: Marketability and Design Process
Abraham Paucar	Member	Primary lead in stress calculations pertaining to gear strength, lead for manufacturing troubleshooting/innovation. Assist in manufacturing, and design. Report Roles: Introduction and Design Process
Ketton James	Member	Primary coordinator for project scheduling and timeline; in charge of compilation of final report. Assist in gear drawings, manufacturing, and design. Report Roles: Project Schedule, Roles & Responsibilities, & Design Process
Andrew Blancarte	Member	Lead in initial testing/troubleshooting of system. In charge of financial reimbursement/allocation of project funds. Assist in design and drawings. Report Roles: Competition and Design Process

* The actual writing of the report is a team effort and thus everyone has worked on the parts of the report as listed in the above table

Schedule

Draft Schedule made on 4/15/14 updated to reflect any changes along the way.

Master Project Draft Schedule			Drafted:	4/15/2014
Team UV	Brian Martin, Ketton James, Andrew Blancarte, Abraham Paucar, Ben Saletta			
ECD	RAA	Description		
4/16/2014	Ben	Brainstorming Session/Design Requirements/Subsystem Decomposition		
4/17/2014	Andrew	Preliminary Draft Report		
4/18/2014	Brian	Conceptual Renderings		
4/20/2014	Ketton	Configure Pricing Requirements/Calculations Deadline		
4/22/2014	Abraham	Purchasing Deadline		
4/26/2014	Ben	Manufacturing Start		
5/6/2014	Brian	Manufacturing Deadline		
5/6/2014	Andrew	Testing/Troubleshooting/Report/Final Drawings Period		
5/6/2014	Abraham	Draft Report #1		
5/13/2014	Ketton	Draft Report #2		
5/20/2014	Brian	Testing/Troubleshooting/Report/Final Drawings Period		
5/20/2014	Team	Project Duedate		

Contact Information

Name	Phone	Email
Brian Martin	(818) 282-5186	bmartin@csupomona.edu
Ketton James	(909) 994-5663	kettonjames@hotmail.com
Abraham Paucar	(562) 810-3002	aipaucar@csupomona.edu
Andrew Blancarte	(909) 510-0593	aeblanarte@gmail.com
Ben Saletta	(760) 877-9860	bdsalletta@csupomona.edu

Project Time Schedules

Name	M	Tu	W	Th	F	Sat	Sun
Andrew	n/a	1500>	n/a	1500>	1100>	All	All
Abraham	1200-1600; <1800	1200-1600	1200-1600; 1800>	1200-1600	1200-1600	<1400	n/a
Ketton	n/a	1100-1600	n/a	1100-1600; 1715>	Appointment	All	All
Ben	<1600; 2200>	n/a	<1600; 2200>	n/a	All	All	All
Brian	<1200; 1400>	<1715	<1200; 1400>	n/a	All	All	All

Good -

Marketability

First and foremost this product is a proof of concept for an underwater propulsion system. While it can be a final product for some very limited applications it is meant to be a component in a larger scale system or attached to control surfaces. The propulsion system itself cost around \$700 (approximately 88% of the initial projected budget of \$800) and about 50 hours of work a week for 5 weeks. The cost is quite low for a project of this scale because the vast majority of the components are constructed using standard pipe or ducting sizes and commercial off the shelf components (COTS). There are only eleven custom parts in the whole design which makes the product cheaper and easier to manufacture. Ten of these custom parts were 3D printed gears. These could easily be replaced with steel or brass gears in the future with a minimal upfront investment. The final custom component was the vane shell. This part contains some significant complexity due to the helix shape of the fin blades. In order to mass produce this part, a custom die would have to be made and this would cause a significant upfront investment cost. If another of these propulsion systems were to be made it would cost around \$400; the prototype cost a bit more due to material waste and finding the proper manufacturing processes for the vanes and the shells. Overall there was not much wasted money because the design process was well thought out and involved detailed designs. There would be a significant tooling investment for the mass production of these propulsion systems due to the need for custom parts such as the gears and the vane shell approximately \$10,000 for all of them, 3 gear dies at \$1,500 and a custom vane die at \$5,000.

While this is only a proof of concept demonstrator, there are no other products on the market that use a propulsion system similar to this design. All other underwater systems use a propeller based propulsion system. Bladed propellers (while historically the propulsion system of choice) can cause problems due to their high susceptibility to cavitation, their tendency to foul upon collision with cable or kelp depending on the size of the application, may cause turbulent flow, and produce a significant amount of noise that can lead to detection of the device (which may be problematic in a stealth environment). This new propulsion system uses a relatively low speed but adds energy into the flow for a longer time and thus enables higher thrust without the threat of cavitation, while also significantly reducing turbulence in the flow, and the noise typically associated with the choppy flow of a propeller. The rotating components are enclosed which prevents fouling due to the debris in the water. The stealth and robustness of this design makes it ideal for research applications where the water is full of debris. This could also be applied to the navy with the stealth characteristics this device would look like a tuna to most detection devices.

6/21/2023

Conclusion

The original objective of this project was to explore the feasibility of using a new, innovative type of underwater propulsion for an underwater vehicle; in this respect, the project was a great success. SHEILA-D provides proof that water can be moved in order to produce a significant amount of thrust in a steady, even manner by rotating it through an annular region along an extruded length. The mechanics associated with this type of flow are little known and have been left virtually unexplored and painfully neglected by the world of marine and sub-marine propulsion. The propulsion demonstrator described in the preceding pages serves a function so as to merely glimpse through the proverbial looking glass into what this untapped innovative source of propulsion has to offer. This means of propulsion has the latent potential to revolutionize how underwater vehicles maneuver through and explore the world's oceans, lakes, and other bodies of water. From a quick, stealthy Information, Surveillance, and Reconnaissance (ISR) drone that may be used by US Navy SEALs behind enemy lines to a hidden-in-plain-sight observation vehicle that may be used by marine biologists to study marine life in an unimposing manner, the future underwater vehicle as will be developed from SHEILA-D will have the ability to provide unprecedented capabilities in a very diverse field of applications. This seemingly straight-forward, yet extremely complex, well thought out, comprehensively developed demonstrator project will have huge implications as it is carried through into the next phase of its existence as it is adapted into a fully operational underwater vehicle.

Lead:

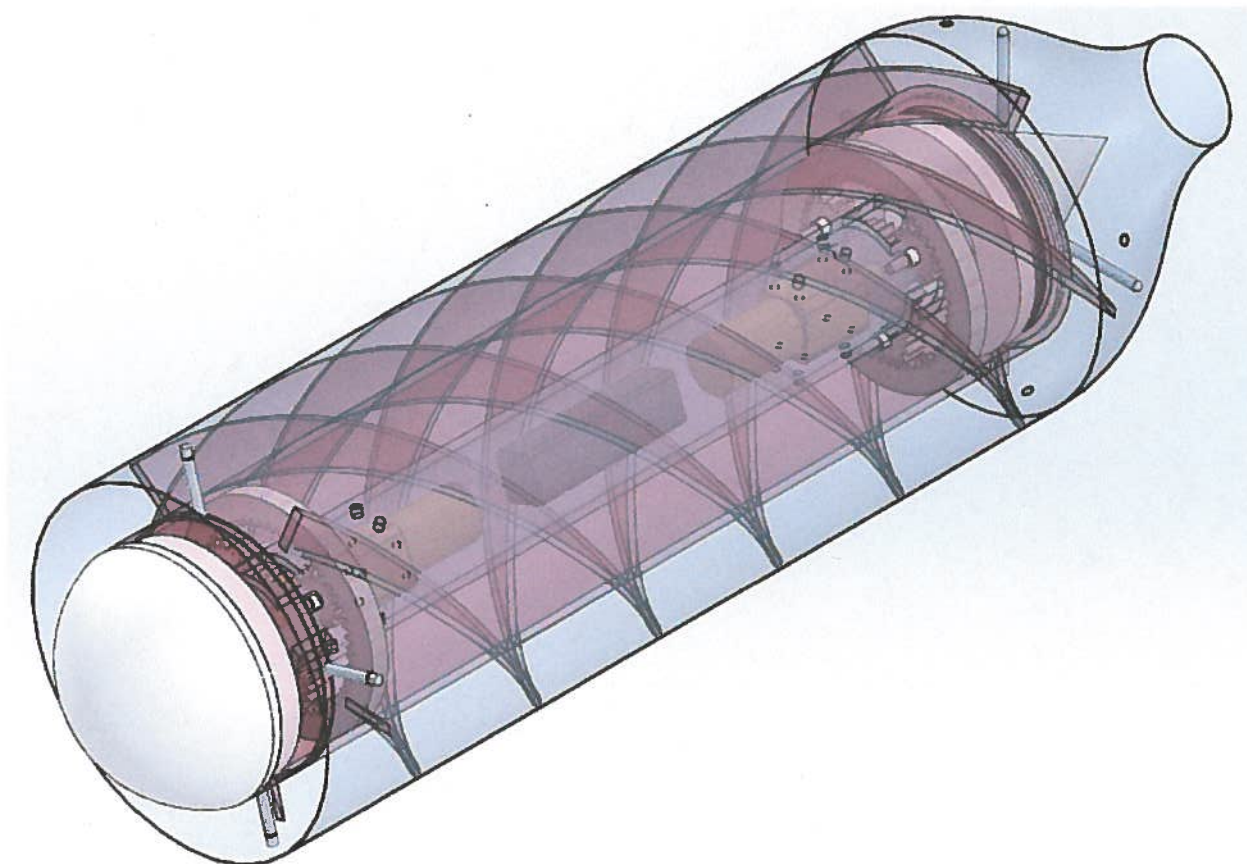


Figure 1: Isometric View of SHEILA-D

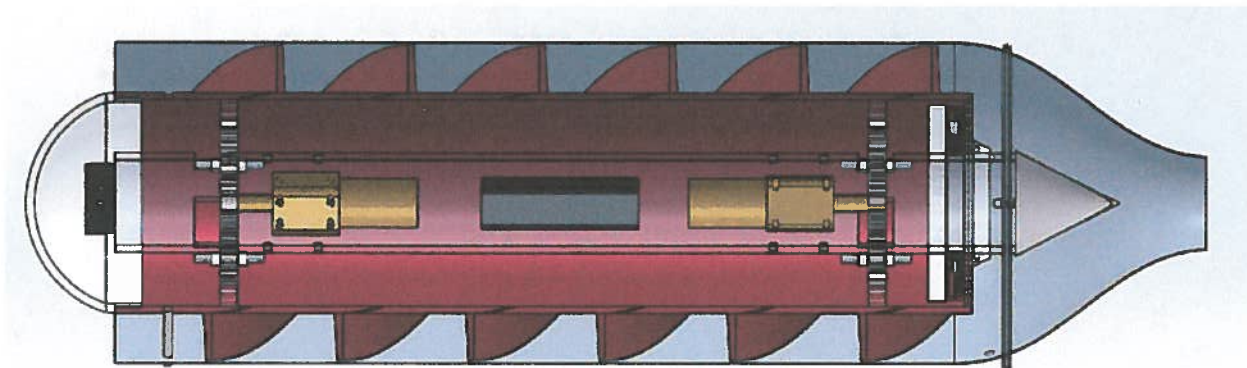


Figure 2: Cutaway Side View

Nice View

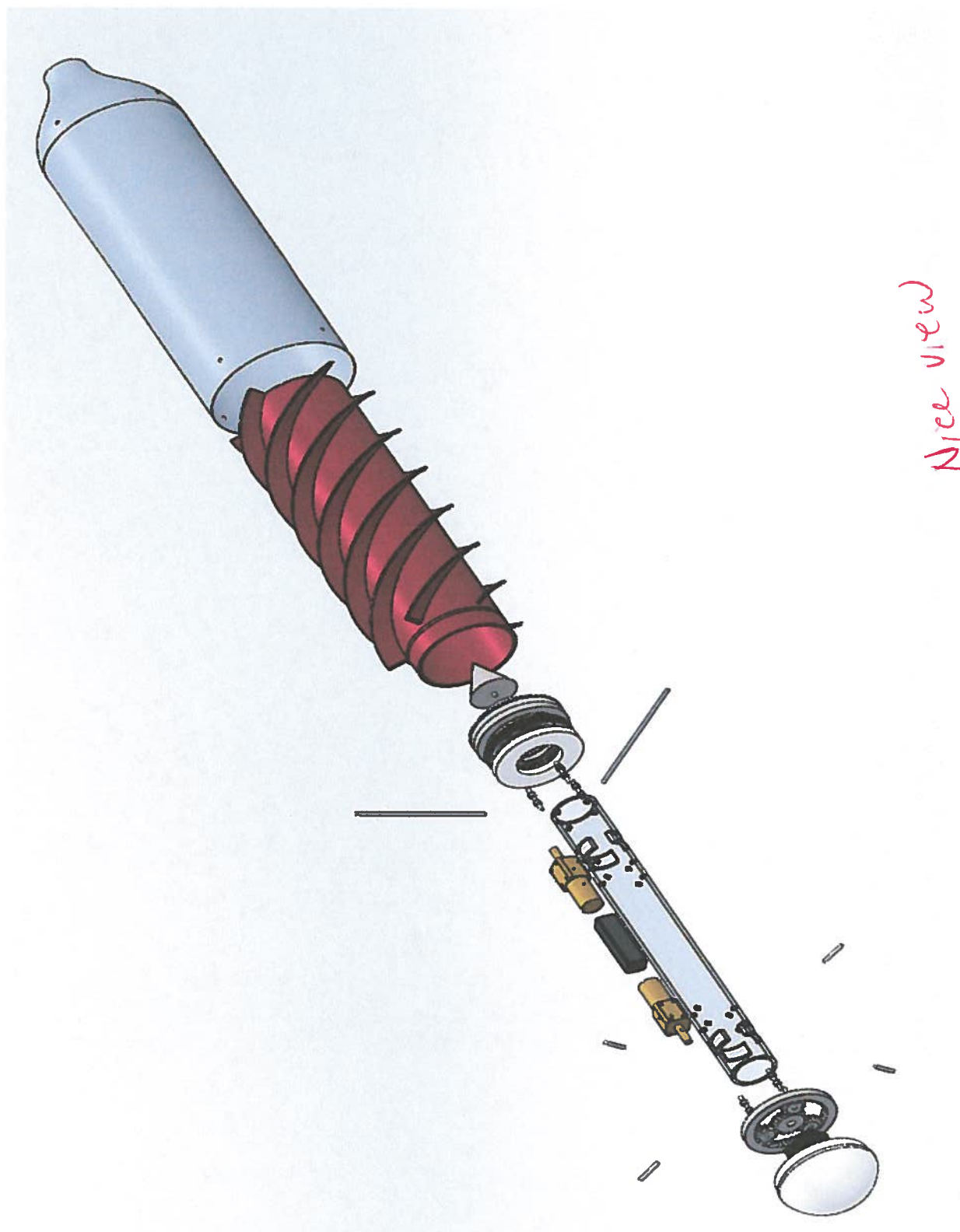


Figure 3: Exploded View of SHEILA-D

Appendix B

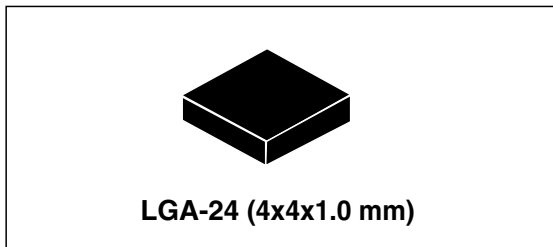
Presentation Format

Appendix C

Electronics Data Sheets

iNEMO inertial module: 3D accelerometer, 3D gyroscope, 3D magnetometer

Datasheet - production data



Features

- 3 acceleration channels, 3 angular rate channels, 3 magnetic field channels
- $\pm 2/\pm 4/\pm 6/\pm 8/\pm 16\text{ g}$ linear acceleration full scale
- $\pm 2/\pm 4/\pm 8/\pm 12$ gauss magnetic full scale
- $\pm 245/\pm 500/\pm 2000$ dps angular rate full scale
- 16-bit data output
- SPI / I²C serial interfaces
- Analog supply voltage 2.4 V to 3.6 V
- Power-down mode / low-power mode
- Programmable interrupt generators
- Embedded self-test
- Embedded temperature sensor
- Embedded FIFO
- Position and motion detection functions
- Click/double-click recognition
- Intelligent power saving for handheld devices
- ECOPACK®, RoHS and “Green” compliant

Applications

- Indoor navigation
- Smart user interfaces
- Advanced gesture recognition
- Gaming and virtual reality input devices
- Display/map orientation and browsing

Description

The LSM9DS0 is a system-in-package featuring a 3D digital linear acceleration sensor, a 3D digital angular rate sensor, and a 3D digital magnetic sensor.

The LSM9DS0 has a linear acceleration full scale of $\pm 2g/\pm 4g/\pm 6g/\pm 8g/\pm 16g$, a magnetic field full scale of $\pm 2/\pm 4/\pm 8/\pm 12$ gauss and an angular rate of $\pm 245/\pm 500/\pm 2000$ dps.

The LSM9DS0 includes an I²C serial bus interface supporting standard and fast mode (100 kHz and 400 kHz) and an SPI serial standard interface.

The system can be configured to generate interrupt signals on dedicated pins and is capable of motion and magnetic field detection. Thresholds and timing of interrupt generators are programmable by the end user.

Magnetic, accelerometer and gyroscope sensing can be enabled or set in power-down mode separately for smart power management.

The LSM9DS0 is available in a plastic land grid array package (LGA) and it is guaranteed to operate over an extended temperature range from -40 °C to +85 °C.

Table 1. Device summary

Part number	Temperature range [°C]	Package	Packing
LSM9DS0	-40 to +85	LGA-24	Tray
LSM9DS0TR	-40 to +85	LGA-24	Tape and reel

1.2 Pin description

Figure 2. Pin connections

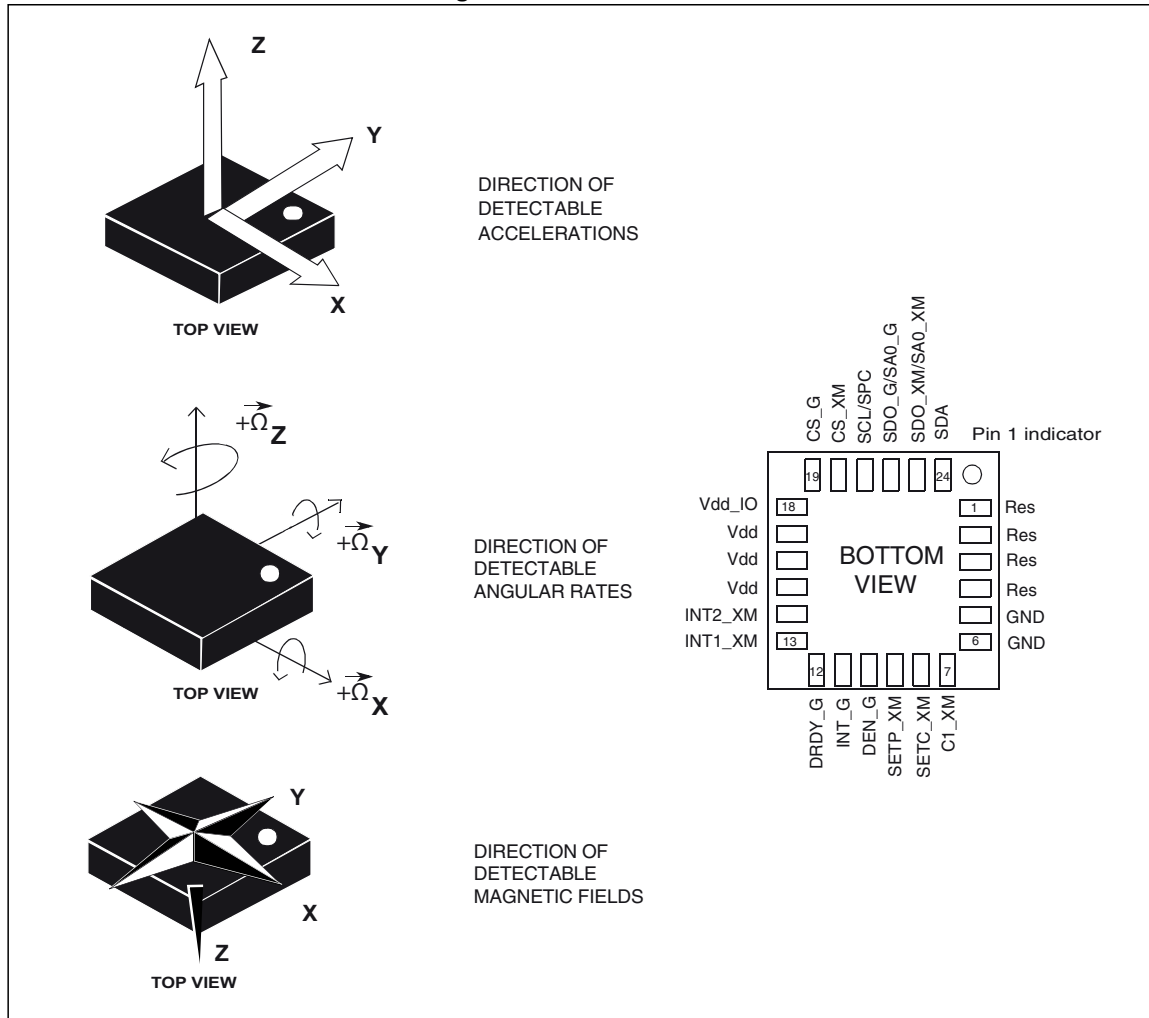


Table 2. Pin description

Pin#	Name	Function
1	Reserved	Leave unconnected
2	Reserved	Connect to GND
3	Reserved	Connect to GND
4	Reserved	Connect to GND
5	GND	0 V supply
6	GND	0 V supply
7	C1_XM	Capacitor connection (C1)
8	SETC_XM	S/R capacitor connection (C2)
9	SETP_XM	S/R capacitor connection (C2)
10	DEN_G	Gyroscope data enable
11	INT_G	Gyroscope programmable interrupt
12	DRDY_G	Gyroscope data ready
13	INT1_XM	Accelerometer and magnetic sensor interrupt 1
14	INT2_XM	Accelerometer and magnetic sensor interrupt 2
15	Vdd	Power supply
16	Vdd	Power supply
17	Vdd	Power supply
18	Vdd_IO	Power supply for I/O pins
19	CS_G	Gyroscope I ² C/SPI mode selection 1: SPI idle mode / I ² C communication enabled 0: SPI communication mode / I ² C disabled
20	CS_XM	Accelerometer and magnetic sensor SPI enabled I ² C/SPI mode selection 1: SPI idle mode / I ² C communication enabled 0: SPI communication mode / I ² C disabled
21	SCL SPC	I ² C serial clock (SCL) SPI serial port clock (SPC)
22	SDO_G SA0_G	Gyroscope serial data output (SDO) Angular rate sensor I ² C less significant bit of the device address (SA0)
23	SDO_XM SA0_XM	Accelerometer and magnetic sensor SPI serial data output (SDO) Accelerometer and magnetic sensor I ² C less significant bit of the device address (SA0)
24	SDA	I ² C serial data (SDA)

2 Module specifications

2.1 Sensor characteristics

@ Vdd = 3.0 V, T = 25 °C unless otherwise noted^(a)

Table 3. Sensor characteristics

Symbol	Parameter	Test conditions	Min.	Typ. ⁽¹⁾	Max.	Unit
LA_FS	Linear acceleration measurement range ⁽²⁾			±2		g
				±4		
				±6		
				±8		
				±16		
M_FS	Magnetic measurement range			±2		gauss
				±4		
				±8		
				±12		
G_FS	Angular rate measurement range			±245		dps
				±500		
				±2000		
LA_So	Linear acceleration sensitivity	Linear acceleration FS = ±2 g		0.061		mg/LSB
		Linear acceleration FS = ±4 g		0.122		
		Linear acceleration FS = ±6 g		0.183		
		Linear acceleration FS = ±8 g		0.244		
		Linear acceleration FS = ±16 g		0.732		
M_GN	Magnetic sensitivity	Magnetic FS = ±2 gauss		0.08		mgauss/ LSB
		Magnetic FS = ±4 gauss		0.16		
		Magnetic FS = ±8 gauss		0.32		
		Magnetic FS = ±12 gauss		0.48		
G_So	Angular rate sensitivity	Angular rate FS = ±245 dps		8.75		mdps/ digit
		Angular rate FS = ±500 dps		17.50		
		Angular rate FS = ±2000 dps		70		
LA_TCS0	Linear acceleration sensitivity change vs. temperature	From -40 °C to +85 °C		±1.5		%
M_TCS0	Magnetic sensitivity change vs. temperature	From -40 °C to +85 °C		±3		%

a. The product is factory calibrated at 3.0 V. The operational power supply range is from 2.4 V to 3.6 V.

Table 3. Sensor characteristics (continued)

Symbol	Parameter	Test conditions	Min.	Typ. ⁽¹⁾	Max.	Unit
G_SoDr	Angular rate sensitivity change vs. temperature	From -40 °C to +85 °C		±2		%
LA_TyOff	Linear acceleration typical zero-g level offset accuracy ⁽³⁾⁽⁴⁾			±60		mg
G_TyOff	Angular rate typical zero-rate level	FS = 245 dps		±10		dps
		FS = 500 dps		±15		
		FS = 2000 dps		±25		
LA_TCOff	Linear acceleration zero-g level change vs. temperature	Max delta from 25 °C		±0.5		mg/°C
G_TCOff	Zero-rate level change vs. temperature			±0.05		dps/°C
M_EF	Maximum exposed field	No perming effect on zero reading			10000	gauss
M_DF	Magnetic disturbing field	Sensitivity starts to degrade. Automatic S/R pulse restores the sensitivity ⁽⁵⁾			20	gauss
LA_ST	Linear acceleration self-test positive difference ⁽⁶⁾⁽⁷⁾	±2 g range, X, Y, Z-axis AST1:0 = 01 see Table 74	60		1700	mg
G_ST	Angular rate self-test output change ⁽⁸⁾⁽⁹⁾	FS = 245 dps	20		250	dps
		FS = 500 dps	70		400	
		FS = 2000 dps	150		1000	
Top	Operating temperature range		-40		+85	°C

1. Typical specifications are not guaranteed
2. Verified by wafer level test and measurement of initial offset and sensitivity
3. Typical zero-g level offset value after MSL3 preconditioning
4. Offset can be eliminated by enabling the built-in high-pass filter
5. Set / Reset Pulse is automatically applied at each conversion cycle
6. "Self-test output change" is defined as: OUTPUT[mg]_{(CTRL_REG2_XM (21h) AST1:0 enabled)} - OUTPUT[mg]_{(CTRL_REG2_XM (21h) AST1:0 disabled)}
7. For polarity refer to [Table 77: Self-test mode configuration](#)
8. "Self-test output change" is defined as: OUTPUT[mg]_{(CTRL_REG4_G (23h) ST1:0 enabled)} - OUTPUT[mg]_{(CTRL_REG4_G (23h) ST1:0 disabled)}
9. For polarity refer to [Table 31: Self-test mode configuration](#)

2.2 Temperature sensor characteristics

The electrical characteristics concerning the temperature sensor are given in the table below.

@ Vdd = 3.0 V, T=25 °C unless otherwise noted.

Table 4. Temperature sensor electrical characteristics

Symbol	Parameter	Test conditions	Min.	Typ. ⁽¹⁾	Max.	Unit
TSDr	Temperature sensor output change vs. temperature	-		8		LSB/°C
TODR	Temperature refresh rate			M_ODR [2:0] ⁽²⁾		Hz
Top	Operating temperature range		-40		+85	°C

1. Typical specifications are not guaranteed.
2. Refer to [Table 84: Magnetic data rate configuration](#).

2.3 Electrical characteristics

@ Vdd = 3.0V, T = 25 °C unless otherwise noted^(b)

Table 5. Electrical characteristics

Symbol	Parameter	Test conditions	Min.	Typ. ⁽¹⁾	Max.	Unit
Vdd	Supply voltage		2.4		3.6	V
Vdd_IO	Module power supply for I/O		1.71	1.8	Vdd+0.1	
Idd_XM	Current consumption of the accelerometer and magnetic sensor in normal mode ⁽²⁾	HR setting CTRL_REG5_XM (M_RES [1,0]) = 11b, see CTRL_REG5_XM (24h)		350		µA
Idd_G	Gyroscope current consumption in normal mode ⁽³⁾			6.1		mA
Idd_G_LP	Gyroscope supply current in sleep mode ⁽⁴⁾			2		mA
Idd_Pdn	Current consumption in power-down mode ⁽⁵⁾			6		µA
VIH	Digital high-level input voltage		0.8*Vdd_IO			V
VIL	Digital low-level input voltage				0.2*Vdd_IO	V
VOH	High-level output voltage		0.9*Vdd_IO			V
VOL	Low-level output voltage				0.1*Vdd_IO	V
Top	Operating temperature range		-40		+85	°C

1. Typical specifications are not guaranteed
2. Magnetic sensor setting ODR =6.25 Hz, Accelerometer sensor ODR =50 Hz, gyroscope in power-down mode
3. Accelerometer and magnetic sensor in power-down mode
4. Sleep mode introduces a faster turn-on time compared to power-down mode. Accelerometer and magnetic sensor in power-down mode.
5. Linear accelerometer, magnetic sensor and gyroscope in power-down mode

b. LSM9DS0 is factory calibrated at 3.0 V

Appendix D

Senior Project Primer Package

Memorandum

To: Professor Coburn

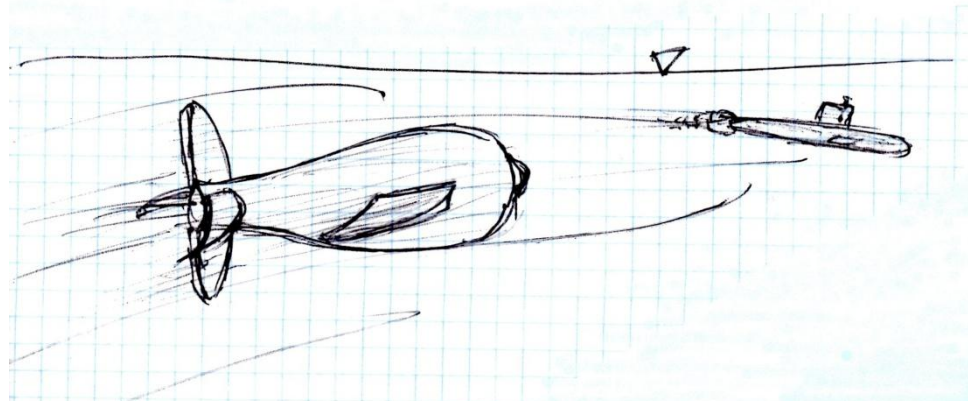
Date: June 8th, 2014

From: Brian Martin

Subject: Senior Project Proposal/Primer Package

The following pages contain the required elements of the senior project proposal package as they relate to the senior project that I wish to launch. The specific section breakdown of this package is as follows:

■ <u>Topic</u>	<u>Page 2</u>
• Phase I (ME 325/L)	
• Phase II (EGR 481/482)	
■ <u>Objective</u>	<u>Page 2</u>
• Mission Objectives	
• Operational & Design Objectives	
■ <u>Partners</u>	<u>Page 5</u>
• Team Member Profile Forms	
■ <u>Schedule/Timeline</u>	<u>Page 10</u>
■ <u>Challenges/Obstacles</u>	<u>Page 10</u>
• Design	
• Analysis	
• Manufacturing	
• Financial	
■ <u>Preliminary assessment of achievability of objectives</u>	<u>Page 12</u>
• Mission Objectives	
• Operational Objectives	
• Challenges/Obstacles	
■ <u>Proof of 300 level coursework completion</u>	<u>Page 14</u>
• Senior Project Eligibility Check Sheet	



Topic

Phase I (ME 325/L)

Design of an innovative underwater propulsion system based off of an annular screw concept

- Resulted in *SHEILA-D (Submerged Hydrodynamically propelled Explorer, Implementation: Los Angeles – Demonstrator)*.

Phase II (EGR 481/482)

Design of an innovative, highly maneuverable, stealthy unmanned underwater vehicle with ISR* capabilities

*ISR here refers to *Information, Surveillance, and Reconnaissance*.

Objective

The objective of this senior project is to develop an unmanned underwater vehicle (UUV) based off of an innovative propulsion system, merit of which was demonstrated through completion and testing of SHEILA-D (as defined above), an innovative propulsion system demonstrator developed through a ME 325/L project.

SHEILA-D (as developed in ME 325/L) was a Phase I concept demonstrator and, in as much, accomplished the goal of producing thrust through the propulsion mechanics that the project was designed to test. The senior project (as will be developed in EGR 481/482) will be Phase II of this effort and will focus on the design, building, and testing of the full solution, namely, the fully operational underwater vehicle (UV). The propulsion mechanism developed through SHEILA-D will either be directly used or adapted for use in the UV, as determined by the results of performance characteristic, flow field, and other types of testing that will be conducted during the Summer 2014 time period.

The senior project will be comprised of many subsystems, which must be integrated together in order to produce the fully operational vehicle; some of these subsystems are as follows:

- Propulsion system (as adapted from SHEILA-D)
- Maneuverability systems
 - Control surfaces
 - Control electrical systems
 - Control module
- Buoyancy system
 - Buoyancy control (mechanical components, etc.)
 - Buoyancy control electrical systems
 - Buoyancy control module

- Body
 - Streamlining
 - Subsystem housing
 - Structural support system
- Communications/Autonomy System
 - More than likely autonomous, not remotely operated, as this compromises stealth and limits the area of operations
 - \Possibly some sort of sensing and avoidance system

The above systems are those that have been selected as the focus of the Phase II effort. This list may be amended or added onto as the project progresses, but the main system decomposition (Propulsion, Maneuverability, Buoyancy, Body, Communications/Autonomy) will remain in place, but may be added to as any issues may arise over the course of the project.

In terms of engineering subject decomposition, the senior project goals will be assessed through the following major subjects/categories:

- Mechanical design
- Electromechanical systems
- Materials selection
- Fluid mechanics
- Heat transfer (see Challenges/Obstacles)

None of these subjects saw optimal usage in the Phase I effort, mostly on account of lack of time and proper funding. Both of these deficiencies will be corrected for in the Phase II effort.

Mission Objectives

(As per the initial Mission Objectives sheet developed in April 2014)

Mission Objectives*

1. Fluid/smooth maneuvering
2. Higher speeds
3. STEALTH
 - i. Thermal signature
 - ii. Magnetic signature
 - iii. Noise
 - iv. Flow signature
 - v. Cavitation
 - vi. Inconspicuous
4. Little to no human interaction necessary

*These objectives were set out in the initial concept stage of this project and must be carried through to the final design/testing phases. Violation/endangerment/jeopardizing of these mission objectives is equivalent to a failure of the mission; as such, these mission objectives should be upheld throughout the project period and must be repeatedly referenced for compliance.

Operational & Design Objectives

The operational and design objectives will be more comprehensively assessed at the end of the Summer 2014 time period; a short list of initial operational objectives which are subject to alteration at the end of the aforementioned time period follows:

- Depth range of ~100-200 ft
- Speed of ~ 5 knots
- Size limited to approximately that of a scuba tank
- Weight which aims to increase thrust-to-weight ratio, but reduce the amount of positive buoyancy that the buoyancy control systems must overcome; the weight might possibly be used to induce neutral buoyancy at a prescribed depth
- Operational times of ~ 1 hour at full power
- Maximization of internal space for stowage of the sensor suite
- Eases of storage and transportation/portability
- Ease of maintenance/reduction in required maintenance

Partners

Brian Martin, Ketton James, Ben Saletta, Andrew Blancarte, Abraham Paucar

Team Member Profile Forms

Team UV Team Member Profile Form

Date: 5/24/14

I. Academic Info

Team Member Name: Brian Martin

Date Joined Team (MM YY): 04/14

Major Curriculum Year: M.E. 09-10

Current Standing (i.e. 5th Year): 5th Year

Expected Graduation Quarter: Winter 2015

Interested in Higher Academic Degrees (Yes/No): Yes

If marked Yes, list any associated interests:

Fluid Mechanics, Materials Science, Aerospace Eng., Automotive Eng., Naval/Marine Eng.

II. Career Info

List any industries/fields/topics of interest:

Defense industry, all topics listed above

List any jobs of interest:

Designing vehicles (sea, air, land, manned, unmanned, etc.) in defense industry.

III. Project Info

List favorite aspect(s) of your role in the project thus far:

Overall system design, fluid mechanics.

List the aspect(s) of the project that you are most interested in going forward:

Fluids/performance characteristics, innovative subsystem & system solutions.

IV. Capabilities Info

List a few strengths that will help the team move forward:

- Ability for experience with innovation.
- Well read/studied.
- Extremely passionate about engineering & this specific project.

List at least one weakness area you think you can improve in:

- Shy, so leading a team can be difficult. - Very busy, need to further improve time management.

V. Additional Comments

(& offloading)

Hobbies: Wakeboarding, hiking/camping, dogs, reading/learning, engineering projects.

Passion: Engineering, defense industry, support for military, dogs, all things waterbased, this project.

If you have anything else you would like to comment on, please list here:

- hope to one day open my own small, special projects type engineering firm for projects like this one.
- Stoked about the future of this project & this team.

Team UV Team Member Profile Form

Date: 6/2/2014

I. Academic Info

Team Member Name: KETTON JAMES Date Joined Team (MM YY): 04/2014

Major Curriculum Year: ME / 2008 Current Standing (i.e. 5th Year): 6th

Expected Graduation Quarter: June 2015 Interested in Higher Academic Degrees (Yes No): Yes

If marked Yes, list any associated interests:

SOLID MECHANICS AND/OR MBA

II. Career Info

List any industries/fields/topics of interest:

OTIS ELEVATOR, BECOMING STRESS ANALYST TO ELEVATOR DESIGN

List any jobs of interest:

DESIGN ENGINEER JET TURBINE ENGINEER

III. Project Info

List favorite aspect(s) of your role in the project thus far:

INITIAL DESIGN/DESIGN REFINEMENT

List the aspect(s) of the project that you are most interested in going forward:

FURTHER DESIGN REFINEMENT/INNOVATION

IV. Capabilities Info

List a few strengths that will help the team moving forward:

ANOTHER VIEW TO CREATE A SOUND DESIGN.

List at least one weakness/area you think you can improve in:

AVAILABILITY AND ANALYSIS

V. Additional Comments

Hobbies: RECREATIONAL SPORTS, & WORKING ON MY CAR.

Passion:

LEARNING NEW THINGS. TAKING ON ANY NEW CHALLENGE.

If you have anything else you would like to comment on, please list here:

Team UV Team Member Profile Form

Date: 5/27/14

I. Academic Info

Team Member Name: Ben Salietta

Date Joined Team (MM/YY):

04

3/14

Major Curriculum Year: ME 10-11

Current Standing (i.e. 5th Year): 4th Year

Expected Graduation Quarter: Spring 15

Interested in Higher Academic Degrees (Yes/No): Yes

If marked Yes, list any associated interests:

Ocean Engineering, Fluid Mechanics

II. Career Info

List any industries/fields/topics of interest:

Ocean, Sustainability, Biomimicry, innovation

List any jobs of interest:

Ones that Pay Money, Design Engineering

III. Project Info

List favorite aspect(s) of your role in the project thus far:

Finding creative solutions to problems & working around obstructions

List the aspect(s) of the project that you are most interested in going forward:

Simplifying & controlling Navigation.

IV. Capabilities Info

List a few strengths that will help the team move forward:

Creative Problem Solving, Some practical experience with electrical controls

Some welding experience.

List at least one weakness area you think you can improve in:

I tend to over invest in my own ideas.

V. Additional Comments

Hobbies: SCUBA Diving, Rock Climbing

Passion:

Underwater exploration,

If you have anything else you would like to comment on, please list here:

Team UV Team Member Profile FormDate: 5/27/14**I. Academic Info**

Team Member Name:	<u>Andrew Blancarte</u>	Date Joined Team (MM YY):	<u>04/14</u>
Major Curriculum Year:	<u>M.E 2008-09</u>	Current Standing (i.e. 5th Year):	<u>6th Year</u>
Expected Graduation Quarter:	<u>Winter 15</u>	Interested in Higher Academic Degrees (Yes/No):	<u>No</u>

If marked Yes, list any associated interests:

II. Career Info

List any industries/fields/topics of interest:

Product Development, Medical Equipment, robotics.

List any jobs of interest:

Testing and/or Quality**III. Project Info**

List favorite aspect(s) of your role in the project thus far:

I really enjoyed the manufacturing phase of our project and testing.

List the aspect(s) of the project that you are most interested in going forward:

Arduino coding, controls, electronics.**IV. Capabilities Info**

List a few strengths that will help the team moving forward:

Willing to commit large amounts of time. Very hands on.

List at least one weakness/area you think you can improve in:

I would like to be more involved with design calculations.**V. Additional Comments**Hobbies: Working on Sheila-D, Driving my Camaro, spending time w/the family

Passion:

Passion for Success :)

If you have anything else you would like to comment on, please list here:

Team UV Team Member Profile FormDate: 5/26/14**I. Academic Info**Team Member Name: Abraham Paurar Date Joined Team (MM/YY): 04/14Major/Curriculum Year: ME / 2009 Current Standing (i.e. 5th Year): 5th YearExpected Graduation Quarter: Spring 2015 Interested in Higher Academic Degrees (Yes/No): _____

If marked Yes, list any associated interests:

Materials / Stress Analysis**II. Career Info**

List any industries/fields/topics of interest:

Materials, Stress analysis

List any jobs of interest:

anything**III. Project Info**

List favorite aspect(s) of your role in the project thus far:

Design of SHEILA, stress calculations

List the aspect(s) of the project that you are most interested in going forward:

Controls and programming**IV. Capabilities Info**

List a few strengths that will help the team moving forward:

Stress analysis, machine design, experience w/ Arduino programming

List at least one weakness/area you think you can improve in:

Design suggestions**V. Additional Comments**Hobbies: Music, Dance, sleeping, Hiking, Jesus

Passion:

If you have anything else you would like to comment on, please list here:

Schedule/Timeline

The following schedule is subject to change and **will** be changed in the coming months as the amount of work completed over Summer Break (06/16/14-09/25/14) will be reflected in a much more polished schedule which will be developed in mid to late September 2014. As such, the schedule below is a *very* rough picture of the objective timeline.

Date		Description	Tasks	Notes
Start	End			
	06/16/14	1st Phase II (Intro) Meeting	Phase I debrief, financial assets, project organization, concept	
06/16/14	09/25/14	Summer Break	Concept, preliminary calcs, preliminary drawings, parts search, redesign (post parts search)	Meetings every other week (possibly more often in September)
09/25/14	12/13/14	Fall 2014	Redesign (post parts search), complex calcs/analysis, manufacturing start	At least weekly meetings
12/13/14	01/06/14	Winter Break	Manufacturing/assembling	At least weekly meetings
01/06/15	03/21/15	Winter 2015	Manufacturing/assembling, testing, final analysis, report preparation	At least weekly meetings Project Deadline: 03/21/15
03/21/15	06/30/15	Spring 2015	Polishing, presentation preparation	Meetings every other week
	06/30/15	Project Symposium	Project presentation	Set sights on Showcase

Challenges/Obstacles

As with any project that ventures into the unknown and attempts to accomplish what has not been done before, this project is born into a nest of challenges and obstacles, a relatively short list of which follows (as classified into one of four categories).

Design

Many of the same design challenges as were faced in the Phase I effort will continue to represent obstacles in the Phase II effort; but, as always, obstacles exist to be overcome. Some of the challenging areas that will be carried over from the Phase I effort include:

- Sealing/waterproofing
- Streamlining/reduction of drag
- Efficient use/transmission of power to produce thrust
- Proper structural support

Along with these continuing challenges will come a whole slew of new challenges, including:

- Navigation (communication/autonomy)
- Maneuverability (directional control)
- Buoyancy control
- Heat transfer (for electronics cooling and reduction of thermal signature)

- Materials selection (for corrosion control, weight control, cost control, manufacturability, reduced thermal, noise, magnetic, signature)

Analysis

Just as was the case in the Phase I effort, virtually any analysis that will be done in the Phase II effort will have to be adapted from a wide variety of theories, which will need to be integrated together to provide the formulas and methodology needed for the analytical portion of this project. This is the case because of the innovative nature of the project. Some of the topics which relate to the analysis that will need to be performed, but which literature cannot be found or does not exist for, include:

- **Annular screw flow**
- Highly dynamic/acrobatic movement of an underwater vehicle
- Stealth on the small scale of this project
- Small scale buoyancy control

Some areas in which literature exists, but is not readily applicable to this project include:

- Sealing/waterproofing of a system subjected to great hydrostatic pressures
- Streamlining/drag reduction for a relatively high speed/highly dynamic, small scale UV
- Control surface design for a relatively high speed/highly dynamic, small scale UV

Lastly there are some areas in which literature has recently become more available with the recent upswing in popularity of underwater vehicles; therefore, these subjects represent less of a challenge with respect to analysis, but will still be time consuming in their adaptation. These areas/subjects are as follows:

- Navigation (more specifically, autonomous underwater vehicles (AUVs) have recently come into the spotlight; however, none of these vehicle are high speed nor high mobility, so this may lead to some interesting challenges)
- Materials selection for weight, cost savings, and corrosion control with respect to ocean-going vehicles (although current literature is unlikely to discuss stealth considerations)

Manufacturing

This specific subset of complications revolves around the fact that in order to fulfill all of the challenges listed in the Design section (as well as *many, many* challenges that were not listed there), many custom parts will have to be manufactured, as Commercial Off The Shelf components (COTS) will simply not fit the needs associated with this project. In addition to this, as was seen in the Phase I effort, many of the tolerances must be held quite tight in order to produce optimal results.

Financial

This is truly the most limiting of all of the challenges that will be faced in the Phase II effort. As was noted before, the mindset of this team is that obstacles exist to be overcome. This is a highly talented, capable, motivated, determined, and innovative team, but these assets cannot be fully taken advantage of without proper funding.

The Phase I effort amounted to \$769.74 and produced a demonstrator that was almost completely constructed by hand and which had loose tolerances, numerous inefficiencies, far less-than-optimal materials (truthfully, it was a materials engineers worst nightmare), and was not aesthetically pleasing. In order to produce meaningful results in Phase II, the project simply cannot be funded by the team itself; the team must obtain financial backing.

The lower limit of funding necessary will more than likely be in the \$3k-\$5k range in order to accomplish what this team has set out to do. There does not exist an upper limit to the amount of funding that the team can receive, as no funding will go to waste. Any extra funding will be used to further the project in as many ways possible or to complete more comprehensive, more polished testing.

Preliminary assessment of achievability of objectives

Mission Objectives

The mission objectives as set forth are all within the realm of achievability. With the Phase I effort, these objectives were at the very least partially addressed, with some of them actually achieved with some degree of success (cavitation, flow signature, thrust which will lead the way to high speeds). As noted in the Mission Objectives portion of the Objective section, failure to meet these objectives will not be tolerated, and as such, they will remain the top project priorities.

Operational & Design Objectives

The depth range listed above is very attainable with proper water proofing and sealing, which will be a major component of the Phase II effort. The speed is well within the range of capabilities that the propulsion system will be able to provide for. Size, weight, portability, internal sensor suite spacing, and maintenance concerns will all be addressed in a highly redundant, iterative manner throughout the duration of the project. Lastly, SHEILA-D had a full power operational time of about 30 minutes (as determined through power calculations) and thus scaling this up to 1 hour will be a challenge as a result of all of the new subsystems, but is certainly doable as the team has already learned quite a bit about providing the necessary power since the conclusion of the Phase I effort.

Challenges/Obstacles

While all of the aforementioned challenges and obstacles might amount to what would be normally viewed as an insurmountable barrier, this is not an average team.

The design challenges can and will all be overcome. SHEILA-D was developed in just over a month and represented something that had never been done before. This team now has 9 months (Summer 2014, Fall 2014, Winter 2015) to complete the rest of the design; this is well within this team's operational capabilities. Overcoming the design challenges is simply a matter of finding time (which we have plenty of) to do so and being motivated enough to do so. The latter is a non-issue for this team.

The analysis challenges are simply stimuli to encourage more learning outside of the class room, which is exactly what this project is all about. It was known going into this project that these challenges would push all of the team members outside of their comfort zones, and thus this is not a deterrent. The team has already begun researching, picking out textbooks, and extending their knowledge for the Phase II effort; the Team UV library currently consists of 13 textbooks, 2 guides, 3 magazines, 36 technical papers, and 2 videos all relating to the Phase II effort and this list is quickly growing.

The manufacturing challenges are simply something that must be worked through in a highly introspective, well-measured manner. This is to say that the trigger will not be pulled on any manufacturing until all possible kinks will be thought out; in addition to this, in order to reduce costs and maintenance, while increasing usability, these challenges will have quite a chunk of time dedicated to them.

Lastly comes the financial hurdles mentioned earlier. In order to remedy this situation, two main means of funding are being looked into:

- Crowd-funding (Through websites like KickStarter, Indiegogo, Smallknot, and RocketHub)
- Sponsorships (Through local companies providing funding, products, or services)
 - One team member was previously part of Formula SAE and thus has experience with this type of funding
- Donations
 - Another team member is part of Cal Poly Pomona's effort to receive school donations/funding and thus is familiar with this kind of funding and is currently looking into tax write offs or other benefits for donators
- We are open to just about any source of funding; however it should be noted that the reason we are not considering research grants as much as these other sources is due to restrictions that may be incurred with respect to the project as well as possible issues with creative rights, as this project is 5 years in development conceptually and the team is in no way willing to risk loss of creative rights.

Proof of 300 level coursework completion

Senior Project Eligibility Check Sheet

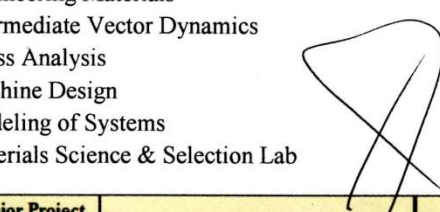
Senior Project Eligibility Check Sheet

Project Duration: Fall 2014-Winter 2014 Project Advisor: Dr. Todd Coburn Email: tdcoburn@csupomona.edu

This page provides verification of completion of all 300 level courses prior to start of the senior project for each team member involved.

300 level courses required to graduate as a Mechanical Engineering undergraduate at Cal Poly Pomona are as follows (as appears on the 2009-2010 curriculum year curriculum sheet):

- 1) ME 301: Thermodynamics I
- 2) ME 302: Thermodynamics II
- 3) ME 311: Fluid Mechanics I
- 4) ME 312: Fluid Mechanics II
- 5) ME 313L: Fluid Mechanics Lab
- 6) ME 315: Engineering Materials
- 7) ME 316: Intermediate Vector Dynamics
- 8) ME 319: Stress Analysis
- 9) ME 325/L: Machine Design
- 10) ME 340: Modeling of Systems
- 11) ME 350L: Materials Science & Selection Lab



Student	Senior Project Eligible (Yes/No)	Remarks	Professor Verification	Date
Brian Martin	Y		E	6/3/14
Ben Saletta	Y			
Ketton James	Y			
Andrew Blancarte	Y			
Abraham Paucar	Y	Student will be taking final 300 level class Fall 2014 (ME 350L) and thus will register for EGR 481 482 Winter 2014.	V	

Additional Notes:

References

- [1] Rorres, Chris. "The Turn of the Screw: Optimal Design of an Archimedes Screw." *Journal of Hydraulic Engineering* (2000): 72. Print.
- [2] Anderson, John D. *Computational Fluid Dynamics: The Basics with Applications*. New York: McGraw-Hill, 1995. Print.
- [3] Sonar. Photo Credit: physicsqazvin.blogfa.com
- [4] Tow tank flow visualization. Photo Credit: 3me.tudelft.nl
- [5] Grotheus spoiler. Photo Credit: schneekluth.com
- [6] Owl wing sections as they relate to stealth. Photo Credit: sciencedaily.com
- [7] Submarine hydrostatics. Photo Credit: Naval Engineering Education Center
- [8] Submarine design process. Photo Credit: Submarine Technology for the 21st Century (Zimmerman)
- [9] Munson, Bruce Roy, T. H. Okiishi, Donald Young, and Wade Huebsch. *Fundamentals of Fluid Mechanics*. 6th ed. Hoboken, NJ: J. Wiley & Sons, 2009. Print.